AN ABSTRACT OF THE THESIS OF

Laurence Alan Montano for the degree of Master of Science

in Chemistry presented on December 9, 1977

Title: DETERMINATION OF TRACE CONCENTRATIONS OF COBALT VIA LUCIGENIN CHEMILUMINESCENCE

Redacted for Privacy

Abstract approved: _____
J. D. Ingle, Jr.

The application of lucigenin chemiluminescence for the determination of trace concentrations of Co(II) is described. This method is based on the enhancing effect that Co(II) has on the reaction of lucigenin and hydrogen peroxide in a basic solution. The chemiluminescence signal from a Co(II) enhanced lucigenin reaction, which is in excess of the signal in the absence of added metal activators, is proportional to the Co(II) concentration.

The instrumentation used in the study was a previously constructed chemiluminescence photometer. The photometer is the discrete sampling system type and the luminescent signal was monitored with a photomultiplier tube. Several improvements were made to the existing instrumentation in order to minimize contamination, improve the reproducibility of the chemiluminescent signals, and decrease the analysis time.

The mixing order of the reagents, their concentration and volumes, and other reaction conditions were optimized. The Co calibration curve is linear from the detection limit, 15 pptr, up to 100 ppm. A comprehensive interference study of 88 species (metals, nonmetals, common anions, and complexing agents) indicated that many species enhance or inhibit the lucigenin reaction. In many samples, most of these potential interferents are not present at a large enough concentration to interfere with the determination of ppb and sub-ppb concentrations of Co(II). A solvent extraction separation procedure was developed to isolate Co from its matrix and the most troublesome interferences (Mg and Fe), and it was used in the analysis of NBS orchard leaves. The analysis of five orchard leaves samples indicated that the Co concentration was 0.12 ppm and the relative precision was 18%. Direct analysis of a spiked tap water sample showed that dilution can be used to eliminate interferences as long as the Co concentration in the sample is at least 5 ppb.

The chemiluminescent reaction of lucigenin in a strongly basic solution in the absence of hydrogen peroxide was studied and various absorption, fluorescence, and chemiluminescent spectra were obtained. The reactivity of several Co(III) complexes was investigated as well as the effect of bubbling the reaction solutions with O_2, N_2, H_2, and Ar.

Determination of Trace Concentrations of Cobalt via Lucigenin Chemiluminescence

by

Laurence Alan Montano

A THESIS

submitted to

Oregon State University

in partial fulfillment of
the requirements for the
degree of

Master of Science

Completed December 1977

Commencement June 1978

APPROVED:

Redacted for Privacy

Associate Professor of Chemistry
in charge of major

Redacted for Privacy

Chairman of Department of Chemistry

Redacted for Privacy

Dean of Graduate School

Date thesis is presented December 9, 1977

Typed by Mary Jo Stratton for Laurence Alan Montano

TO LAURENCE, CAROLINE AND

ESPECIALLY KAY

TABLE OF CONTENTS

Table of Contents (Continued)

LIST OF TABLES

LIST OF FIGURES

List of Figures (Continued)

DETERMINATION OF TRACE CONCENTRATIONS OF COBALT VIA LUCIGENIN CHEMILUMINESCENCE

INTRODUCTION

Chemiluminescence (CL) is the emission of light from an excited intermediate or a product in a chemical reaction. The emission process falls in the category of luminescence because the excited electronic state is produced by a nonthermal process. Any type of luminescence is a potential tool for analysis since the number of photons emitted due to the luminescence is related to the concentrations of the luminescing species and of other species which affect the rate of luminescence. In the case of chemiluminescence analysis, the luminescence signal produced by mixing certain reagents with the analyte is related directly to the concentration of the analyte.

Chemiluminescence analysis is an attractive technique and the recent reviews (1, 2, 3, 4) attest to its growing popularity. The instrumentation is simple and easily made portable for possible field use. The detection limits are low for many metals and analyses can be carried out over a wide range of concentrations. In addition, the technique is often specific for a certain oxidation state of some metals.

Recently, three chemiluminescent systems have been described and used for the determination of Co. The luminol system (3, 5), the

gallic acid system (6), and the lucigenin system (7) are applicable to the determination of Co(II) to the ppb level. Co(II) is of great biological importance and routine determination of Co(II) at ppb and sub-ppb levels is difficult since few analytical techniques are available to the analyst. Those techniques which are available can be expensive, time consuming, and require specialized instrumentation.

This investigation is concerned with the application of a simple chemiluminescence photometer (8, 9, 10) to the determination of ppb and sub-ppb concentrations of Co(II). The instrument uses a discrete sample system in which the reagents and analyte solution are mixed in a standard spectrophotometer cell for each determination. The resultant radiation peak is detected by a photomultiplier tube and the peak height is recorded.

The instrumentation was applied to the chemiluminescent reaction between lucigenin and hydrogen peroxide in a basic solution. The reaction and resultant chemiluminescent signal is greatly enhanced by Co(II). The effect of reagent concentrations and instrumental parameters on the chemiluminescence signal was studied to learn more about the nature of the reaction and to choose optimal conditions for analysis of Co(II). The linear range on a log-log calibration plot of peak chemiluminescence signal versus Co(II) concentration is from a detection limit of 15 pptr to 100 ppm. A comprehensive interference study was completed and relevant

spectra were obtained. A number of metal ions interfere with the determination of Co(II) with the most troublesome being Fe and Mg. A simple analysis procedure for Co(II) was developed and applied to biological and water samples. The feasibility of the digestion, separation, and chemiluminescence analysis procedures were checked with a NBS standard reference material.

INSTRUMENTATION

Introduction

As discussed in the background section, the three basic CL sampling systems are the discrete sampling system, the flow cell system, and the centrifugal analyzer. A previously constructed and tested (8, 9, 10) discrete sampling system was used in this study with only slight modification.

The advantages of this discrete sampling system over previous and commercial units include temperature control for the sample cell, a large light-tight compartment to allow room for modifications to the cell holder, compatibility with a monochromator, a magnetic stirrer, a cooled PMT housing to reduce dark current noise, and a versatile electronics system.

The basic components of the discrete sampling system are shown in Figures 1 and 2 and the components are identified in the figure captions. A cell holder inside the sample module (a) holds a spectrophotometer cell (i) in which the chemiluminescent reagents and the analyte are mixed. The resultant chemiluminescence is detected by the photomultiplier tube (PMT) in the PMT module (b). The signal from the PMT is then modified so that the instantaneous chemiluminescence signal and the peak area can be measured. The sample module, the PMT module, the electronics, and precision

Figure 1. Photograph of the exterior of the CL instrument and identification of components.

Letter	Description
a	sample module
b	PMT module
c	sample module lid
d	Swagelock injection port
e	hinge
f	access port cover
m	shutter handle
n	water reservoir
o	pipet rack
p	Eppendorf pipet
q	weighing bottle
r	polyethylene bottle (KOH reservoir)
s	precision liquid dispenser

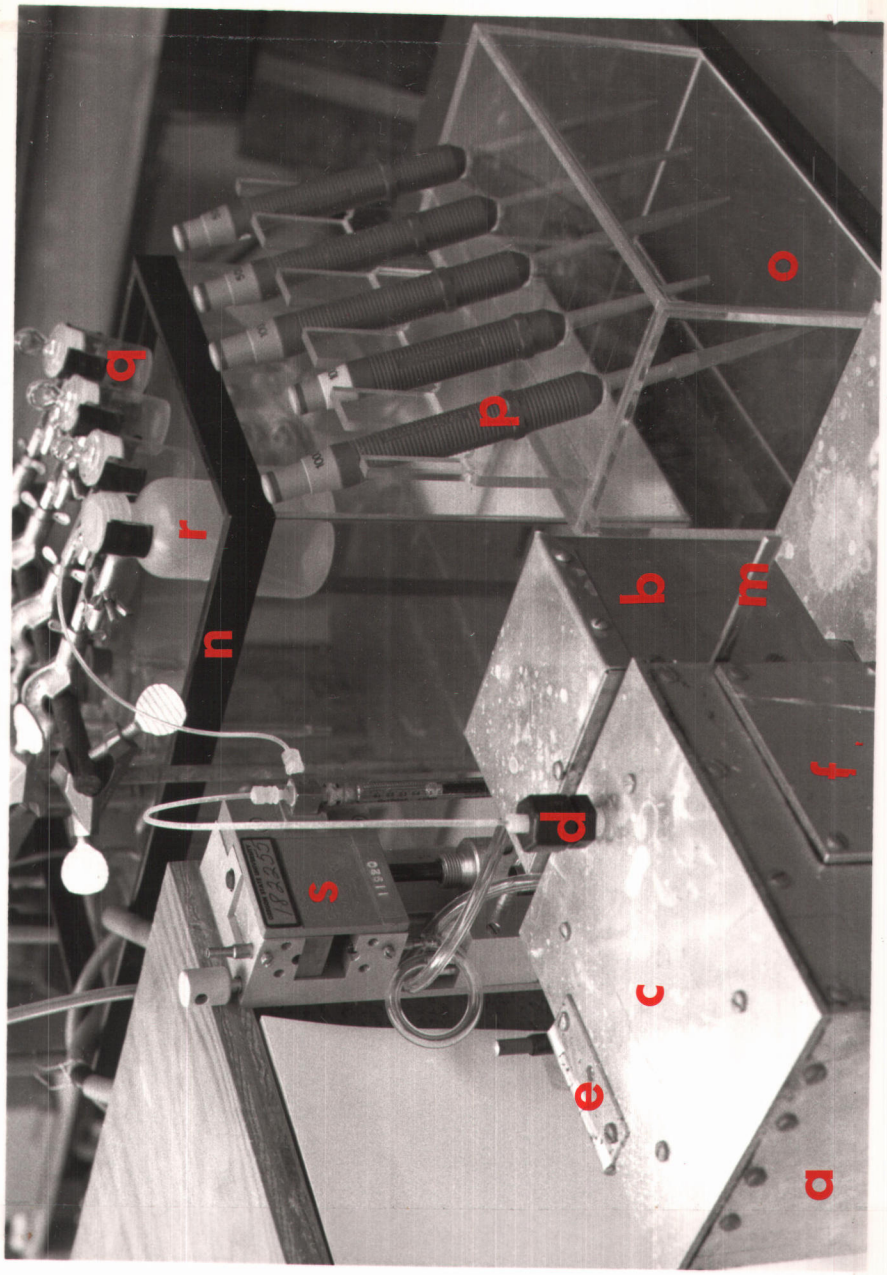

Figure 1

Figure 2. Photograph of the interior of the CL instrument and identification of components.

Letter	Description
g	bulkhead Swagelock fitting
h	sample cell holder
i	sample cell
j	movable block
k	carriage
l	machine screw

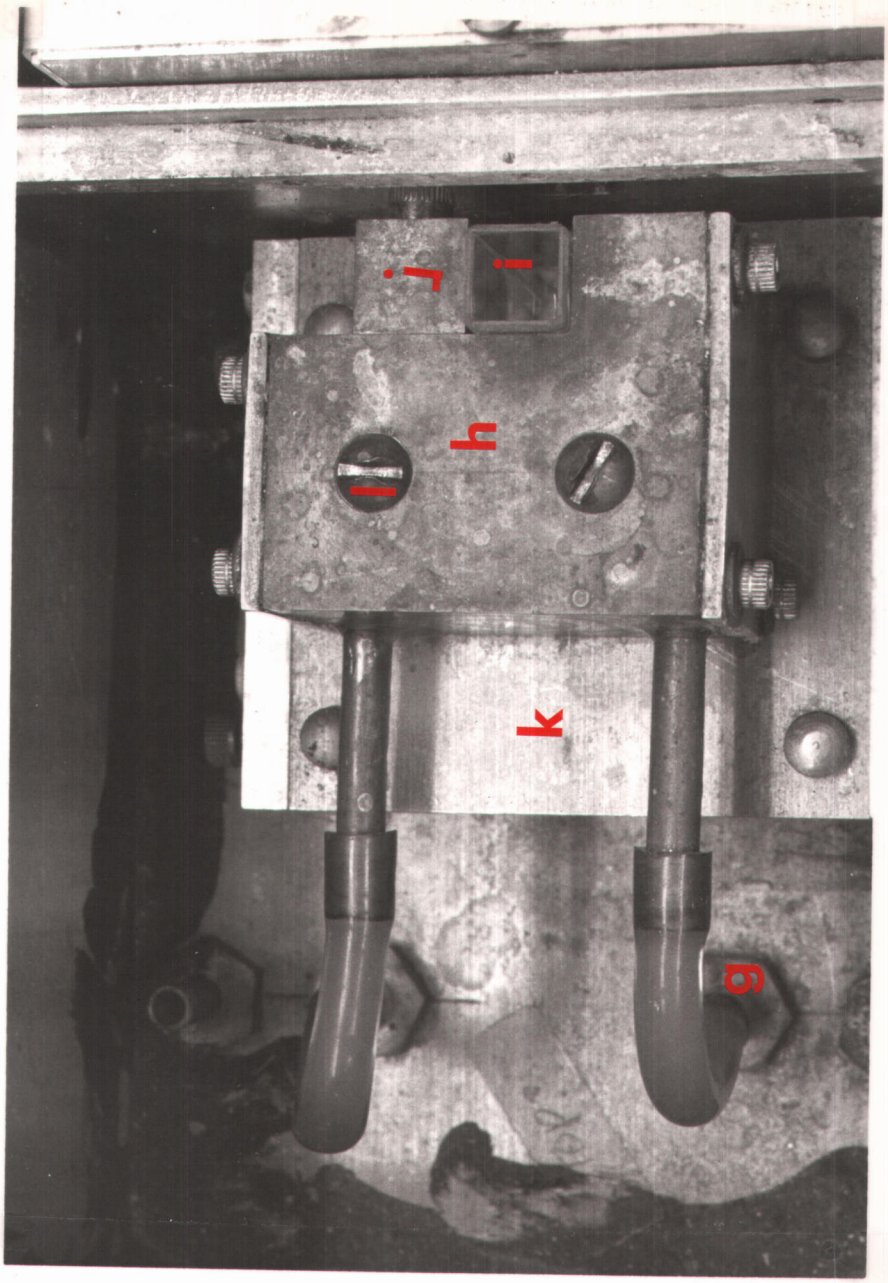

Figure 2

liquid dispenser are covered in the rest of the chapter. Modifications to the original instrumentation will be noted.

Sample Module

The three essential parts of the sample module are the housing, the sample cell holder, and the stirring mechanism. The box shaped housing is 3/32 in. aluminum plates which are fastened together with machine screws. The inside edges of the box are sealed with a black rubber compound to prevent light leaks. Directly above the sample cell in the lid (c) is a polypropylene pipe to tubing Swagelock fitting (d) which holds a rubber septum. This replaced the brass Swagelock fitting in the original instrument which was thought to be a potential source of metal contamination. A 3 in. brass hinge (e) was added to the instrument to permit the lid to be opened and closed quickly. An access port (f) permits the adjustment of the movable carriage and oiling of the stirring motor. The access port and lid have felt gaskets.

The sample module is divided into an upper (main) compartment and a lower (motor) compartment. Water and gas (if needed) enter the motor compartment through bulkhead Swagelock fittings attached to the back plate and flow through 1/4 in. copper tubing to a second set of bulkhead fittings (g) when entering the main sample compartment.

The temperature controlled sample cell holder (h) is brass and provides temperature control by water circulating through holes drilled in the block. When constructed, the water was circulated by a Haake model FJ temperature bath and pump. This unit was replaced by a submersible pump (Little Giant model 1) which pumps the water from a 5 gal. reservoir (n) maintained at a constant temperature by a Polyscience model 73 immersion circulator. The sample cell is surrounded on three sides by the cell holder. The sample cell (i) is a 1 cm square glass cell and is held in position by a movable block (j) which keeps the cell in thermal contact with the cell holder.

The cell holder is attached to a movable carriage (k) which provides a 3/4 in. adjustment in height and can accommodate different sample cell holders and cells. The sample cell holder is secured to the carriage by two brass screws (l) on top of the cell holder which allow easy removal for cleaning.

A stirring magnet centered below the sample cell is connected to a motor with a brass shaft. The shaft is hollow and is held in position with a set screw so it can adjust with the height of the carriage. The induction motor speed is controlled by a Variac outside the sample compartment. For stirring, a round, slotted, Teflon coated magnetic stirring bar was driven by the motor.

Between the sample module and PMT module, a simple shutter mechanism is provided to prevent light from reaching the PMT when the sample module lid is open. The shutter handle (m) is pushed in to close the shutter.

Photomultiplier Tube Module

The design and construction of the cooled PMT module has been described previously (10). Cooled PMT housings are used to reduce the dark current noise caused by thermionic emission. For low light levels, the reduction in dark current noise will improve the signal-to-noise ratio (S/N) if dark current noise is significant. In this study, the PMT was never operated under low temperature conditions for CL measurements because dark current noise was not limiting.

The side-on PMT photocathode is 1-1/2 in. from the CL reaction cell in order to ensure efficient light collection. For all CL measurements an RCA C-37025C PMT with high spectral responsitivity from 200-900 nm was used. Response in the UV is possible since the PMT has a quartz window and quartz sample cells are available.

Electronics

The photoanodic current from the PMT is amplified and converted to a voltage by a Keithley model 124 current amplifier. The

signal from the amplifier is monitored and modified by different types of circuitry and readout devices as shown in Figure 3. The specific electronic components are listed in Table I along with the other instrumental components.

The chart recorder was the principal readout mode in this study. The storage oscilloscope was only used during the initial portion of the study when signals too fast for the chart recorder were being studied. The integrator configuration has been previously reported (8).

Precision Liquid Dispenser

To record the initial CL output of the lucigenin system, it is necessary to inject the final reagent into the sample cell through a rubber septum in the lid. The original procedure was to use a gas-tight syringe to inject the final reagent. During this study this was changed with the installation of a Hamilton model 77000 precision liquid dispenser (s). This air operated device draws a solution from a reservoir into a 1.0 mL gas-tight Hamilton syringe and delivers it to the reaction cell with a measured precision of 0.03%. This modification significantly increases the speed of analysis and reduces the amount of handling since the dispenser is automatic filling and dispensing. The precision of analysis is also increased since the reproducibility of sample delivery is much better than with a manual

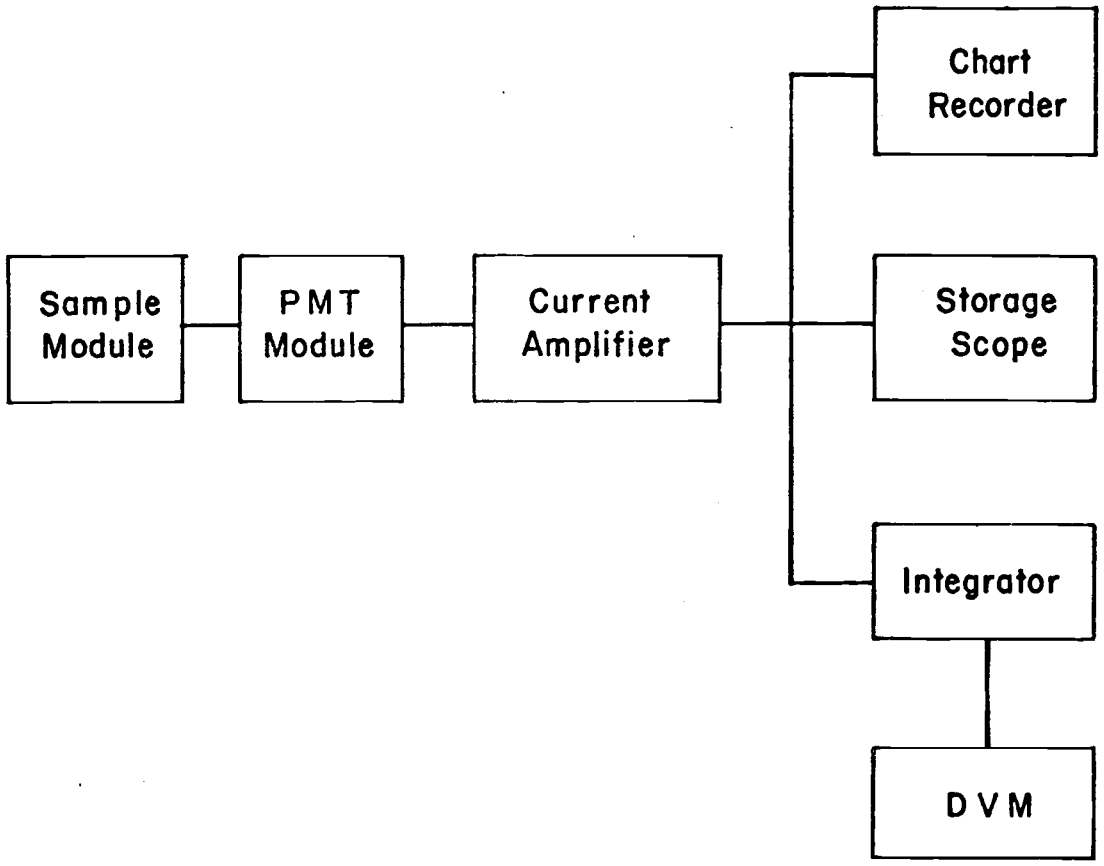

Figure 3. Block diagram of CL instrumentation.

Table I. Instrumental components.

Component	Manufacturer	Model
PMT	RCA	C-31025C
PMT power supply	Keithley	244
Current amplifier	Keithley	124
Chart recorder	Heath	SR-205
Storage scope	Tektronix	564B
Digital voltmeter	Fluke	8000A
Submersible pump	Little Giant	1
Immersion circulator	Polyscience	73
Precision liquid dispenser	Hamilton	77000

syringe and the speed and position of delivery into the sample cell is always the same. Contamination is also reduced since the delivery and reservoir system for the injected reagent is closed.

HISTORY

Introduction

Chemiluminescence (CL) arises when a chemical reaction produces a species in an electronically excited state which emits light as it returns to its ground state. Bioluminescence (BL) is a specific type of CL which involves an enzyme reaction. Usually CL and BL reactions are oxidation-reduction reactions of the general form:

$$A + B + C \longrightarrow L^* \longrightarrow P + h\nu \qquad (1)$$

where A represents an oxidizing or reducing agent or coenzyme; B represents an activator, inhibitor, or enzyme; C is a molecule which undergoes oxidation or reduction to produce a CL species; L^* is an excited product or intermediate; P is the product of the reaction; and $h\nu$ represents a photon. The quantum efficiency of a CL reaction is defined as:

$$\Phi = \frac{\text{number of photons emitted}}{\text{number of molecules reacting}} \qquad (2)$$

In general, the highest efficiencies are associated with BL reactions.

The most important application of BL to chemical analysis is the determination of ATP (adenosine triphosphate) based on the luciferin-luciferase system. The reaction provides a detection limit of 0.1-1 picomoles, and the BL signal is linear with respect to ATP concentration over five orders of magnitude (1). If it is assumed that

the percentage of ATP in living matter is constant, the determination of ATP concentration provides a direct measure of the biomass. There are other BL systems used for analysis, such as the bacterial system for FMN (flavine mononucleotide) determinations (1) and the Aequorea system for determination of the cations Ca(II), Co(III), Pb(II), and Yb(III) (11).

CL analysis has not received much attention until recently because the quantum efficiencies are much lower than with BL. The smaller CL signal was difficult to measure with the photographic film used by early researchers. The use of the photomultiplier tube to measure low light levels has led to the development of CL analytical techniques. CL methods of analysis can be divided into gas phase analysis and solution analysis. Gas phase analyzers are commercially available and are used primarily for measuring pollutants such as S, SO_2, P, O_3, NO, NO_2, CO, and BO_2 (12, 13, 14).

For analysis in solutions, the two common organic CL substances are luminol (5-amino-2, 3-dihydro-1, 4-phthalazendione) and lucigenin (N, N'-dimethylbiacridinium dinitrate). Analysis is based on the activation or deactivation by certain metals of the luminol (or lucigenin) CL in basic solutions with hydrogen peroxide. For the luminol-peroxide system, analytical procedures based on catalysis of the reaction have been developed for V (15), Cr(III) (8, 9, 16), Mn(II) (17), Fe(II, III) (18, 19), Co(II) (5), Cu(II) (20), and Hg(II) (21). Zr (22),

Ce (23), and Th (24) analysis is possible because these metals inhibit the metal catalyzed reaction of luminol. For the lucigenin-peroxide system, analytical procedures based on catalysis of the reaction have been developed for Mn(II) (25, 26), Co(II) (7, 35), Ag(I) (27, 28), Os(VIII) (29), Tl(I) (30), Pb(II) (31, 32, 33), Bi(III) (34), Ni(II) (35), Cu(II) (36), Ce(III) (37), Cr(III) (38), and Fe(II) (39).

The following sections will provide background information on lucigenin chemistry, the mechanism of the lucigenin reaction, cobalt chemistry, hydrogen peroxide chemistry, instrumentation for CL analysis, and CL cobalt analysis.

Lucigenin

Lucigenin (Lc) belongs to a class of acridine molecules called the biacridines. The structures of acridine and Lc are shown in Figure 4 along with the numbering system currently used to name these molecules. Of all the possible molecules that can be formed from two acridine ring systems, only those joined at the 9, 9', 10, 10', and 9, 10' positions are known (40).

The first preparation of Lc from acridine was reported by Decker and Dunant in 1909 (41). This synthesis was modified in 1935 by Decker and Petsch (42) and these two methods appear to be equally employed by researchers who synthesize their own lucigenin. The reagent is commercially available from K and K Laboratories.

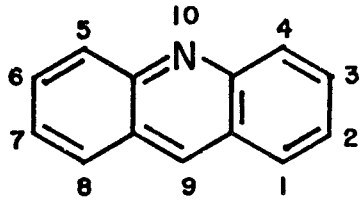

Acridine

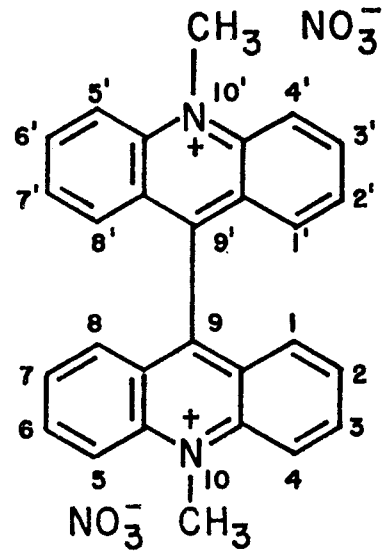

10, 10'-dimethyl-9, 9'-biacridinium dinitrate (lucigenin)

Figure 4. Numbering system and structure of acridine and lucigenin.

The application of Lc in analytical chemistry (beyond CL metal analysis) has been in the areas of titration, biological assay, and metal extraction. Erdey and Buzas (43) have reported that Lc can be used as a CL indicator for the titrimetric determination of Cu, Pb, and Hg. They also report a titrimetric procedure for the argentometric determination of iodide and standardization of EDTA solutions, again using the appearance or disappearance of Lc CL as an indicator of the equivalence point. The use of Lc CL as a pH indicator has been reported by Lurie (44) where use is made of the fact that no CL is visible when the pH of the solution is below nine. An indicator which contains Lc, fluorescein, and H_2O_2 has been used as a CL indicator for acid-base titrations in colored, dark, and turbid solutions (45). It is also possible to determine milligram amounts of potassium by precipitating the potassium with sodium tetraphenylborate ($NaBPh_4$). The excess BPh_4^- is titrated with a basic Lc + H_2O_2 solution where the equivalence point is indicated by the appearance of CL (46).

A biological assay for an enzyme that induces Lc CL has been patented (47) and several studies have been made of the xanthine oxidase induced CL of lucigenin (48, 49). Cell free extracts of Serratia marcesoens also activate the Lc CL in the absence of H_2O_2 or alkali (50).

The extraction of a Cu(II) complex from CL solutions of lucigenin has been used to spectrophotometrically determine Cu (51). The

complexing ligand is presumably an intermediate or end product of the CL reaction. This benzene extraction technique appears to have fewer metal interference problems than the conventional CL analysis, and the detection limit is quite low.

Mechanism of the Lucigenin Reaction

The mechanism of the Lc chemiluminescent reaction in the presence or absence of added metal catalysts has not been finalized. Following is a brief review of the proposed mechanisms and the data that support these mechanisms. The structural formulas and names for the acridine molecules in this section are presented in Figure 5.

In 1935, Gleu and Petsch (52) discovered that the addition of H_2O_2 to an alkaline, aqueous solution of Lc (a) produced CL. The duration of the CL was several hours under certain conditions and the intensity could be increased, at the expense of the duration, by adding traces of osmium tetroxide. After further studies, they proposed a mechanism that was consistent with these findings:

1. N-methylacridone (d) is the chief reaction product.
2. When other oxidizing agents, such as sodium hypochlorite and potassium ferricyanide, replace H_2O_2 no CL is observed.
3. Lucigenin loses its fluorescence properties in a basic solution due to formation of the bicarbinol (b).

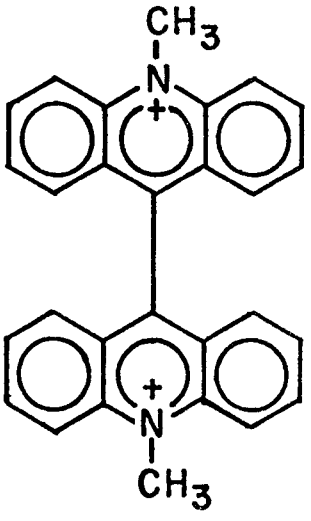

(a) lucigenin

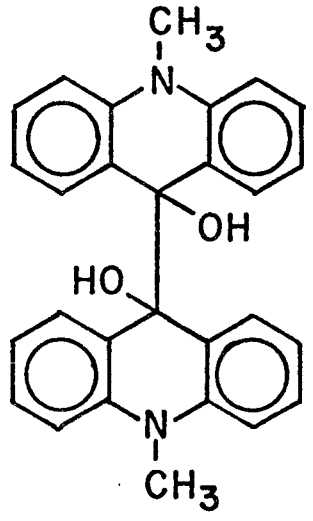

(b) bicarbinol

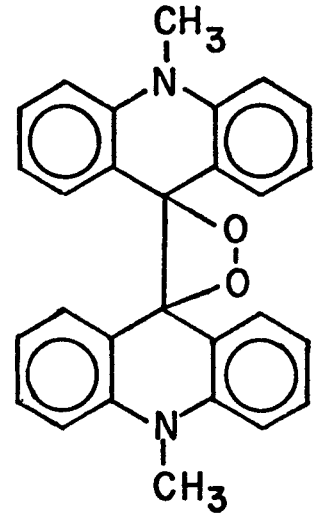

(c) annular peroxide

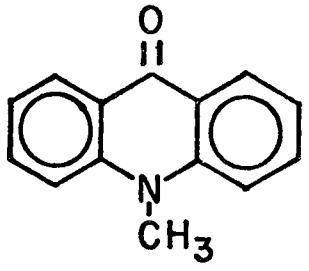

(d) N-methyl-acridone

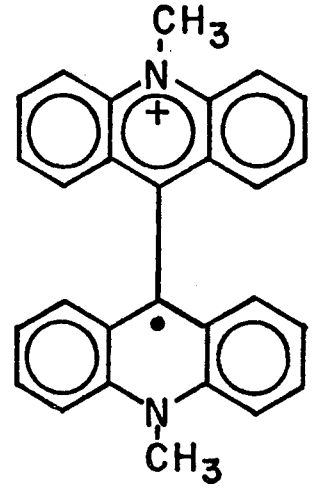

(e) dimethylbiacridine radical cation

Figure 5. Structures of molecules proposed in the mechanism of the Lc reaction.

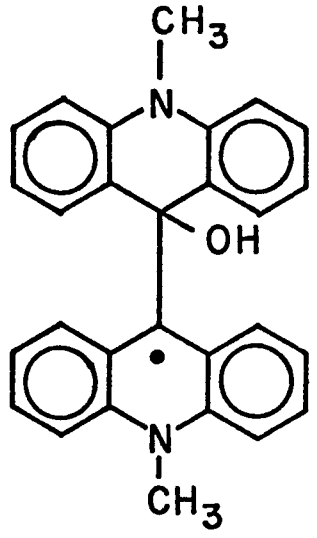

(f) hydroxide addition product of (e)

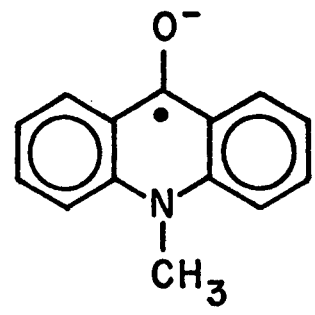

(g) N-methylacridine ketyl

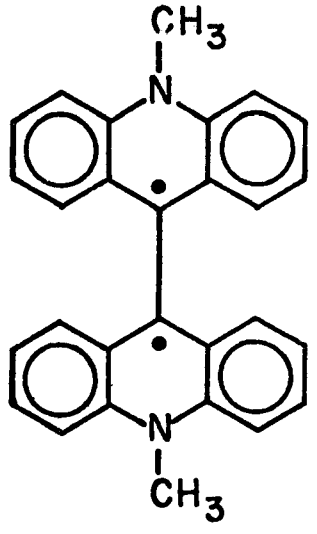

(h) dimethylbiacridine biradical

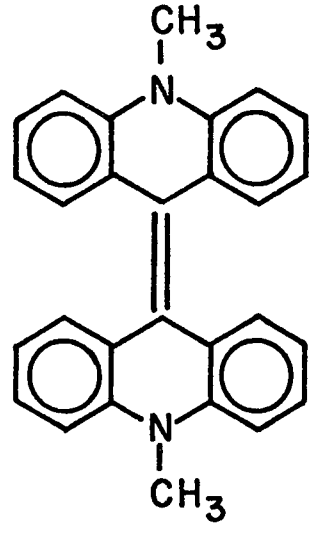

(i) dimethylbiacridene

Figure 5. (Continued)

4. Chemiluminsecence is observed in alkaline solutions with a high Lc concentration when molecular oxygen is present.
5. Chemiluminescence eventually ceases even when unreacted H_2O_2 is present.

Their mechanism, shown in Figure 6, involves the formation of a bicarbinol (b) which can be oxidized by H_2O_2 to the annular peroxide (c). The reduction of this peroxide species by H_2O_2 was believed to be the chemiluminescent step. The bicarbinol (b) was presumed to react irreversibly to form N-methylacridone (d), the major end product. Although this mechanism was invalidated when N-methylacridone (d) was identified as the light emitting molecule, the formation of the bicarbinol (b) and/or the annular peroxide (c) are essential features of all subsequent mechanisms.

In the following years, other investigators examined the Lc reaction and the additional mechanistic information derived from these studies showed that:

1. Dissolved molecular oxygen is an essential reactant for the chemiluminescent reaction of Lc in alkaline solutions (no H_2O_2 present) (53).
2. As the reaction temperature increases (Lc + H_2O_2 + base system), the duration of the CL decreases and the intensity increases (53).

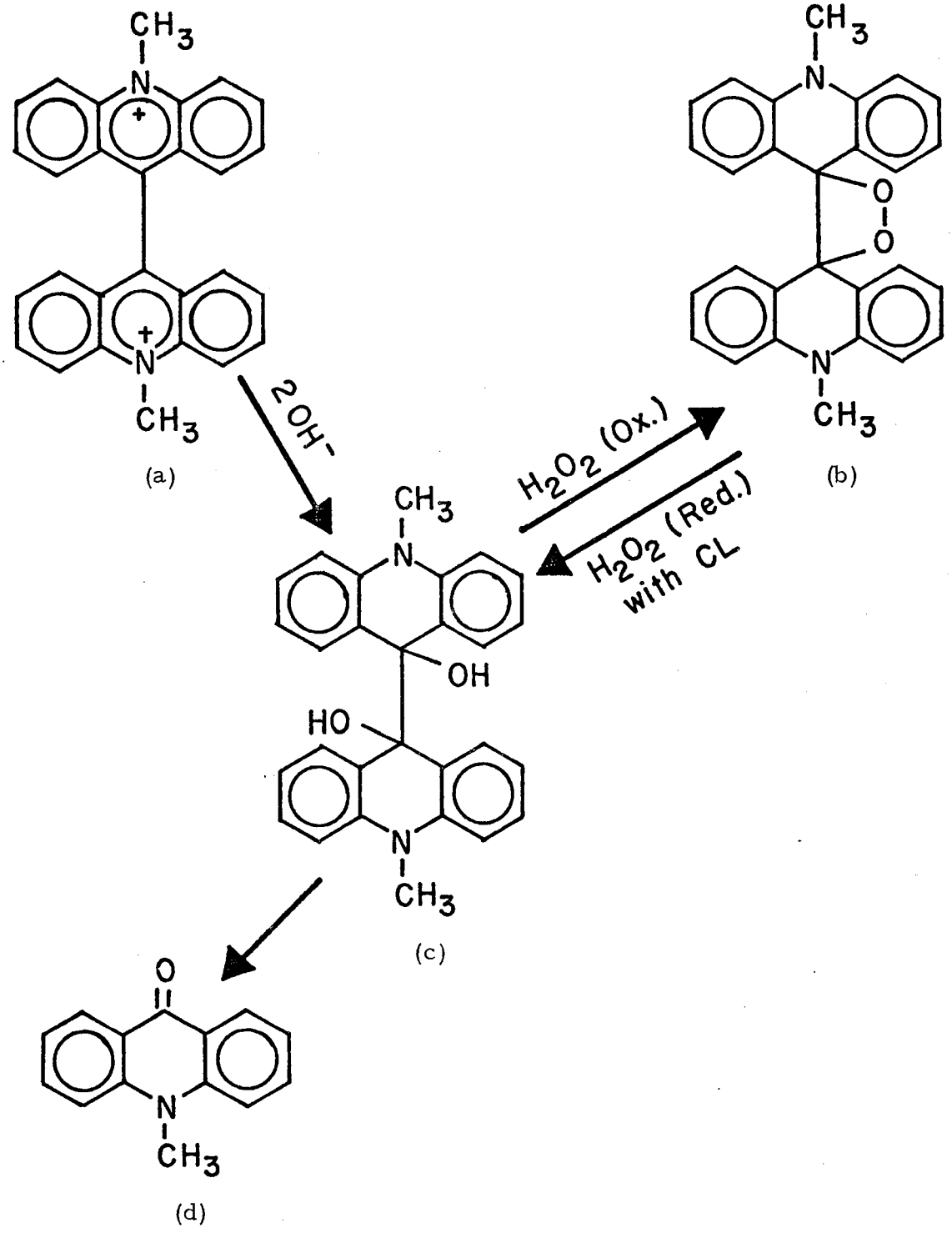

Figure 6. Mechanism proposed by Gleu and Petsch (52).

3. When alkaline solutions of Lc are electrolyzed, luminescence is observed at the cathode, where reduction takes place (53).

4. The maximum of the CL spectrum is at 515 nm when the Lc concentration is high (54).

In his review of the acridines in 1959, Acheson (40) pointed out that substitution at various positions of the Lc molecule was a factor in the weakness or absence of CL exhibited by these molecules. In Table II (from Acheson, p. 282), it is clear that substitutions away from the bond that joins the two acridine moieties has little effect on the visible CL while substitution at the 1, 1' or 2, 2' positions hinders the CL.

Totter (55) obtained various fluorescence and CL spectra which are summarized in Table III. He showed that in mixed organic solvent systems the CL spectrum of the Lc-H_2O_2 reaction matched the fluorescence spectrum of N-methylacridone (d). Dimethylbiacridene (i) in alkaline alcohol solutions is chemiluminescent and its CL spectrum is also identical to the fluorescence spectrum of N-methylacridone (d). The CL reaction of Lc in a completely aqueous system, however, did not have the same spectrum as it did in mixed organic solvents. The shift of the maximum wavelength to a slightly higher wavelength in aqueous solutions is attributed to the formation of a short lived hydrate of N-methylacridone (d). Totter determined that the quantum yield of the Lc-H_2O_2 reaction (based on the

Table II. Chemiluminescence of lucigenin analogs.

9, 9'-Biacridinium Salt	Chemiluminescence Color
10, 10'-dimethylbiacridinium dinitrate (Lc)	Intense green
10, 10'-diethylbiacridinium, trinitrate[1]	Intense green
10, 10'-diphenylbiacridinium, tetrachloride[1]	Intense green
1, 1'-dimethoxy-10, 10'-dimethylbiacridinium, borofluoride	No CL
2, 2'-dimethoxy-10, 10'-dimethylbiacridinium, trinitrate[1]	Weak yellow
3, 3'-dimethoxy-10, 10'-dimethylbiacridinium, dinitrate	Blue-green
1, 1', 10, 10'-tetramethylbiacridinium, borofluoride	Weak blue-green
2, 2', 10, 10'-tetramethylbiacridinium, tetranitrate[1]	Yellow-green
3, 3', 10, 10'-tetramethylbiacridinium, trinitrate[1]	Intense blue-green
1, 1', 2, 2'-tetramethoxy-10, 10'-dimethyl-3, 4-3', 4'-bismethylenedioxybiacridinium, dinitrate[1]	No CL

[1]Means the acid salt.

Table III. Luminescence spectra data from Totter (55).

Reaction or Species	Type of Spectrum	λ_{max} for Observed Peaks (nm)	Solvent
N-methylacridone (d)	Fluorescence	435, 450	Unknown
Lc + H_2O_2 + KOH	CL	435, 450	Alcohol, pyridine, 0.01 M KOH (1:1:2)
Dimethylbiacridene (i) + H_2O_2	CL	435, 450	50% Alcohol
Lc + H_2O_2 + KOH	CL	475	Aqueous, pH = 10.4

N-methylacridone formed) was about 0.014 and noted that dimethylbiacridene (i) was formed when Lc is in excess.

Maeda and Hayashi (56) also studied the pertinent CL and fluorescence spectra of the Lc reaction. Their systematic examination of the CL spectrum showed that the maximum wavelength of the CL emission shifted from 510 nm to 485 nm when the Lc concentration varied from 2×10^{-4} to 5×10^{-6} M. This shift is attributed to the fact that Lc absorbs strongly at wavelengths below 490 nm, and hence distorts those spectra in which the Lc concentration is relatively large. When the Lc concentration is varied from 1 to 5×10^{-6} M the maximum wavelength of luminescence remains constant, indicating that absorption by Lc no longer has an effect on the CL spectrum.

The fluorescence emission spectrum of Lc at concentrations from 4×10^{-6} to 4×10^{-3} M in 0.12 M sodium hydroxide showed that the maximum of the emission spectrum is at 508 nm (56). Once this solution has been prepared, however, the fluorescence spectrum begins to change. Within 20 minutes, the spectrum is predominantly the fluorescence emission spectrum of N-methylacridone (d) which has maxima at 435 and 450 nm. This reaction, which is accompanied by CL, was known to occur (52, 53), but N-methylacridone had not previously been demonstrated as a product. During the following years, the reaction in the absence of H_2O_2 became the focus of

mechanistic studies because of the complexity of the reaction when H_2O_2 is present.

McCapra and Richardson (57) proposed the mechanism shown in Figure 7 on the basis of its similarity to the CL reaction of an acridine derivative which also produces excited N-methylacridone (d). This mechanism includes the bicarbinol (b) and the annular peroxide (c) of Gleu and Petsch (52). N-methylacridone (d) is not regarded as the CL species and this differs from all subsequent postulated mechanisms which accept the data of Totter (55) showing that N-methylacridone is the CL species.

Janzen et al. (58) employed Electron Spin Resonance (ESR) spectroscopy to study the reaction of hydroxide ion and Lc in dimethylsulfoxide-water mixtures. Two radical species were readily detected, but neither could be conclusively identified. On the basis of comparison to ESR spectra of structurally similar radicals, they postulated that one of the radicals is the hydroxide addition product (f) of the dimethylbiacridine radical cation (e). However, this could not be confirmed experimentally since species f could not be produced independent of the Lc reaction.

Radicals e and g were produced independently of the Lc reaction, but their ESR spectra did not correspond to the spectra readily observed during the lucigenin reaction. It was reported that no

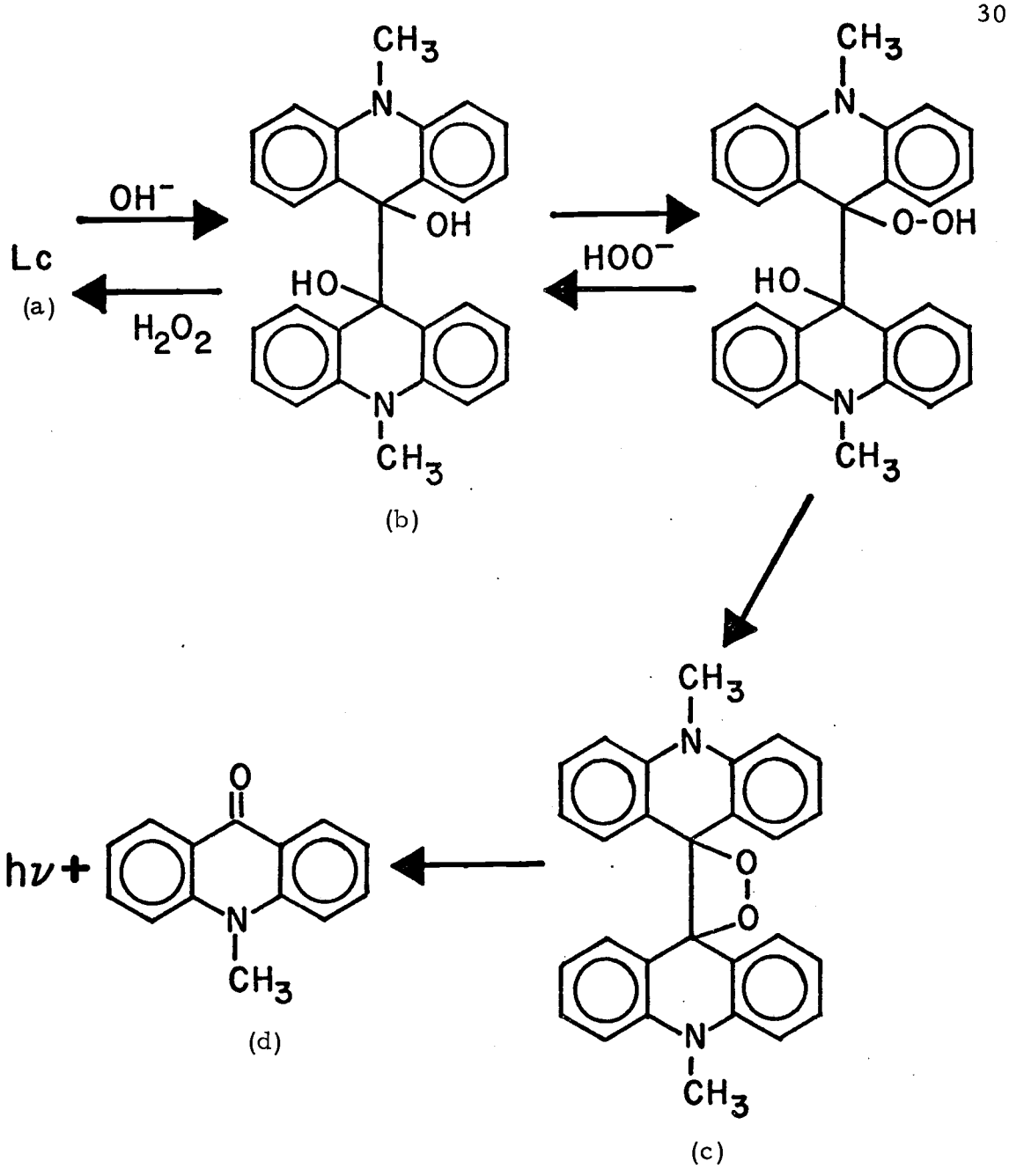

Figure 7. Mechanism proposed by McCapra and Richardson (57).

radicals were detected when the lucigenin reaction was carried out in the presence of added H_2O_2.

The authors (58) reported that the intensity of CL is much greater and the appearance of CL upon mixing the reagents is much sooner when H_2O_2 is present. This prompted them to present a mechanism which involved three routes to the production of N-methylacridone (d). The first route, which occurs in the absence of H_2O_2, is considered to be the slowest route for the production of N-methylacridone (d) because of the number and nature of steps involved. As shown in Figure 8, it starts with formation of the bicarbinol (b) by hydroxide addition to Lc (as in previous mechanisms) but does not involve formation of the annular peroxide (c). According to the authors, there is ample precedence for each step and their inability to detect the N-methylacridine ketyl (g) during the Lc reaction in the absence of H_2O_2 is considered unimportant. Presumably, the radicals that were detected in their studies lead to side products and hence were not incorporated into the mechanism.

In the presence of H_2O_2, two routes for the Lc reaction are believed to be important. They are similar to the mechanism proposed by McCapra and Richardson (57) (Figure 7) in that the annular peroxide (c) is formed and it dissociates into excited N-methylacridone (d). All three basically differ in the order of addition of hydroxide

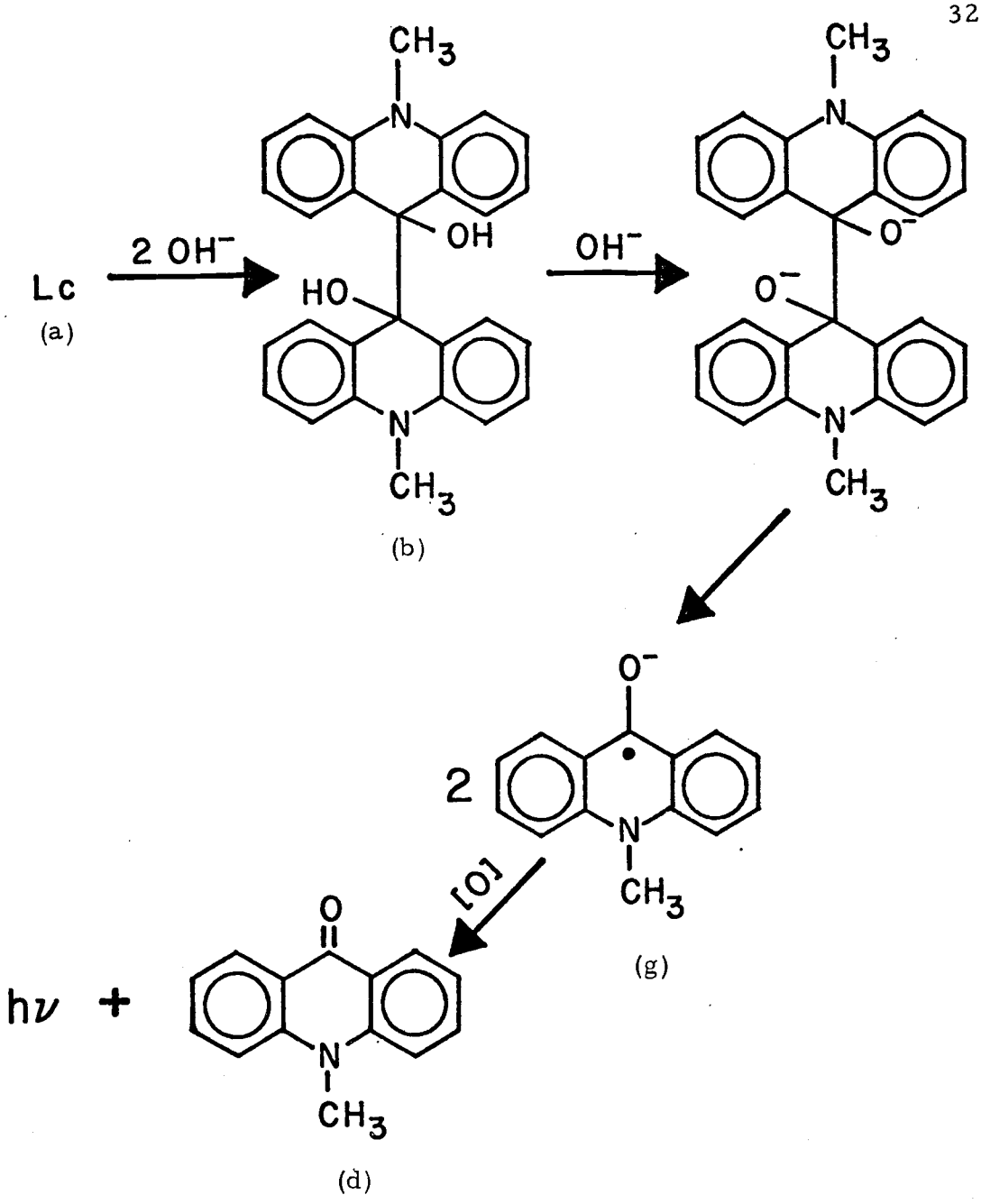

Figure 8. Mechanism proposed by Janzen et al. (Route #1) (58).

and perhydroxyl ions and the rearrangements that occur to form the annular peroxide (c).

The most recent paper concerning the mechanism of the Lc CL reaction, by Maeda et al. (59), again relies on the application of ESR spectroscopy to study the free radicals formed in the absence of H_2O_2. Their approach is more general in that they studied the reaction of many nucleophiles other than hydroxide ion with Lc. They found that in the absence of dissolved molecular oxygen in an aqueous solution:

1. Cl^-, Br^-, SCN^-, I^-, and NO_3^- form charge transfer complexes with Lc.
2. $C_6H_5COCH_2^-$ and $CH_3COCH_2^-$ produce the dimethylbiacridine radical cation (e) by one electron transfer via the charge transfer complex.
3. OH^-, CN^-, CCl_3^-, and $C_6H_5S^-$ produce the dimethylbiacridine biradical (h) by two-electron transfer via the cation radical (e).

The reaction of Lc in the presence of dissolved molecular oxygen with all nucleophiles of the same type as hydroxide ion (strong electron donors) produces CL so the ability to form the biradical (h) is the key that distinguishes the nucleophiles studied. Formation of the dimethylbiacridine radical cation (e) when oxygen is present will not result in CL.

Maeda et al. noted that McCapra and Hann (60) had demonstrated that production of the annular peroxide (c) by two methods (other than Lc CL) resulted in the formation of excited N-methylacridone (d). Accordingly, the mechanism shown in Figure 9 was proposed by Maeda et al. for the reaction in the absence of H_2O_2. They did not advance a mechanism for the case when H_2O_2 is present in solution.

Another aspect of Lc chemistry is the electrochemically generated CL (ECL) studies of Legg and Hercules (61). In organic solvents, they found that N-methylacridone (d) is the primary emitter as in normal aqueous Lc CL. This was accomplished by spectroscopically observing the reduction of Lc at the cathode. Lc was believed to react with superoxide (also being formed under the conditions of the ECL) to eventually produce excited N-methylacridone (d). A two-electron reduction product of Lc, identified as dimethylbiacridene (i), is formed as a side product. The spectra in organic solvents changed with time as ECL continued and this was correlated with the fact that N-methylacridone (d) is able to transfer its energy to Lc or dimethylbiacridene (i) via singlet-singlet interactions. Comparable studies for aqueous systems were not possible because the side product of the reaction, dimethylbiacridene (i), is insoluble in water and hence was deposited on the electrode and reaction cell surfaces.

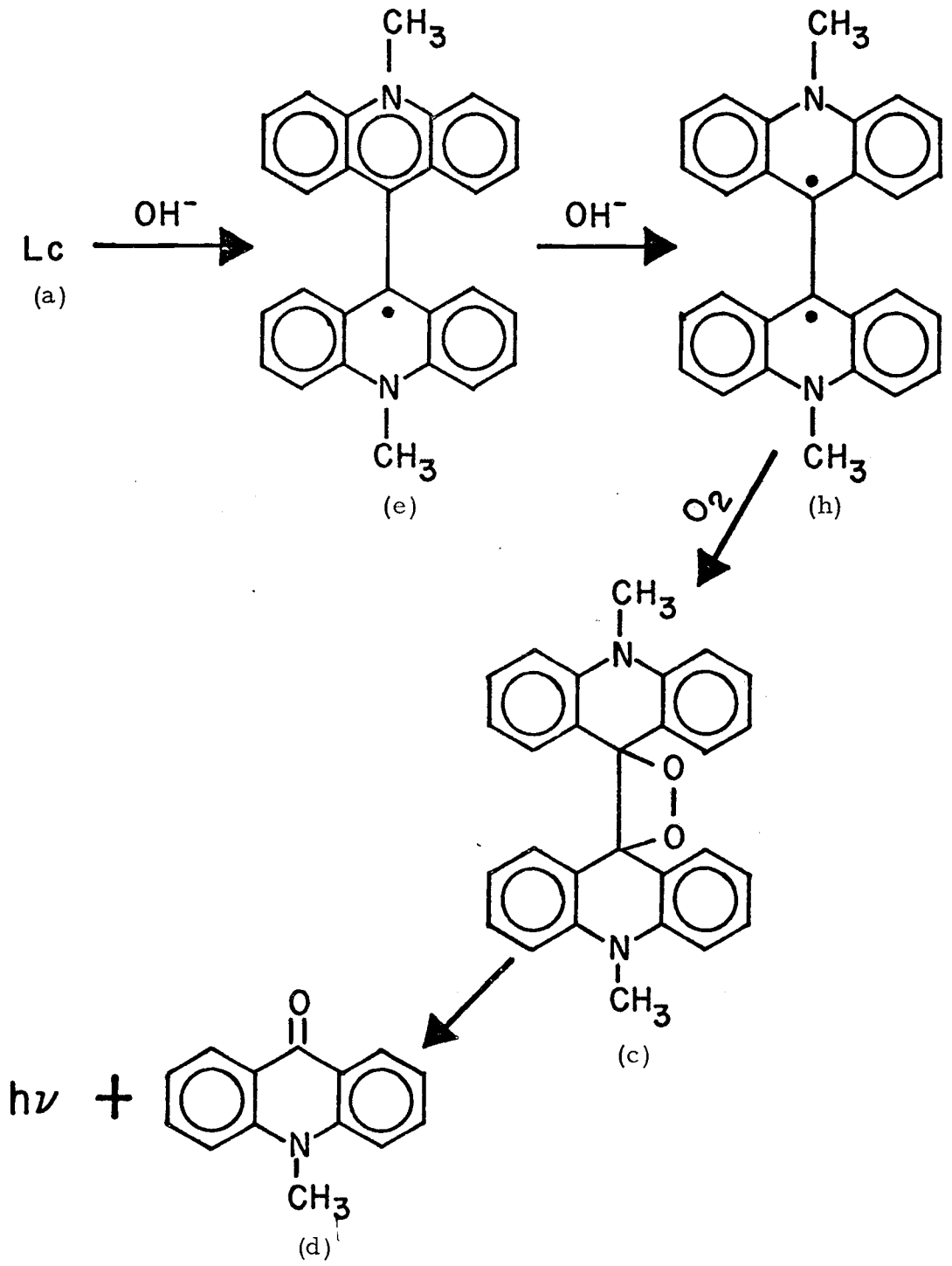

Figure 9. Mechanism proposed by Maeda et al. (59).

The final literature source for observations that can provide information about the mechanism comes from those papers that are directed toward the analytical (metal analysis) applications of the Lc reaction. These papers deal exclusively with the reaction in the presence of H_2O_2. Dubovenko and Guz (31) found that addition of EDTA decreased the CL intensity of the Pb(II) catalyzed reaction (Pb(II) + Lc + H_2O_2 + hydroxide ion), and concluded that formation of the stable Pb-EDTA complex prevented Pb from participating in the Lc reaction. Sulfate, acetate, and carbonate anions also had the same effect on the CL intensity. Complexation of the metal ion was deemed preferable in a Mn analysis paper by Dubovenko and Tovmasyan (26). They found that addition of triethanolamine (TEA) to the Mn(II) + H_2O_2 + Lc + hydroxide ion reaction greatly lowered the detection limit for Mn relative to analysis in the absence of the amine. The increased analytical signals were attributed to the formation of a catalytically active Mn(III)-TEA complex. Dubovenko and his coworkers have been able to extract metal-"Lc" complexes. The Pb complex is formed in the ratio of 1:2 (Pb:Lc) during the early part of the CL reaction, but at the end of the reaction the complex has a ratio of 1:1 (32). It is believed that the complex actually involves a reduced form of Lc and that the unstable 1:2 complex decomposes to give the 1:1 complex. A Co containing complex (7) has been extracted from solutions which initially were Co + Lc + H_2O_2 + hydroxide ion. Again, the complex is

believed to contain a reduction product of Lc. A 1:2 (Bi:Lc) complex is reportedly extracted by benzene and its concentration parallels the intensity of the CL reaction solution that it is extracted from (62). The extraction of a Cu complex from a Cu enhanced CL reaction solution is so reliable that the Cu concentration can be determined spectrophotometrically with a detection limit for Cu of 10 ppb (51).

The effect that metal catalysts have on the rate of H_2O_2 decomposition has been studied in several of the analytical application of Lc papers. As the pH of the CL reaction solution increases, the rate of H_2O_2 decomposition increases if the determination is made within the first 10 minutes of the Co enhanced CL reaction (7). When the CL reaction is allowed to proceed for 30-60 minutes, the maximum percent H_2O_2 decomposition occurs near the middle of the pH range studied (13.5). The Ag enhanced CL reaction shows the opposite tendency in that as the pH increases, the initial rate of H_2O_2 decomposition decreases (28). A pH of 11.5 is the optimum for the Pb(II) enhanced CL reaction and corresponds to the maximum rate of H_2O_2 decomposition (33). In the analysis for Mn, it was found that the addition of triethanolamine suppressed the rate of H_2O_2 decomposition in the Mn enhanced Lc reaction (26).

As stated previously, it is not possible to present a unified mechanism for the CL reaction of Lc. For the reaction between Lc and hydroxide ion, the authors of the most recent mechanism proposal,

Maeda et al. (59), seem to ignore the major point of a reference which is supposed to support a key step in their mechanism. The alternate mechanism for this reaction, offered by Janzen et al. (58), incorporates a radical that the authors could not observe via ESR and omits the radical they did observe and identify.

The mechanism for the reaction of Lc in the presence of H_2O_2 is more complicated. It is reasonable to concur with Janzen et al. (58), that more than one pathway toward the production of the light emitting molecule is possible. Even greater complexity is achieved when metals are introduced into the system. The wide range of effects that these metals have on the Lc reaction would seem to imply that enhancement of the reaction could occur by different mechanisms according to which metal is present.

Cobalt Chemistry and Analysis

The observed oxidation states of cobalt range from -1 to +4 (63), but the most frequently encountered are the Co(II) and Co(III) states (63). Co(II) forms a wide variety of simple and hydrated salts as well as numerous binary compounds. This ion is the only d^7 ion of common occurrence and numerous kinetically labile complexes are formed by it. The predominant stereochemistry of these complexes is tetrahedral and octahedral, and the stability difference between these two forms is small (63). In Table IV, some standard reduction

Table IV. Standard reduction potentials for cobalt.

Half Cell Reaction	Standard Reduction Potential (E^o) (V)
$Co^{3+} + e^- \rightleftarrows Co^{2+}$	1.82
$[Co(NH_3)_6]^{3+} + e^- \rightleftarrows [Co(NH_3)_6]^{2+}$	0.1
$Co(OH)_3 + e^- \rightleftarrows Co(OH)_2 + OH^-$	0.20
$[Co(CN)_6]^{3-} + e^- \rightleftarrows [Co(CN)_6]^{4-}$	-0.83
$CoO_2 + H_2O + 2e^- \rightleftarrows CoO + 2OH^-$	0.90
$Co^{2+} + 2e^- \rightleftarrows Co$	-0.277

potentials for Co(II) complexes are listed (64). As indicated in Table IV, the hexaaqou Co(II) complex is not readily oxidized; but in the presence of ligands which stabilize the Co(III) complex, the oxidation is very favorable.

In contrast to Co(II), there are few simple salts or compounds formed by Co(III). Co(III) complexes, however, are numerous and well studied because of their kinetic inertness. All discrete complexes have octahedral symmetry. Ligands with nitrogen donor atoms (amines, ammonia, nitro groups, and nitrogen-bonded thiocyanate) form stronger bonds than ligands which bond through oxygen or sulfur (63).

The known biological chemistry of Co is characterized by its occurrence in the various coenzyme forms of vitamin B_{12}. In its biologically active form, a Co(III) atom has four bonds to the planar corrin ring system and in the fifth coordination position is a 5, 6-dimethylbenzimidazole group. The last position is occupied by the 5'-deoxyadenosyl group. This molecule is shown in Figure 10. Commercial vitamin B_{12} is cyanocobalamin, in which the 5'-deoxyadenosyl group of the coenzyme has been replaced by cyanide during the isolation of the molecule. B_{12} is the only vitamin which is a coordination compound (65). Unlike other Co(III) complexes, vitamin B_{12} and its coenzyme are not kinetically inert (66).

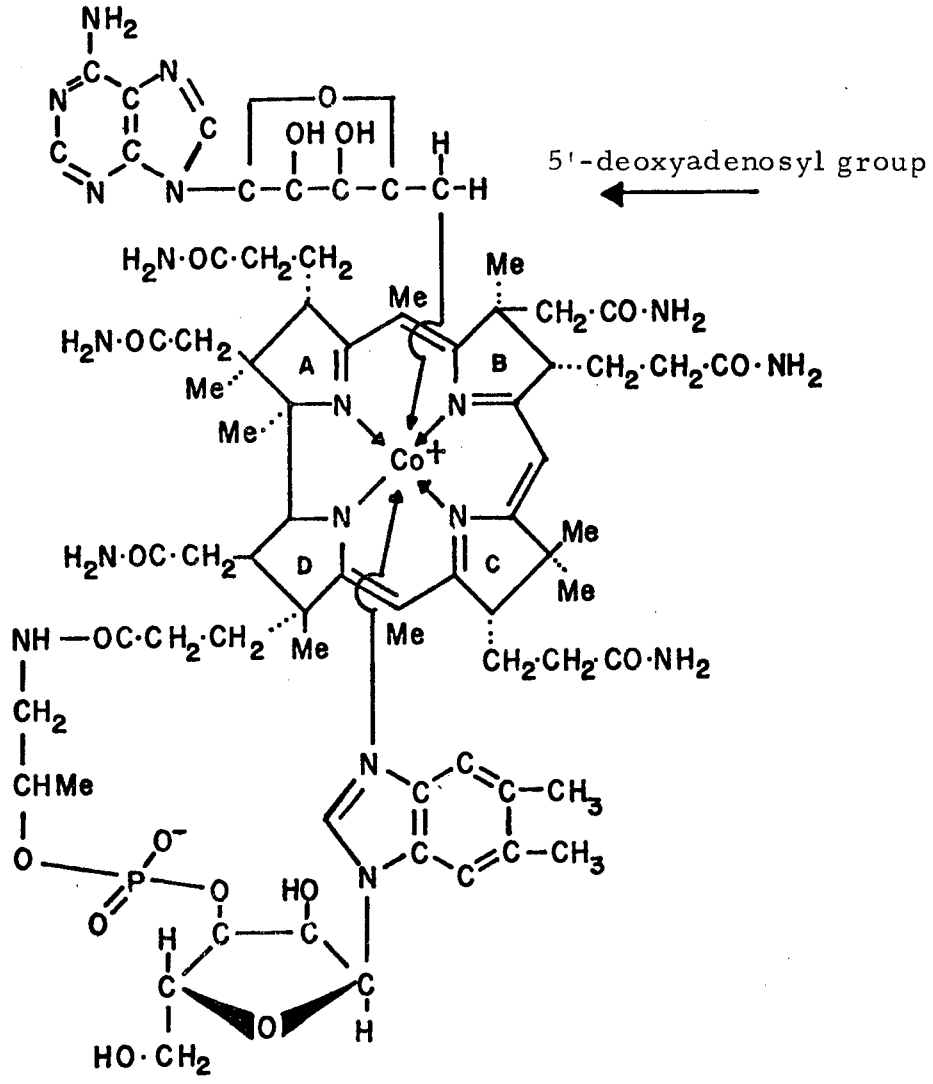

Figure 10. Structure of B_{12} coenzyme.

Vitamin B_{12} coenzyme is required by all animals, but its biosynthesis is effected only by microorganisms. The small requirement of approximately 10-15 μg/day (65) for man is amply filled by a diet which includes animal protein and leafy vegetables. Ruminants absorb B_{12} coenzyme synthesized by bacteria in their fore-stomach (67). For other animals, the source is animal protein, plant roots, or their feces (B_{12} coenzyme producing bacteria inhabit the lower digestive tract of many animals). In animals, B_{12} coenzyme is usually concentrated in the liver and kidneys (67). Its concentration in human blood has been estimated as 7×10^{-5} to 6×10^{-3} μg/mL.

All of the metabolic functions of B_{12} coenzyme in animals are not known, but four reactions that have been identified are (68):

1. Isomerization of glutamic acid to β-methylaspartic acid.
2. Isomerization of methylmalonyl coenzyme A to succinyl coenzyme A.
3. Conversion of propanediol to propionaldehyde.
4. Biosynthesis of methionine.

An important aspect of the biological chemistry of Co is its association with plants and bacteria that fix atmospheric nitrogen. Co is required for the growth of blue-green algae which fix nitrogen (69). It is also necessary for the growth of and nitrogen fixation by leguminous plants which live in symbiotic association with Rhizobium species (69). This symbiotic relationship results when bacteria invade

roots of the plants and root nodules are formed. Nitrogen fixation takes place in these root nodules, but the mechanism of the fixation is not clear. It has been established that these Rhizobium require Co for growth and that they synthesize coenzyme B_{12} as well as other related B_{12} compounds (69). Leguminous plants grown in the absence of these bacteria do not require Co, if they are supplied with fixed nitrogen. Thus, coenzyme B_{12} is not implicated in the actual process of fixing nitrogen, but it (and hence Co) is required by free living bacteria which can fix nitrogen and bacteria which symbiotically participate in nitrogen fixation (69).

The analytical chemistry of Co has been reviewed extensively and three books devoted exclusively to Co (70, 71, 72) more than adequately present the techniques available up to 1969. More recent analytical methods for Co analysis can be found in Winefordner's book on trace element analysis (73). Table V lists a variety of means for Co determination at trace level concentrations. The analyses based on the enhancement of chemiluminescent reactions will be covered in detail in the final section of this chapter.

Hydrogen Peroxide

Hydrogen peroxide is not an essential reactant for the chemiluminescent reaction of lucigenin, but in metal analyses based on the enhancement of the lucigenin reaction it is always used. Hydrogen

Table V. Methods for Co analysis.

Method	Detection Limit (ppb)	Sample Volume	Reference
Atomic Absorption (flame)	5	-	74
Atomic Absorption (carbon rod)	1	5 μL	75
Atomic Emission (inductively coupled plasma)	0.1	-	76
Colorimetry (nitroso-R salt)	2	5 mL	77
X-ray Fluorescence (energy dispersive, kα)	1.06 ng	-	78
Neutron Activation Analysis ($^{59}Co(n, \gamma)^{60}Co$)	0.5	10 mL	79
Biological Assay (Rhizobium meliloti)	0.005[1]	5 mL	80
Anodic Stripping Voltametry (pre-electrolysis time, 10 min)	3	-	81

[1]Based on incubation period of 47 hours.

peroxide is slightly more acidic than water with a pK_a of 11.85. It acts as a strong oxidizing agent at all pH's (63), but in basic solutions the oxidation takes place much faster.

Hydrogen peroxide solutions are most stable when the concentration is high and the pH is in the range 4-5 (82). The solutions are best stored in metal-free polyethylene, Teflon or brown borosilicate glass containers (82). This reagent is unstable with respect to heat.

The standard reduction potentials for the H_2O_2-oxygen couple and the water-H_2O_2 couple are shown in Table VI (82). The formal reduction potentials in unit molal base for the perhydroxyl ion are also listed (82).

The decomposition of H_2O_2 solutions has received considerable attention. The overall reaction can be written:

$$2\ H_2O_2 \rightleftharpoons 2\ H_2O + O_2 \qquad (3)$$

in which both oxygen atoms in the O_2 molecule are derived from the hydrogen peroxide molecule (63). Many metals are known to catalyze the decomposition and some are active as both heterogeneous and homogeneous catalysts. Non-metallic catalysts include Cl^-, Br^-, I^-, Se, and As (82). Ionizing radiation and UV radiation (200-400 nm) also cause H_2O_2 to decompose. The mechanisms of decomposition reactions have been studied extensively and some will be briefly

Table VI. Standard and formal reduction potentials for hydrogen peroxide.

Half Cell Reaction	Standard or Formal Reduction Potential (V)
$O_2 + 2H^+ + 2e^- \rightleftarrows H_2O_2$	$E^o = 0.693$
$H_2O_2 + 2H^+ + 2e^- \rightleftarrows 2H_2O$	$E^o = 1.76$
$O_2 + H_2O + 2e^- \rightleftarrows OH^- + HO_2^-$	$E' = -0.084$
$HO_2^- + H_2O + 2e^- \rightleftarrows 3OH^-$	$E' = 0.87$

reviewed according to their applicability to the lucigenin reaction and Co analysis.

In the simplest case, acids and alkali have been reported to increase the decomposition rate of H_2O_2. Acidification with phosphoric, hydrofluoric, perchloric, or sulfuric acid causes hydrogen peroxide decomposition and the increasing rate of decomposition with decreasing pH is independent of the acid anion (82). Nitric acid also causes accelerated decomposition, but in this case, the nitrate ion appears to be directly involved in the reaction (82).

The kinetics of the decomposition when H_2O_2 solutions are made basic have been studied extensively. This work is difficult to carry out because of the necessity to totally eliminate metals in the system because catalysts generally exert their greatest effect at higher pH's. The reaction has been shown to be heterogeneously catalyzed by some glass containers (83, 84). This problem has been overcome by the use of polyethylene and paraffin lined reaction vessels.

Duke and Haas (84) studied the decomposition reaction in aqueous basic solutions and found that the maximum rate occurred when the H_2O_2 was 50% ionized, that is, when the H_2O_2 concentration equals that of the perhydroxyl ion (HO_2^-). Thus, the maximum rate was at the pH which corresponds to the pK_a value of H_2O_2. Their mechanism, rate law expression, and rate constant are shown in Figure 11.

$$H_2O_2 + OH^- \rightleftarrows HO_2^- + H_2O$$

$$H_2O_2 + HO_2^- \xrightarrow{rds}$$

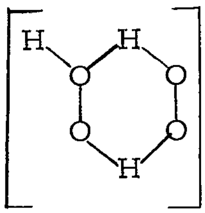

$$\longrightarrow H_2O + O_2 + OH^-$$

$$\frac{-d[H_2O_2]_{total}}{dt} = k[H_2O_2]\,]HO_2^-]$$

$k = 2.65$ L/mole-hr (35°C)

Figure 11. Mechanism, rate law, and rate constant proposed by Duke and Haas (84).

Goodman and Robson (85) concurred with the above observations after their study of the uncatalyzed decompositions of peroxymonosulfuric acid and H_2O_2. Both systems exhibited the same form for their rate law equation and the rate had its maximum when the starting species was 50% ionized. This led them to propose a general mechanism for the decomposition of peroxy-compounds.

The work of Koubek et al. (86) cast some doubt on the validity of earlier work when they studied three peroxy compounds as well as H_2O_2. For the organic acids (peroxoacetic, peroxochloroacetic, and peroxomonophosphoric), the rate law assumed the form given by Duke and Haas and the features of the reaction, as far as the optimum pH equalling the pK_a, were the same. However, the rate of H_2O_2 decomposition was about 1/100th of the rate reported previously. The rate was so slow that reliable kinetic data could not be obtained. Koubek et al. attributed this result to the fact that they had more effectively purified their sodium hydroxide. Duke and Haas (84) purified concentrated sodium hydroxide solutions by coprecipitating the metals, using Fe and Mg as carriers. The solid metal hydroxides were then filtered out and the Fe remaining in the filtrate was extracted. Apparently, Goodman and Robson followed this same procedure but Koubek et al. used only Mg as a carrier. Thus, it appears that early studies of the uncatalyzed decomposition were in fact metal catalyzed. In highly purified basic solutions, H_2O_2 may

not decompose at an appreciable rate. A literature search indicated that no more mechanisms have been advanced for the homogeneous decomposition of hydrogen peroxide in aqueous solutions.

The metal catalyzed decomposition reaction has been studied by numerous authors and because the lucigenin reaction is carried out at high pH's (11-14) the heterogeneous decomposition should be considered. A qualitative indication of the relative catalytic activity of solid metal hydroxides is given in Schumb et al. (82). This study shows that Pb, Ag, Co, and Os are among the most active in the group of 11 metals studied. These same metals also enhance the lucigenin reaction to the greatest extent, hence, it was logical for investigators to attempt to correlate their effects. No conclusive correlation has been demonstrated, however, as discussed in the Mechanism section. Radiotracer methods have shown that when H_2O_2 is added to a solution of Mn(II) and colloidal MnO_2 the H_2O_2 is catalytically decomposed and complete exchange takes place between the Mn in the two phases (87). When the experiment was repeated with Co(II) and solid cobaltic hydroxide (which probably exists as $Co_2O_3 \cdot x H_2O$), H_2O_2 decomposition again occurred but there was no exchange of Co between the two phases (87).

In the area of homogeneous catalysis, a wide variety of studies have been reported. The Co catalyzed decomposition will be considered in some detail, but for the other elements it is sufficient to

say that nearly all transition metals have been shown to catalyze the reaction. Schumb et al. (82) contains references for work prior to 1955 but unfortunately, a newer H_2O_2 monograph with this type of data has not been prepared.

Three studies have been carried out in which the reaction between a Co(III) complex and H_2O_2 in an aqueous perchloric acid medium were examined (88, 89, 90). These systems involved quite acidic conditions and hence their applicability to the Lc reaction, which takes place under basic conditions, is very limited and they will not be discussed. Bobtelsky and Simchen (91) examined the decomposition of H_2O_2 by Co-citrate complexes. The complex was found to exist in two forms; a pink complex which is stable in solution and a green complex which is formed when H_2O_2 is added to a solution of the pink complex. The appearance of the green complex results in rapid decomposition of H_2O_2 and it was shown that the greatest rate occurred when there was a ratio of 1:1:1 for Co(II), citrate, and H_2O_2. No rate law was proposed for the reaction but it was pointed out that Cu, Mn, Ni, Pb, Al, Mg, Cd, and Zn-citrate complexes are all poor catalysts for the decomposition of H_2O_2.

In one paper related to the reaction of a Co(III) complex and H_2O_2 in a perchloric acid medium, a dinuclear Co species was advanced as a possible intermediate (90). Some time earlier Reibel studied a series of dinuclear Co(III) complexes and their effect on the

the decomposition of H_2O_2 (92). He included the aqueous Co(II) ion and studied the decomposition from pH 1 to 12. The rate law he proposes applies only to the dinuclear complexes, but from his data some features of the kinetics for the aqueous Co(II) ion are apparent. First, the rate of H_2O_2 decomposition is linearly related to the Co(II) concentration from 10^{-4} to 1.6×10^{-3} M. At the same molar concentration, other dinuclear Co(III) complexes produced larger and smaller decomposition rates. In the pH study, H_2O_2 decomposition was not observed for solutions which contained Co(II) at a pH of less than 7. When the pH of these solutions was increased from 7 to 12.5, the decomposition rate increased up to pH 11 and then leveled off. The dinuclear Co(III) complexes were able to catalyze the decomposition at pH's as low as 1. Experiments with methyl methacrylate indicated that the decomposition of H_2O_2 is not a free radical process when aqueous Co(II) ion is present or for any of the dinuclear species studied.

Thus, it is clear that the mechanism of the catalytic decomposition of H_2O_2 by Co is not known. It may be some time before this reaction is as well understood as the Fe catalyzed decomposition reaction.

Instrumentation for Chemiluminescence

CL and BL instrumentation is simple and the common configurations for measurement of the luminescence signal are shown in Figure 12. All require a light-tight sample module which contains a cell in which the sample and reagents are mixed and a means of measuring the radiant power emitted during the reaction. The measurement can be the instantaneous intensity, the peak height, the integrated intensity, or the integral between selected times. Early workers used the photographic detection system (Figure 12a) and hence measured the total integrated CL by desitometer analysis of the film. More recently phototubes or photomultiplier tubes (Figure 12b) have been used in place of photographic plates. Generally, this improves the detection limit for most systems and increases the speed of analysis. The signal modifier consists of a current-to-voltage converter and a peak detector or integrator in more complex systems.

The instrumentation shown in Figure 12c utilizes a monochromater so that a CL spectrum may be obtained by running samples at a number of different wavelengths and making a composite spectrum. The double beam feature is needed if the total CL for each sample is different. Some workers use a fluorometer (with the excitation source masked) and scan the emission monochromater over a small

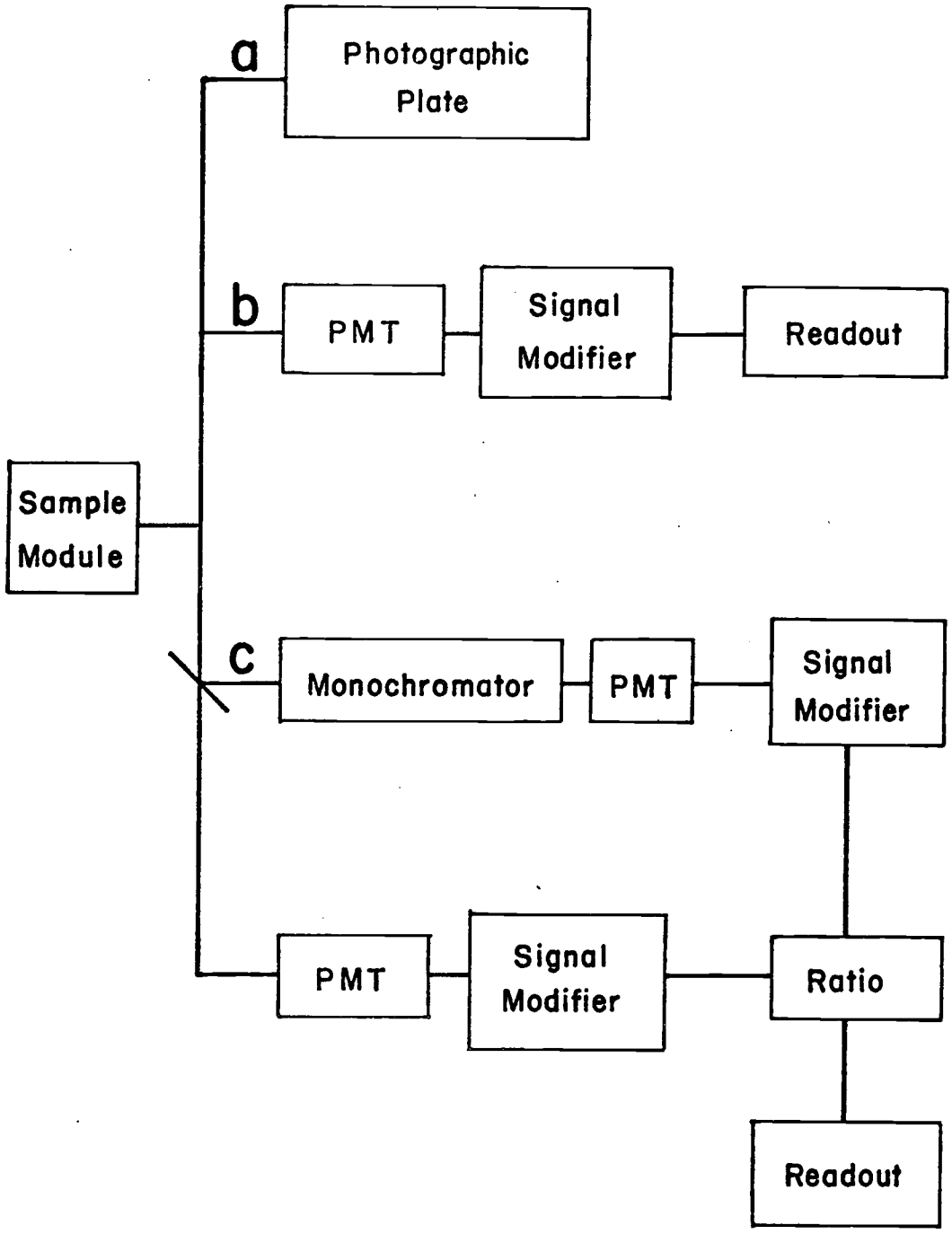

Figure 12. Instrumental configurations for measuring CL.

wavelength range. A linear diode array can be used to obtain CL spectra quickly.

The three types of sample modules that have been developed are the discrete sampling system, the flow system, and the centrifugal analyzer. In the discrete sampling system, all reagents except one are placed in a reaction cell in front of the PMT. A lid is placed over the reaction cell, the last solution needed to initiate the reaction is injected into the sample cell with a syringe, and the photocurrent output is measured as peak height or peak area. In the flow system, the reagents and analyte are continuously pumped through a reaction chamber. This means the integral of the light intensity for the time spent in the reaction chamber is measured. The centrifugal analyzer uses a spinning action to mix the samples, and then measures them as they pass a PMT. The advantages and limitations of each system have been described previously (8).

CL Determination of Cobalt

Gleu and Petsch (52) noted in the original paper describing the chemiluminescent reaction of lucigenin and H_2O_2 that addition of OsO_4 appeared to catalyze the reaction because it increased the intensity of the CL and decreased its duration. Co appears to be an equally effective catalyst and analyses based on the enhancement of the lucigenin CL by Co have been reported.

The first such article by Bognar and Sipos (93) relied on the visual comparison of the CL intensity of several simultaneous reactions to determine the Co concentration. The CL of the sample and several standards were initiated in glass comparator tubes (in a darkened room) and then an estimation of which standard solution most closely matched the intensity of the sample was made. The detection limit for Co was 200 ppb and the linear range extended up 10 ppm. Several elements, which also enhance the lucigenin reaction, were reported as interferents.

Babko et al. (35) surveyed a number of metals to determine what their respective detection limits were in the Lc + H_2O_2 system. A PMT was used to detect the resulting CL in a discrete sampling system. The detection limits and optimum conditions for different metals are shown in Table VII. The detection limit for Co was 0.5 ppm.

The most recent paper for Co determination via lucigenin CL appeared in 1974 (7). Dubovenko and Beloshitski used photographic plates to measure the CL from transparent cells placed directly on the plate. With an exposure time of 5 minutes, the detection limit for Co was 1.4 ppb and the linear range of the calibration curve extended up to 14 ppb. The optimum lucigenin, H_2O_2, and KOH concentrations for CL Co determinations are shown in Table VIII. The reported interferents are also listed.

Table VII. Optimum conditions for metal determination via Lc CL.

	Lc[2]	H_2O_2[2]	Final pH	Detection Limit (ppm)[3]	Reference
Co(II)[1]	1×10^{-6}	1×10^{-4}	13	0.5	35
Ni(II)[1]	1×10^{-6}	1×10^{-4}	13	200	35
Mn(II)	1×10^{-6}	4×10^{-2}	13	1	25
Ag(I)	7×10^{-7}	7×10^{-2}	13.5	0.2	27
Os(VIII)	-	-	10.3	0.001	29
Tl(III)	2×10^{-5}	2×10^{-2}	12.5	0.1	30
Pb(II)	5×10^{-6}	3×10^{-2}	11.5	0.2	31
Bi(III)	2×10^{-6}	1×10^{-1}	12.3	1	34
Cu(II)	-	-	>14	0.5	36
Ce(III)	3×10^{-6}	3×10^{-3}	>14	1	37
Cr(III)	1×10^{-6}	5×10^{-3}	9.5	0.005	38
Fe(II)	-	-	12.6	0.006	39

[1] Lc and H_2O_2 concentrations not optimized for each individual metal. Optimum conditions for Co(II) analysis in Table VIII.

[2] Concentration in moles/l at final cell volume.

[3] Concentration of the metal at final cell volume, this may be 25-50 times greater before metal solution added to sample cell.

Table VIII. CL methods for Co analysis.

System	Conditions[1]	Detection Limit[1] (ppb)	Known Interferences	Reference
Lc+ H_2O_2 + KOH + Co	Lc; 1×10^{-5} M H_2O_2; 5×10^{-3} M final pH; 13.5 discrete system	1.4	Tl, Fe, Ni, Ag, Bi, Cu, Cr, Os, Ce, Mn, Pb	7
Luminol + H_2O_2 + KOH + Co	Luminol; 1×10^{-3} M H_2O_2; 1×10^{-2} M final pH; 11.4 flow system	0.12	Al, Sn, Pb, Bi, Cr, Fe, Cu, Zn, Ag, Mn, Ce	3, 95
Gallic acid + H_2O_2 + NaOH + Co	Gallic acid; 2×10^{-2} M H_2O_2; 3×10^{-3} M final pH; 12.2 flow system	0.4	Pb, Cu, Ag, Mn	6

[1] Lc, H_2O_2, and Co concentrations are before introduction of the solution into the sample cell.

As mentioned in the introduction, Co analysis based on the enhancement of the reaction of luminol and H_2O_2 have been reported. The specification of the best detection limit and optimum conditions for the determination of Co are, however, somewhat ambiguous for several reasons. The first is that the original paper which deals with the determination of Co in the absence of other metals is fairly old (1963) and relies on photographic plates to measure the CL (5). The reported detection limit for Co in this paper is 40 ppb (5).

The second reason is that Seitz and Hercules (3) reported the detection limit for Co as 0.6 pptr (parts per trillion) in a flow system. They pointed out, however, that this value was based on extrapolation of data obtained at much higher concentrations. Unfortunately, this value has been perpetuated in subsequent articles by these and other authors, making it seem that the detection limit for Co in the luminol system is about 1/1000th that in the lucigenin system. The belief that this detection limit of 0.6 pptr is unreasonably low is based on examination of some luminol papers. These papers also provide a good estimate of the detection limit for Co in this system.

Hartkopf and Delumyea (94) described a chemiluminescent metal ion detector for liquid chromatography based on the reaction of the eluted metals with luminol and H_2O_2. No detection limit for Co(II)

was reported, but the lowest concentration actually determined was 60 ppb.

Sheehan and Hercules (95) constructed a flow system for the determination of vitamin B_{12}. The apparatus incorporated a Jones reductor to reduce the Co(III) of the B_{12} molecule to Co(II). The Co was then able to react with luminol and H_2O_2 and the resulting CL was detected with a PMT. The detection limit for vitamin B_{12} was reported as 2.7 ppb which works out to 0.12 ppb Co. This value will be representative for the detection limit only if the following two assumptions are true: the conversion of Co(III) to Co(II) by the Jones reductor is complete, and the remnants of the B_{12} molecule present in the solution do not affect the reaction between Co(II) and the CL reagents.

An indication of the ability of Co to enhance the luminol reaction can be obtained by examination of data which show the magnitude of the CL signal when Co and another metal are both present in a solution. In a study of the determination of Cr via luminol CL, Seitz et al. reported the relative CL peak height for three Cr-Co mixtures (96). The Cr(III) concentration in all three solutions was 5.2 ppb and the Co concentration was 5.9, 17.7 and 29.6 ppb. The relative CL signals observed for these solutions (Cr(III) alone = 100 units) were 125, 175, and 219 units, respectively. Extrapolation of a log-log plot shows that at a concentration of 3 ppb Co all of the observed

signals can be attributed to Cr(III) present in the solution. Assuming that Co and Cr exert their catalytic effect independently, it follows that the detection limit for Co is about 3 ppb. If this same assumption is true for mixtures of Fe(II) and Co(II), a paper by Seitz and Hercules (97) for Fe analysis via luminol CL can also be used to estimate the Co detection limit. Data in this paper show that when the Co concentration has decreased to 1.5 ppb it no longer has an effect on the determination of 2 ppb Fe(II).

The flow cell system for Co determination described by Seitz and Hercules (3) is the same as that described in the other two references for Cr(III) and Fe(II) analyses (96, 97). The optimum reagent concentration is similar for each system so accordingly these values are shown in Table VIII. The lowest detection limit, in light of the preceding discussion, is nominally 0.12 ppb Co and the interferences are those from reference 94.

The final chemiluminescent system for Co analysis is gallic acid (6). The technique is based on the enhancement of the gallic acid + H_2O_2 reaction by Co(II). The instrument is the flow cell type with a PMT as the light detector. The optimum pH and other reagent conditions are shown in Table VIII along with the reported interferences. It should be noted that the gallic acid system is more specific for Co since it has fewer interferences. This is a disadvantage, however, in applications where CL is used as the

basis for metal detection following chromatographic separation (94, 98, 99).

PROCEDURE

Analysis Procedure

The basic injection procedures used during these studies are outlined below. With the shutter closed and the lid of the sample module raised, 1.0 mL of water is added to the sample cell with an Eppendorf pipet (Catalog No. 22 35 070-6). This is followed by 0.5 mL portions of H_2O_2 and Lc, each solution being delivered by a 0.5 mL Eppendorf pipet (Catalog No. 22 35 080-3). The lid is lowered, the shutter opened, and 0.5 mL of KOH is injected through the rubber septum into the cell by the precision liquid dispenser. The CL signal is recorded and then the shutter closed. The lid of the sample module is raised and the sample cell solution removed by suction with a glass, disposable pipet connected to a vacuum aspirator bottle. The sample cell is rinsed four times using Millipore water in a polyethylene wash bottle. When necessary, the insoluble reaction product is removed from the interior surface of the cell by filling it with 50% (V/V) HNO_3 for 5 minutes. When this is completed, the HNO_3 is removed via aspiration and the cell rinsed about 20 times with Millipore water. This same cell cleaning procedure is repeated if a series of Co solutions whose concentration is greater than 1 ppb has been run. This eliminates memory effects in the system.

The above injection procedure constitutes a blank run since the CL signal produced is that which occurs in the absence of added metal catalysts. A metal run is accomplished by substituting 1.0 mL of a metal solution for the 1.0 mL of water which was initially placed in the cell. The H_2O_2, Lc, and KOH are then added in the same manner as a blank run. Since many metal solutions were acidic, it was necessary to run an acid blank to account for any effect the contaminants in the acid of for the slight change in final pH of the reaction solution. This was done by substituting 1.0 mL of water of the same pH as the metal solution for the 1.0 mL of water in a blank run, and then adding the other reagents as usual.

It should be noted that the volumes of reagents employed during the optimization and interference studies were different from that described above. In these experiments, the initial 1.0 mL of water of a blank run was split into two 0.5 mL portions. In metal runs, the first solution to be added to the cell is 0.5 mL of the metal, followed by an equal amount of water. In blank runs, 0.5 mL of water replaced the 0.5 mL of metal solution so these runs are exactly as described initially. Volumes of the other reagents were unchanged. The purpose of this change was to permit the addition of two metal solutions to the cell at the same time without premixing any two reagents or adjusting the volumes of the H_2O_2, Lc, or KOH. The total solution volume in the cell was always 2.5 mL.

Another important change that took place during this study was the installation of the precision liquid dispenser. With this device, it was no longer necessary to use a 0.5 mL Hamilton gas tight syringe (Catalog No. 175 OLTN) to inject the KOH into the cell. The outlet of the dispenser is a one mm (i.d.) polyethylene tube joined to a syringe needle. The needle was securely lodged in the rubber septum so that the KOH was injected reproducibly into the center of the sample cell.

The output on the chart recorder with the optimum mixing order and reagent concentrations is shown in Figure 13. In a blank run, a quick initial peak is observed as soon as the KOH is injected and this is followed by a second peak. Observable CL continues for about an hour, but the run is terminated as soon as the second peak has appeared. It is apparent from Figure 13 that the difference between the height of the second peak for the blank and Co run is proportional to the Co concentration and, as the Co concentration increases, the peak time (time from injection of the base to appearance of the second peak) decreases. At higher Co concentrations, the second peak is so large and peak time so short that only a single peak is observed. Even so, the height of this peak above the second peak of the blank is proportional to the Co concentration.

The blank signal (height of second peak) tends to drift over a period of a few hours and its value for successive runs is not

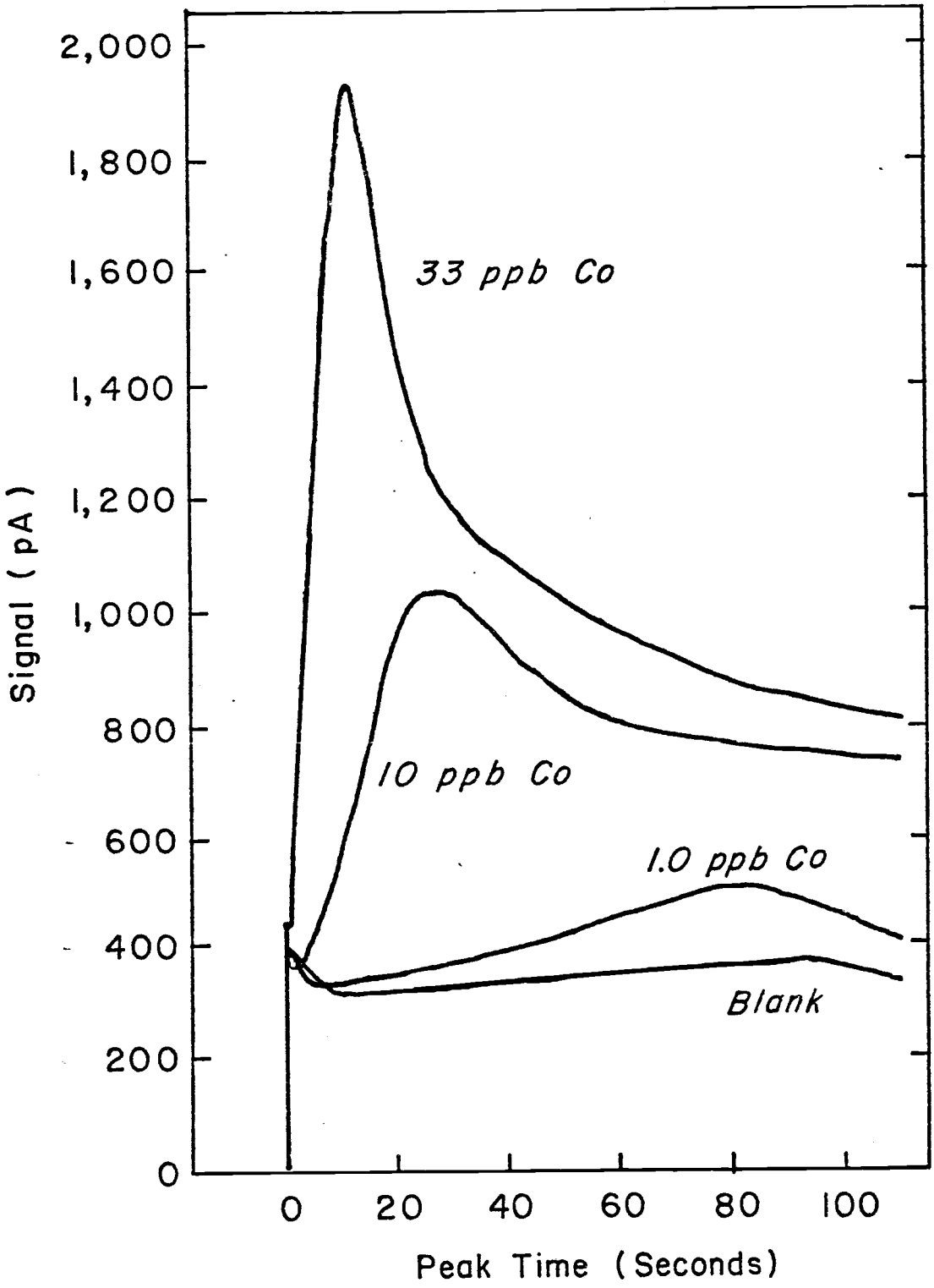

Figure 13. Peak shapes of blank, 1.0, 10, and 33 ppb Co.

constant. Therefore, it is necessary to make three blank runs, three metal runs, and then three more blank runs in order to obtain the analytical signal (the difference between the metal signal and its blank). The three blank values that preceed the metal runs are averaged and this value is averaged with the average of the other three blank runs. The average blank signal was then subtracted from the average of the three metal runs to yield the analytical signal for the metal solution. The peak area can be measured using the available peak integrator, but in practice this output mode was used only slightly. The bias voltage of the PMT was either 760 or 800 V for the majority of this study.

Solutions

All solutions were prepared with water from either a Corning still (Model AG-3) or a Millipore (Milli-Q) reagent-grade water system. The feed water for both systems was central distilled water. Millipore water was used almost exclusively once this unit was operational because it can deliver water faster and with a greater resistivity than the Corning still. The resistivity of Millipore water used to prepare solutions or to clean glassware was at least 17 megohm-cm.

Lc stock solution was prepared by dissolving 0.1276 g of N,N'-dimethylbiacridinium dinitrate (K & K Laboratories, M.W. = 510.5)

in 1.0 L of water. This gives a solution of 1.89×10^{-4} M Lc whose pH is about 5.5. The solution was then diluted by a factor of four on a daily basis to provide a working concentration of 4.73×10^{-5} M. Generally, 100 mL of this solution was sufficient for a day's work and fresh dilutions of the stock solution were prepared each day. An additional stock solution was prepared later in the study whose concentration was 2.19×10^{-3} M (0.7385 g Lc dinitrate in 1.0 L water). A 1:46 dilution of this solution gives a working solution of 4.76×10^{-5} M, and these were prepared using a 1.0 mL Eppendorf pipet and a 50 mL L/I Repipet dispenser (Catalog No. 3050-A-L). When it was necessary to prepare Lc working solutions whose concentration was 6.84×10^{-5} M, 1.0 mL of the 2.19×10^{-3} M stock solution was mixed with 31.0 mL of water dispensed by the Repipet dispenser.

The Lc stock solution was initially stored in a 1 L polyethylene bottle in a refrigerator to retard decomposition. This was not necessary, however, as unrefrigerated stock solutions are stable for at least 9 months. Polyethylene and glass are acceptable materials for storage containers. The only precaution that needs to be mentioned is that Lc solutions must not be made basic as this rapidly deactivates them.

H_2O_2 solutions were prepared by dilution of unstabilized, reagent grade, concentrated H_2O_2 (Mallinckrodt #5240). The 0.10 M solutions were prepared by weighing out 11.34 g of 30% (w/v) H_2O_2

and diluting to 1.0 L. Before filling to the mark, the pH of the solution was adjusted to 4-4.5 with dilute HNO_3. The solution was then separated into four 250 mL polyethylene bottles and the bottles were refrigerated until needed and experience showed they were stable for at least 3 months. When a bottle was removed from the refrigerator for use, it was not returned and the reagent was stable for at least 3 weeks at room temperature. The concentrated 30% H_2O_2 was always kept refrigerated.

An attempt was made to purify 1 L of a 0.10 M H_2O_2 solution via electrodeposition, using an ESA Reagent Cleaner (Model 2014 PM). A potential of -1.4V was maintained across the deoxygenated H_2O_2 solution for 5 hours to electrodeposit metals into a Hg pool. The H_2O_2 solution was then removed and used to run a blank reaction. The blank signal (height of second peak) was the same for the "purified" solution and the starting material so the purity of the H_2O_2 solution was acceptable.

The 5.0 M KOH solution was prepared by dissolving 330.1 g of reagent grade KOH (Mallinckrodt #6984) in 1.0 L of water. The solution was transferred from the volumetric flask to a 1 L polyethylene bottle and kept at room temperature. J. T. Baker reagent grade KOH (#3228) was found unacceptable because it produced a larger than normal blank signal. Some lots of Mallinckrodt KOH were also not usable for this same reason so it was necessary to compare newly

purchased material against known good solutions. Comparison of the blank signal for an acceptable lot of Mallinckrodt KOH against E. Merck Suprapur NaOH (#6466) showed no difference. Purification of 5 M KOH made from acceptable lots of Mallinckrodt was attempted using the ESA reagent cleaner and conditions described above. No improvement was seen, but it is possible to purify solutions made from rejected Mallinckrodt lots to the point that they are the same as solutions made from acceptable lots.

A 200.4 ppm Co stock solution was prepared by first dissolving 0.2004 g of Co metal (in shot form) in about 35 mL of dilute HNO_3. This solution was quantitatively transferred from the beaker to a volumetric flask and diluted to 1.0 L. The pH of the solution was adjusted to 1.0 using dilute HNO_3. Two additional stock solutions were prepared, 10 ppm and 100 ppb, from this solution, but their pH was adjusted to 2.0. When stored in glass containers at these pH's all the Co solutions were stable. Working solutions were prepared easily from these stock solutions with the use of Eppendorf pipets and a 10 mL L/I Repipet dispenser (Catalog No. 3010-A-L). This dispenser was filled with Millipore water adjusted to pH 2.0 with HNO_3 so that all Co solutions would be at the same pH.

Metal solutions for the interference study were prepared using the compounds and procedures found in the "Handbook of Flame Spectroscopy" (100). The acidity of transition metal solutions was kept

at approximately pH 1 and an acid blank solution was always prepared which had the same concentration of acid as the metal solution. All materials were analytical reagent grade or better, and when the recommended primary standard was not available, an appropriate reagent grade compound was substituted for it. Table IX lists compounds which were used in place of the prescribed primary standard compounds. Complexing agents and some common anions were also investigated in the interference study. The compounds used in their preparation are shown in Table X.

Precautions for Trace Analysis

All glassware in this study was cleaned according to the following procedure:

1. The vessel was cleaned using a laboratory detergent (Alconox or Micro) and rinsed with house distilled water.
2. The vessel was filled with a solution of about 0.1 M $KMnO_4$ and 10% H_2SO_4 and left standing 24 hours.
3. The MnO_2 on the interior surface of the glass was removed with concentrated HCl and the vessel rinsed three times with Millipore (or twice distilled) water.
4. The vessel was rinsed with 50% HNO_3 and then rinsed three more times with Millipore water.

Table IX. Compounds substituted for the recommended primary standards.

Element	Compound	100 ppm Metal Solution Matrix
Be	BeO	0.12 M HCl
Ti	$Ti(SO_4)_2 \cdot 9H_2O$	0.12 M HCl
Ga	$GaCl_3 \cdot 6H_2O$	0.12 M HCl
Rb	$RbCl$	H_2O
Zr[1]	$ZrCl_4$	0.12 M HCl
Mo	$Na_2MoO_4 \cdot 5H_2O$	0.12 M HCl
Rh	$RhCl_3 \cdot 3H_2O$	0.24 M HCl
Pd	$PdCl_2$	0.12 M HCl
Pr	$PrCl_3 \cdot 6H_2O$	0.12 M HCl
Hf[1]	$HfCl_4$	0.12 M HCl
Os	OsO_4	0.12 M HCl
Ir	$K_3IrCl_6 \cdot 3H_2O$	0.12 M HCl
Bi	$Bi(NO_3)_3 \cdot 5H_2O$	0.12 M HCl
U	$Na_2U_2O_7$	0.02 M HNO_3
Y	$Y(NO_3)_3$	0.02 M HCl
Lanthanides[2]	$X(NO_3)_3$	0.02 M HNO_3

[1] These solutions were prepared by diluting commercial 1,000 ppm stock solutions (Alfa-Ventron).

[2] These solutions prepared by diluting 1,000 ppm stock solutions (made from the appropriate nitrate) provided by Dr. R.A. Schmitt of Oregon State University: Nd, Sm, Gd, Tb, Ho, Er, Tm, Yb, Lu.

Table X. Compounds used to prepare anion and complexing agent solutions.

Species	Compound
NO_3^-	$NaNO_3$
SO_4^{2-}	K_2SO_4
NH_4^+	$(NH_4)_2SO_4$
PO_4^{3-}	K_3PO_4
ClO_4^-	$LiClO_4$
S_2O_8	$K_2S_2O_8$
CO_3^{2-}	K_2CO_3
HCO_3^-	$NaHCO_3$
OCl^-	5% NaOCl solution
CH_3COO^-	KCH_3COO
$C_2O_4^{2-}$	$K_2C_2O_4 \cdot H_2O$
EDTA	$Na_2H_2EDTA \cdot 2H_2O$
TBP	liquid TPP
Acac	liquid Acac

Plastic beakers and bottles were cleaned by filling them with hot 50% HNO_3 and letting them sit 24 hours. They were then rinsed three times with Millipore water. Polyethylene bottles and glass volumetrics were stored filled with Millipore water and all beakers and flasks were stored upside-down or covered to keep out dust.

When it was necessary to reclean a vessel, generally a rinse with 50% HNO_3 followed by three Millipore water rinses was sufficient. Occasionally, it was necessary to resort to the initial cleaning procedure for some items.

The plastic tips for Eppendorf pipets were cleaned by individually dipping them into 50% HNO_3 such that solution completely filled the tip. The tips remained in the acid for 20 minutes and were then transferred to a large, plastic jar. The tips in the jar were rinsed six times with Millipore water and placed into clean, covered beakers and dried in an oven at 100°C. Storage of these tips was in plastic bags and they were removed in a way that minimized contamination.

At the beginning of this study, Eppendorf pipets were placed in large test tubes (16 x 145 mm) between runs, but this was unsuitable due to contact between the side of the pipet tip and the inside of the test tube. This problem was eliminated with the construction of a Plexiglass pipet rack which ensured that the pipet tips did not contact anything once they were in the rack. Unlike some commercial pipet

racks, this rack prevents dust or liquids from reaching the pipet tip when the pipet is in place. The pipet rack (o) is shown in Figure 1.

The Lc, H_2O_2, and KOH working solutions were initially kept in 125 mL polyethylene bottles during CL runs. Contamination, however, proved to be a problem so 100 mL Eppendorf dual-chamber polyethylene bottles (Catalog No. 22 34 070-1) were used. These bottles have an upper chamber whose capacity is about 5 mL. A plastic tube connects the upper and lower chambers, and squeezing the bottle transfers the solution from the lower to the upper chamber. If contamination of the upper chamber occurs, it can be emptied and cleaned and then filled with uncontaminated solution from the lower chamber. An added advantage of these bottles is that it is easier to pipet from the upper chamber than from 125 mL polyethylene bottles.

When it was decided that the reagent bottles should be placed in the constant temperature bath, the dual-chamber bottles were replaced with small, glass weighing bottles. Three of these could be conveniently placed side-by-side at the front of the water reservoir and they were small enough that pipetting from them was easy. They contained the Millipore water for blank runs, the H_2O_2, and Lc solution. The KOH solution was always in a 125 mL polyethylene bottle and when the precision liquid dispenser was installed the 125 mL polyethylene bottle was partially submerged in the water bath. A plastic tube connected this KOH reservoir to the intake of the precision liquid

dispenser. The glass weighing bottles (q) and KOH reservoir (r) are shown in Figure 1.

RESULTS AND DISCUSSION

Optimization

Introduction

Many criteria were recognized as important in the optimization of the Lc system for Co(II) analysis. It is difficult to rank them in order of importance since compromises were made when two criteria conflicted. The criteria emphasized in this study were:

1. A low detection limit for Co(II) analysis.
2. Good analytical sensitivity (ability to differentiate between similar concentrations).
3. Freedom from interferences.
4. A linear calibration curve over a large concentration range (log-log plot).
5. Rapid analysis.
6. Good reproducibility of blank and Co(II) signals.
7. High signal to background ratio (S/B).
8. Using reagent concentration such that small changes in concentration do not significantly affect the metal or blank signals.

The appropriate calculations and definitions used in this section should be discussed. First, the analytical signal is the difference in height of the second peak of a blank and Co analyte run. Elements

which enhance the Lc reaction have positive analytical signals and those which inhibit have negative analytical signals. All analytical signals are referenced to the three blank signals which precede and follow the three metal signals. The S/B ratio is the ratio of the analytical signal to the blank signal. The standard deviation of the blank signal is computed using the following formula:

$$s_b = \sqrt{\frac{(n_1 - 1)s_1^2 + (n_2 - 1)s_2^2}{n_1 + n_2 - 2}} \qquad (4)$$

where s_1 is the sample standard deviation of the n_1 blank signals which preceded the metals signals and s_2 is the sample standard deviation of the n_2 blank signals which followed the metal runs. This pooled estimator properly weights s_b when n_1 is not equal to n_2. The units of s_b are pA. The detection limit (C_l) for this method is defined as:

$$C_l = \frac{2s_b}{|\text{slope}|} \qquad (5)$$

where the slope of the calibration curve is expressed in pA/ppm or pA/ppb. Because the calibration curve slopes exhibit positive or negative deviation with this method, the slope was always calculated near the detection limit.

It was recognized early in this study that this technique had a low detection limit for Co and so the predominant consideration was to maintain this low detection limit with a reasonable analysis time.

Interferences are an inherent problem with the Lc system and it is doubtful that they can be entirely eliminated without prior separation. A great deal of effort was directed toward improving the reproducibility of the blank and Co signals and this led to substantial improvements in the instrumentation and analysis procedures. The optimization of the reagent conditions and instrumental parameters, as well as the results for Co analysis, will now be covered.

Mixing Order

There are four possible mixing orders for a Co run, if it is considered that the solution injected last is added to a mixture of the first three reagents already in the sample cell. These were systematically investigated by observing the peak shape of the blank and a Co solution for all four mixing orders. Two different KOH concentrations were used and the peak shapes when the final pH is 12.5 are shown in Figure 14. These tracings indicate the peak shape for about the first minute of the CL reaction. The first three mixing orders are not acceptable for these reasons. When H_2O_2 is added last (Figure 14a), only a slight increase in the CL signal at the beginning of the reaction is seen and the detection limit would not be much lower than 5 ppb for Co. No effect was seen as the delay time (time from mixing the first three reagents in the sample cell to time the last reagent is injected) was increased.

Figure 14. Peak shapes for each possible mixing order (final pH 12.5).

Letter	Last solution added
a	H_2O_2
b	Co
c	Lc
d	KOH

Initial conditions

Lc, 5.0×10^{-5} M

H_2O_2, 0.10 M

KOH, 0.08 M

Co, 5.0 ppb

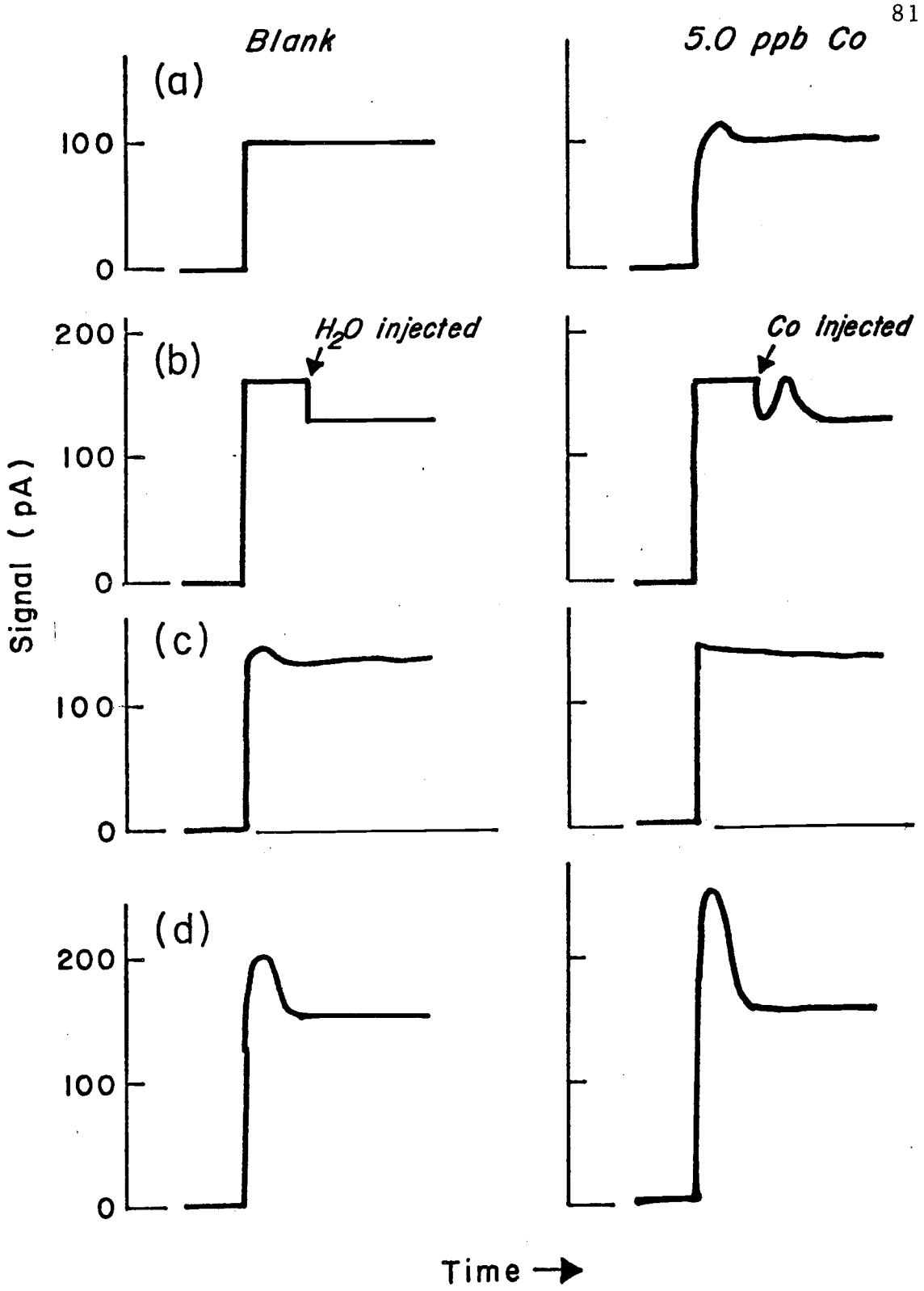
Blank
5.0 ppb Co
(a)
100
0
200
(b)
H_2O injected
Co injected
100
0
Signal (pA)
(c)
100
0
(d)
200
100
0
Time →

Figure 14

For the second mixing order (Co added last), a major disadvantage is that CL is occurring before the Co is injected into the cell (Figure 14b). The size of the Co peak was greatly affected by the speed of injection. A syringe was being used to inject this solution so it would be difficult to get reproducible peaks. The step decrease in the CL intensity when H_2O_2 is injected into the cell (blank run) is due to dilution of the solution in the sample cell.

In the third mixing order (Lc added last), a slight change in the peak shape is noticed, but no measurable effect can be attributed to the Co (Figure 14c). This does not rule out the possibility that at higher concentrations Co may have a measurable affect on the peak shape. A slight increase (10%) in the initial peak height of a Co run was noted when the delay time was increased from 10 s to 2 minutes.

The last mixing order (Figure 14d), where KOH is added last, was certainly the most promising since the height of the first peak increased as the Co concentration increased. The 5 ppb Co peak is about 5 mV above the blank and a 100 ppb Co solution gave a peak which was about 20 mV above the blank. However, it was discovered that Co analysis was more attractive at initial concentrations of KOH greater than 0.08 M (final pH 12.5) so mixing orders at this pH were not evaluated further.

Figure 15 shows the peak shapes for the same four mixing orders, but in this set the concentration of KOH at final cell volume was 2.0 M. Under these very basic conditions, it is possible to observe CL from the reaction of Lc and KOH in the absence of H_2O_2. This background reaction causes a small increase in the CL intensity before the last reagent, the H_2O_2, is added to the cell (Figure 15a). The effect of 5 ppb Co is to slightly increase the maximum signal above the blank, but this mixing order was determined to not be feasible for two reasons. The first is that the detection limit was not much lower than 5 ppb, and the second is that as the delay time increases the maximum signal decreases and hence, for good reproducibility, the delay time would have to be kept identical from run to run.

Adding the Co last (Figure 15b) is again not optimal for the same reasons as noted when this mixing order was studied at pH 12.5. There was too strong a dependence on the injection speed of the Co and it was felt that a mixing order which did not involve CL prior to the introduction of the last reagent would be better.

Injection of the Lc last initially appeared to be quite attractive because it offered the possibility of a low detection limit and rapid analysis time. As shown in Figure 15c, the very sharp peak for the Co run is about ten times greater than the blank. This peak and the blank peak increased as the delay time increases. A study to

Figure 15. Peak shapes for each possible mixing order (final KOH concentration 2.0 M).

Letter	Last solution added
a	H_2O_2
b	Co
c	Lc
d	KOH

Initial conditions

Lc, 5.0×10^{-5} M

H_2O_2, 0.10 M

KOH, 5.0 M

Co, 5.0 ppb

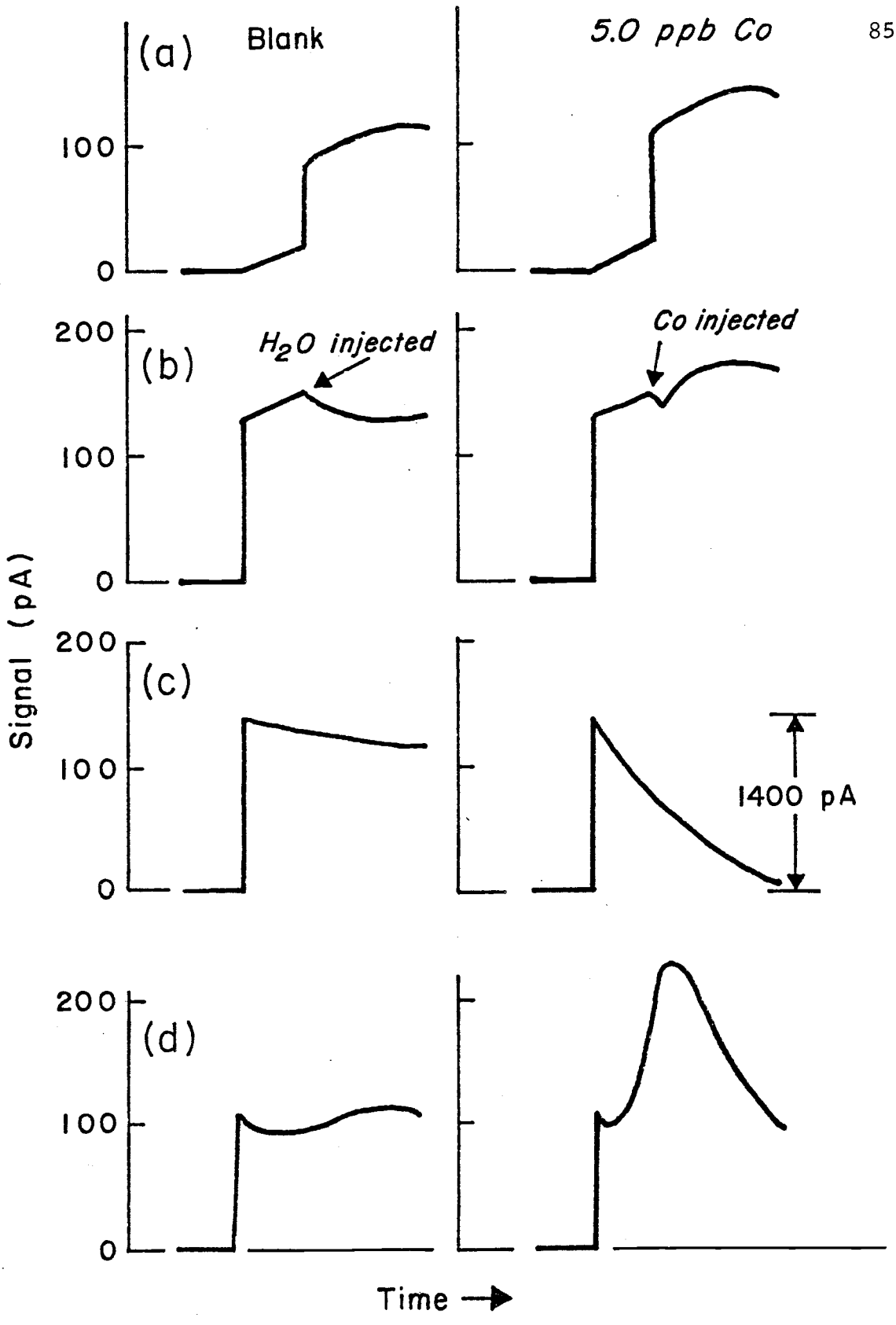
(a)
Blank
5.0 ppb Co
100
0
200
(b)
H_2O injected
Co injected
100
0
200
(c)
100
0
1400 pA
200
(d)
100
0
Signal (pA)
Time

Figure 15

determine the optimum delay time showed that the analytical signal increased as the delay time increased (up to 5 minutes) so a delay time of 90 s was employed. The disadvantage of having to reproduce the delay time would be outweighed by the achievement of a low detection limit. The detection limit under these conditions was 0.1 ppb, but the Co calibration curve on a log-log plot was linear only over about one order of magnitude above the detection limit. The major disadvantage of this particular mixing order is that the reproducibility of the blank and Co peaks was extremely poor. No procedures could be found to improve the reproducibility so the combination of this problem with the restrictive linear calibration range and 90 s delay time resulted in the abandonment of this mixing order.

When KOH is added last (Figure 15d), the effect of the Co is to increase the height of the second peak above the value it has for the blank and as the Co concentration increases the analysis time decreases (as shown in Figure 13). For Co concentrations of 30 ppb or greater, there was only one peak which appears in a matter of 5 s or less. At this KOH concentration, adding KOH last is certainly the optimal mixing order. It was used for all further studies because it offered a low detection limit (30 pptr), no delay time effect, and good reproducibility. This is the same mixing order that was used in the most recent paper on Co determination (7) via Lc CL. The order

of addition of the first three reagents was not important in this mixing order or in any other mixing order.

Optimum Lc Concentration

To find the optimum Lc concentration, a determination was made of the blank, 0.1, 1.0, and 10 ppb Co peak shapes for Lc concentrations from 2.2×10^{-7} to 2.2×10^{-3} M. Figure 16a is a log-log plot of the height of the second peak of the blank and 10 ppb Co versus the initial Lc concentration. The peak height is linearly related to the Lc concentration for the blank, that is, the slope is nearly one. In separate studies, it was found that the same linear relationship holds for the blank reaction when Lc or H_2O_2 is added last. No such simple relationship exists for the Co reaction. The curves for 0.1 and 1.0 ppb Co lie between the two curves in Figure 16.

Examination of Figure 16b, which is a log-log plot of the analytical signal versus the initial Lc concentration, shows that for 10 ppb Co analyses the optimum Lc concentration is about 2.2×10^{-4} M. The optimum Lc concentration range is rather large, however, and a variation by a factor of three from the maximum value does not affect it very much. The same behavior occurs for 0.1 and 1.0 ppb Co, with the optimum of the 0.1 ppb Co curve being even broader than for the other two Co concentrations (2.4×10^{-5} to 2.2×10^{-3} M).

Figure 16. Signal and analytical signal versus initial Lc concentration. Initial conditions: H_2O_2, 0.10 M; KOH, 5.0 M (final pH 14).

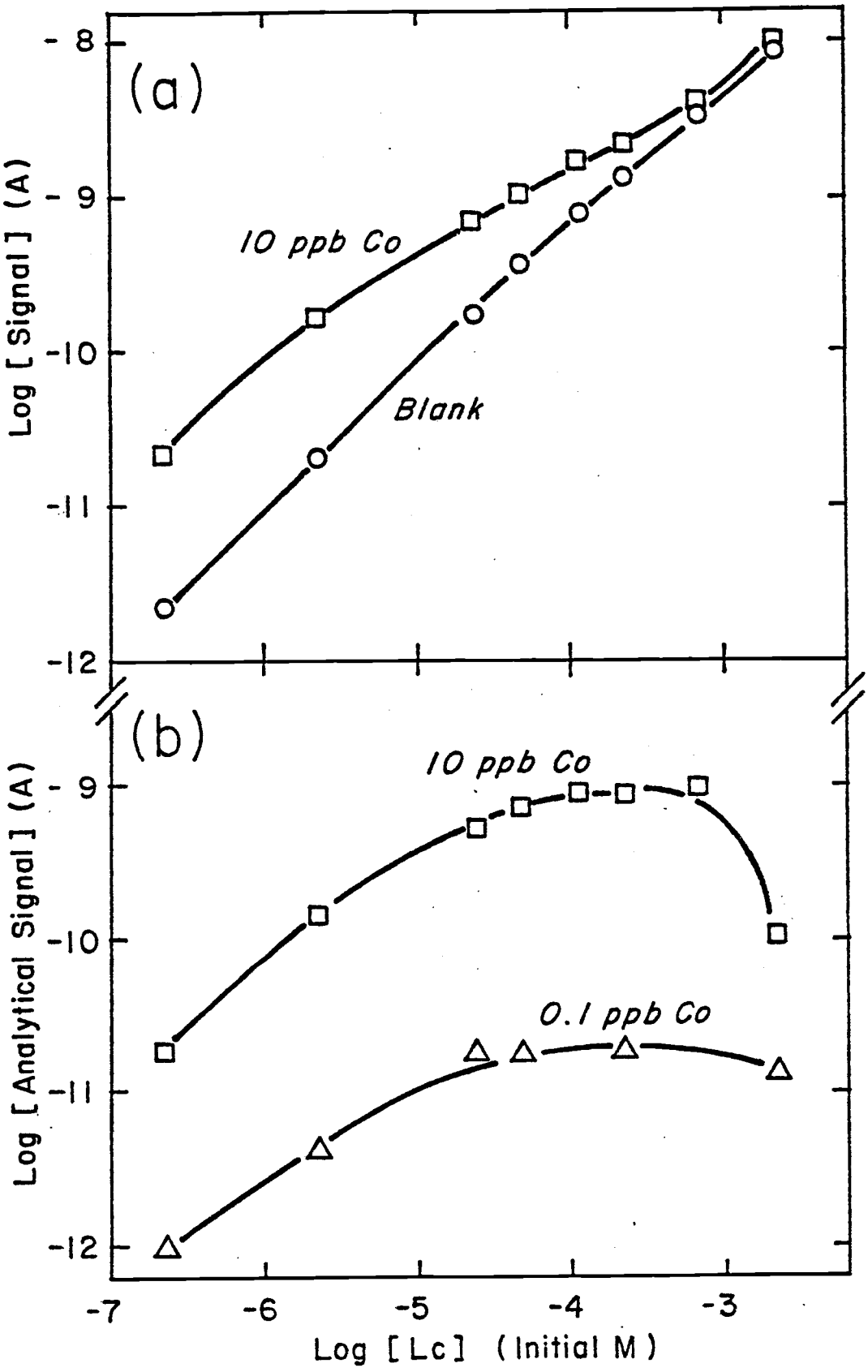
(a)
10 ppb Co
Blank
Log [Signal] (A)
- 8
- 9
-10
-11
-12
(b)
10 ppb Co
0.1 ppb Co
Log [Analytical Signal] (A)
- 9
-10
-11
-12
-7
-6
-5
-4
-3
Log [Lc] (Initial M)

Figure 16

Another criterion to be considered is the signal to background ratio (S/B) which is plotted (linear-log) in Figure 17 as S/B versus initial Lc concentration. The figure clearly shows that the optimum (largest) S/B ratio for 1.0 and 10 ppb Co analysis is at the lowest Lc concentration studied. The S/B ratio for 0.1 ppb Co changes less dramatically, but it does increase as the initial Lc concentration decreases. A mitigating factor in the choice of a low Lc concentration for analysis is that as the Lc concentration decreases the peak time for blank and Co runs increases. This is shown in Figure 18 which is a linear-log plot of peak time versus initial Lc concentration for the blank and 10 ppb Co runs. Under the best S/B ratio conditions, the peak time for the blank is 6 minutes and about 1.7 minutes for 10 ppb Co. This long of an analysis time for a single determination was clearly prohibitive since it is usually necessary to make three blanks before and after three Co runs in order to obtain the analytical signal. The longer the solutions are in the sample cell the more often it is necessary to perform a major cleaning of the cell (50% HNO_3 for 5 minutes followed by 20 water rinses) instead of just rinsing the cell with water between runs. At the optimum initial Lc concentration, based on the analytical signal (2.2×10^{-4} M), the peak time for the blank is about 47 s and about 13 s for 10 ppb Co. As expected from the S/B ratio data, the analytical sensitivity decreases as the Lc concentration increases. During these particular runs the

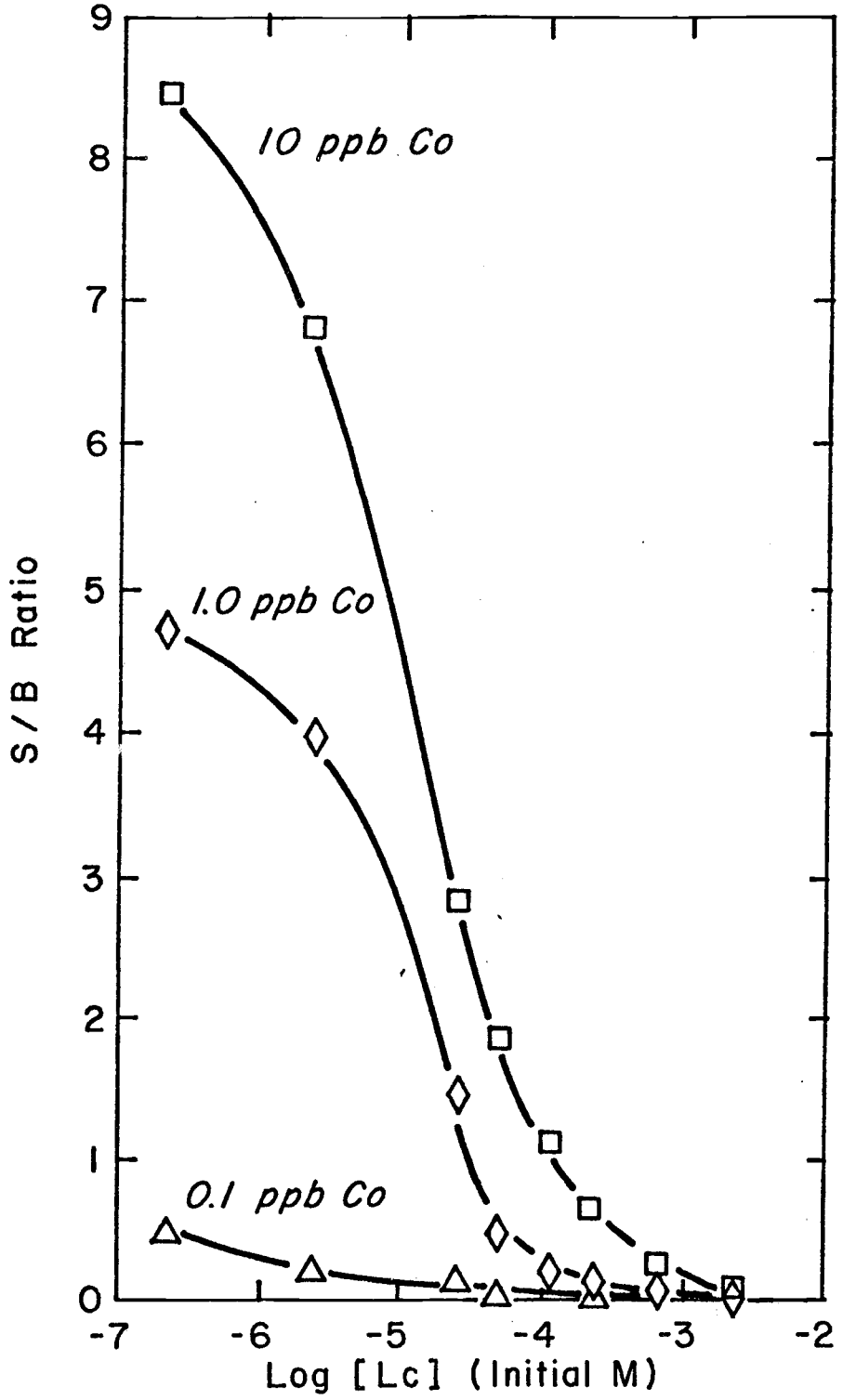

Figure 17. S/B ratio versus initial Lc concentration. Initial conditions: H_2O_2, 0.10 M; KOH, 5.0 M (final pH 14).

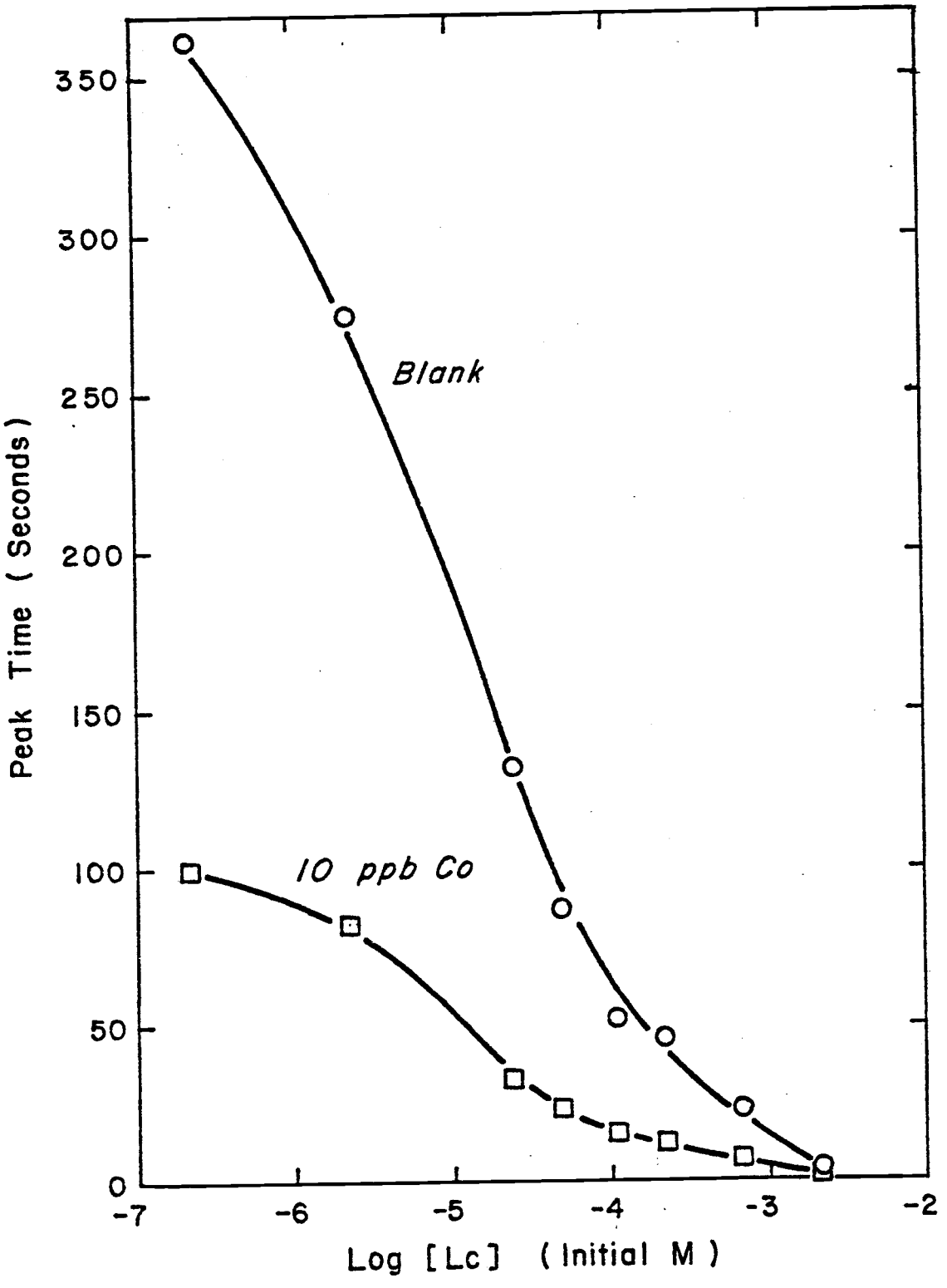

Figure 18. Peak time versus initial Lc concentration. Initial conditions: H_2O_2, 0.10 M; KOH, 5.0 M (final pH 14).

detection limit was 20 pptr for the lowest Lc concentration and increased to 600 pptr for the highest.

The choice of the optimum Lc concentration clearly involves compromises since important criteria are in direct conflict. A large S/B ratio and low detection limit can be achieved only at the expense of a considerably longer analysis time. In terms of the analytical signal, the optimum Lc concentration extends over a wide range and this range increases in size as the Co concentration decreases. It was anticipated that the Co concentration in the analysis of real samples would be 0.1 to 1 ppb, so a detection limit of 50 pptr or less was desirable. Accordingly, the concentration of Lc used to optimize the H_2O_2 and pH was 4.8×10^{-5} M. At this concentration, the analytical signal for 0.1 ppb Co is only 9% less than the optimum which occurs at 2.2×10^{-4} M. Similarly, the S/B ratio is 90% less and the detection limit is 1.5 times greater compared to the optimum Lc concentration for these two criteria (2.2×10^{-6} M). However, the analysis time for six blanks and three Co runs (10 ppb) decreased by a factor of 8 in going from a Lc concentration of 2.2×10^{-6} to 4.8×10^{-5} M.

Optimum Hydrogen Peroxide Concentration

To find the optimum H_2O_2 concentration, a determination was made of the blank, 0.1, 1.0, and 10 ppb Co peak shapes for H_2O_2

concentrations from 9.7×10^{-5} to 0.61 M. During this experiment a change in the actual peak shapes of the blank and Co peaks was noted. As the H_2O_2 concentration decreased, the height of the first peak also decreased. At the lowest H_2O_2 concentration, this peak was entirely absent. As in the optimization study, Co does not affect the height of the first peak very much. It is also noticed that for H_2O_2 concentrations greater than 0.61 M, the second peak appears as a small shoulder on the first peak, and estimation of its height is difficult. Consequently, no data are presented for runs made at H_2O_2 concentrations above 0.61 M.

Figure 19a is a plot of the height of the second peak of the blank and 10 ppb Co versus the initial H_2O_2 concentration. The blank signal is linearly related to H_2O_2 concentration above 0.01 M with a slope of 0.90. Below 0.01 M the slope is much less than one. In separate studies, it was found that when H_2O_2 is added last the same plot for the blank is linear with a slope of one from 4.0×10^{-3} to 0.78 M. When Lc is added last the same plot is linear with a slope of 0.9 from 1.0×10^{-3} to 5 M. At the upper end of the plot for 10 ppb Co (Figure 19a) the slope is about 0.5. When Lc is added last the slope of the corresponding curve for a 1.0 ppb Co solution is linear with a slope of about 0.9.

In Figure 19b, which is a log-log plot of the analytical signal of 0.10 and 10 ppb Co versus the initial H_2O_2 concentration, it is clear

Figure 19. Signal and analytical signal versus initial H_2O_2 concentration. Initial conditions: Lc, 4.8×10^{-5} M; KOH, 5.0 M (final pH 14).

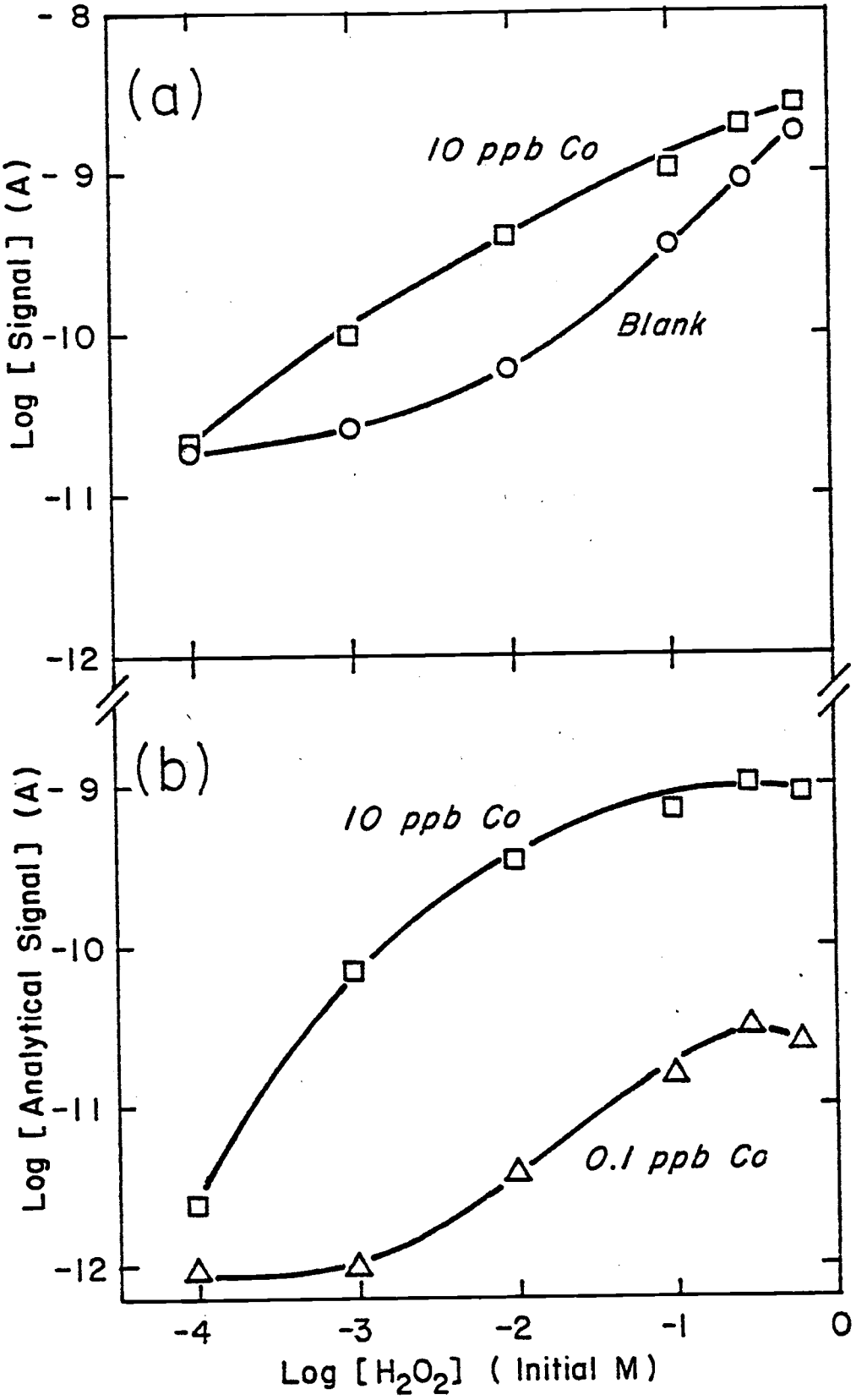
(a)
10 ppb Co
Blank
Log [Signal] (A)
- 8
- 9
-10
-11
-12
(b)
10 ppb Co
0.1 ppb Co
Log [Analytical Signal] (A)
- 9
-10
-11
-12
-4
-3
-2
-1
0
Log [H2O2] (Initial M)

Figure 19

that the optimum is at the higher H_2O_2 concentrations. For both Co solutions, any H_2O_2 concentration from 0.1 to 0.6 M would be optimal because the analytical signal is large and it changes little in this region. When the S/B ratio is considered, however, the optimum H_2O_2 concentration is no longer in this region. Figure 20 is a plot of the S/B ratio versus the initial H_2O_2 concentration. It shows that the optimum H_2O_2 concentration for the determination of 1.0 and 10 ppb Co is 0.01 M. The curve for 0.10 ppb Co is not as clearly defined, but the largest value is also at 0.01 M. The analytical sensitivity parallels the S/B ratio in this study and consequently indicates that 0.01 M is the optimum H_2O_2 concentration.

Just as in the Lc study, it was determined that the peak time is longer at lower reagent concentrations. Figure 21 is a plot (linear-log) of the peak time for the blank and 10 ppb Co versus the initial H_2O_2 concentration.

As in the Lc optimization study, the criteria evaluated are in conflict as to what the optimum H_2O_2 concentration is. The detection limit for Co is quite high at the two extremes of the H_2O_2 concentration range studied, but in the middle of the range it is fairly constant with a value of 20 to 60 pptr. A large S/B ratio for 1.0 and 10 ppb Co and good sensitivity can only be achieved if analysis time is increased. In terms of the analytical signal, the optimum H_2O_2 concentration is 0.10 M or greater for each of the three Co solutions. As mentioned in the

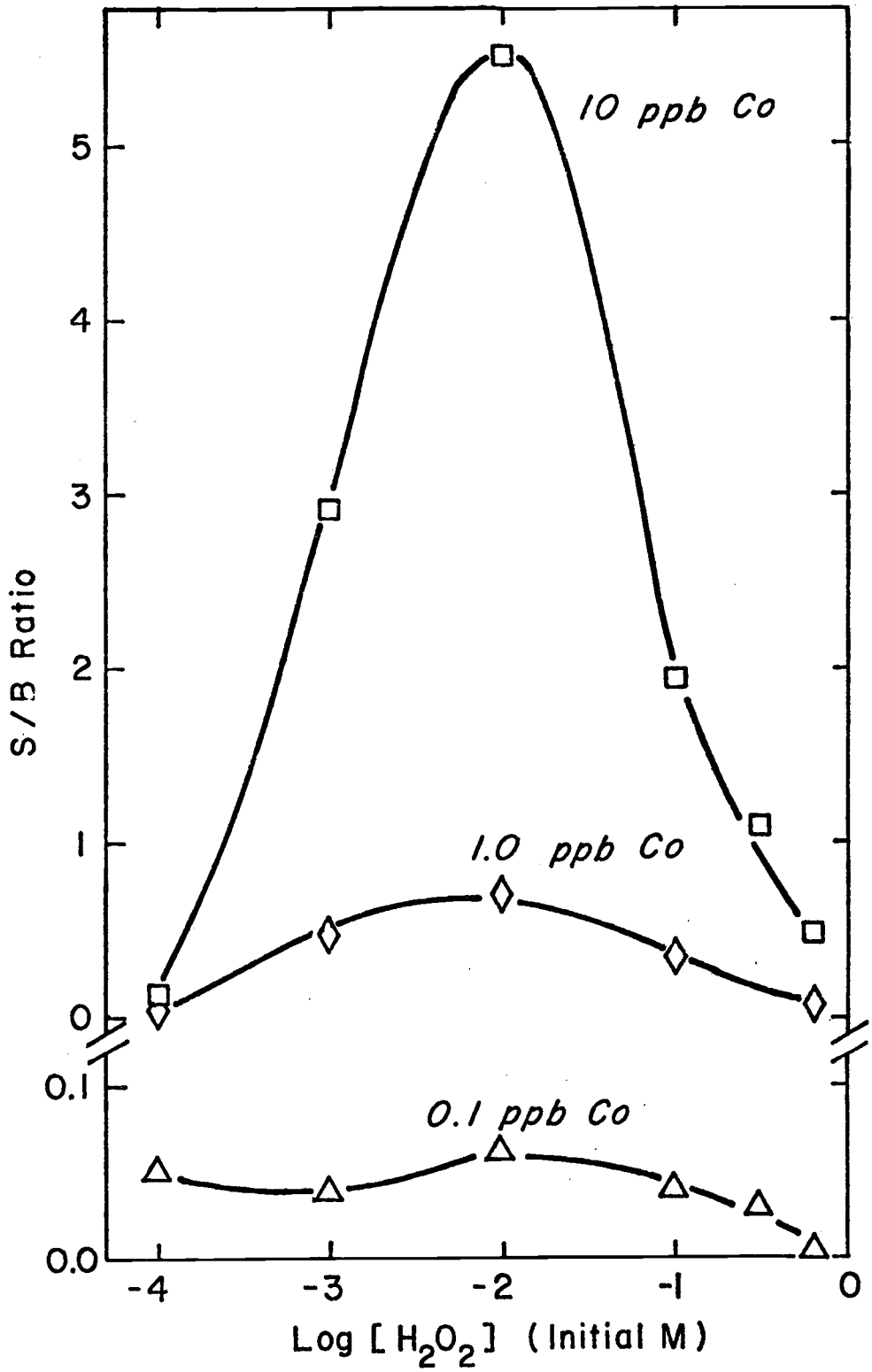

Figure 20. S/B ratio versus initial H_2O_2 concentration. Initial conditions: Lc, 4.8×10^{-5} M; KOH, 5.0 M (final pH 14).

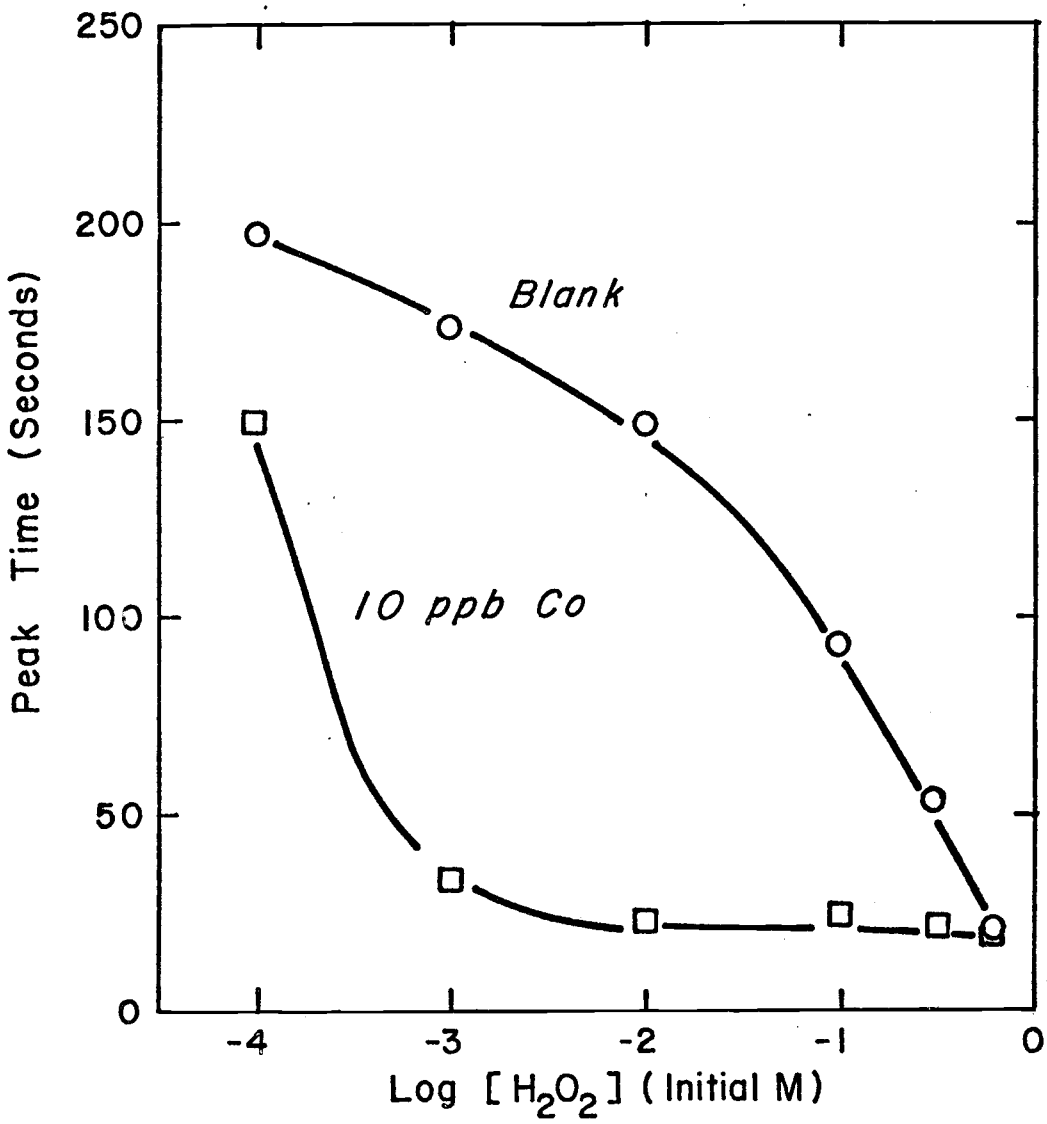

Figure 21. Peak time versus initial H_2O_2 concentration. Initial conditions: Lc, 4.8×10^{-5} M; KOH, 5.0 M (final pH 14).

Lc optimization section, the analysis of real samples was expected to entail the determination of Co at concentrations of 0.1 to 1 ppb. Accordingly, the H_2O_2 concentration chosen as the optimum for the remainder of the optimization study was 0.10 M. At this concentration the analytical signal for 0.10 ppb Co is about half the optimum value, which occurs at 0.29 M. The S/B ratio is 33% less and the detection limit is twice that which is found at the optimum H_2O_2 concentration for these two criteria (0.01 M). However, the analysis time for six blanks and three Co runs (10 ppb) is about half that compared to analysis using 0.01 M H_2O_2. Since this was the same concentration that was used in the Lc optimization, there was no need to evaluate the characteristics of the Lc dependence again with a new H_2O_2 concentration.

Optimum Hydroxide Concentration

The optimum hydroxide ion (OH^-) concentration was found by making determinations of the peak shapes of the blank, 0.10, 1.0, and 10 ppb Co over the OH^- range from 5.6×10^{-5} to 2.0 M (final cell concentration). Below 1 M OH^-, the OH^- concentration was calculated from the measured pH of the CL solutions.

The results are shown in Figure 22a, which is a log-log plot of the blank and 10 ppb Co signal versus the final OH^- concentration. The blank signal has a maximum at about 2×10^{-2} M and minimum at

Figure 22. Signal and analytical signal versus final OH^- concentration. Initial conditions: H_2O_2, 0.10 M; Lc, 4.8×10^{-5} M.

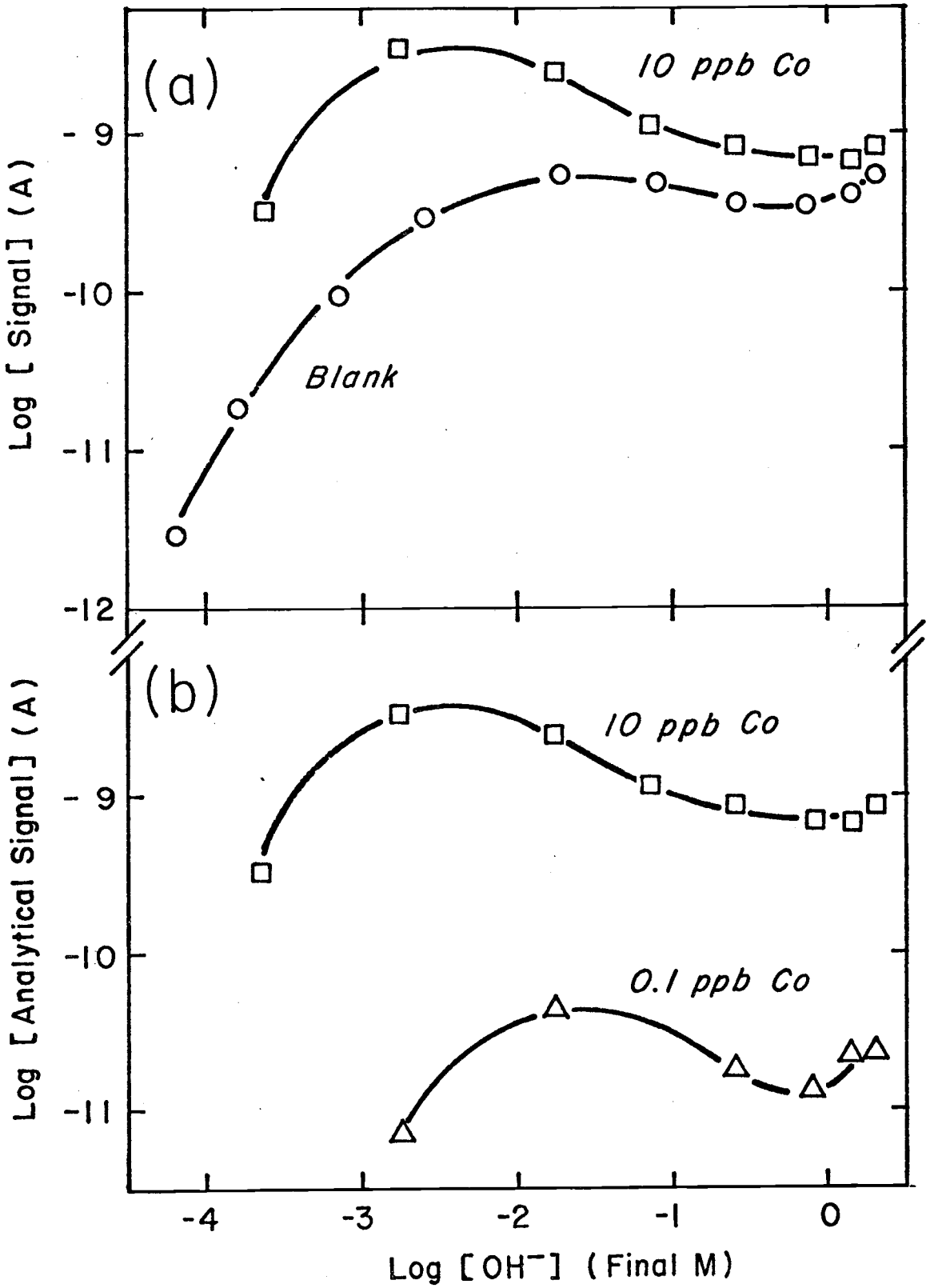
(a)
10 ppb Co
Blank
Log [Signal] (A)
- 9
-10
-11
-12
(b)
10 ppb Co
0.1 ppb Co
Log [Analytical Signal] (A)
- 9
-10
-11
-4
-3
-2
-1
0
Log [OH⁻] (Final M)

Figure 22

7×10^{-1} M. The 10 ppb Co signal also has a maximum and minimum, but the maximum is at a lower OH^- concentration than the blank while the minimum occurs at about the same place. The maxima for 0.1 and 1.0 ppb Co signals lie between those of the blank and 10 ppb Co. Other studies showed that the OH^- dependence for the blank is the same whether Lc or H_2O_2 is injected last and that when the peak area is measured the presence and location of the maximum and minimum remains unchanged.

The analytical signals of 0.10 and 10 ppb Co solutions versus the final OH^- concentration are shown in Figure 22b. The maximum analytical signals are found at 2×10^{-3} M for 10 ppb Co and 2×10^{-2} M for 0.10 ppb Co. When the final OH^- concentration is 0.25 to 2 M, the analytical signals are relatively constant with no signal being more than a factor of 1.5 different from the average in that region. The choice of an OH^- concentration in the range of 0.25 to 2 M would involve no more than a five-fold decrease in the signal or analytical signal compared to the maximum value at the lower OH^- concentrations.

The S/B ratio for the three Co solutions versus the final OH^- concentration is shown in Figure 23. The optimum OH^- concentration for determination of 1.0 and 10 ppb Co is 1.7×10^{-3} M and for 0.10 ppb Co it is 1.7×10^{-2} M. The detection limit increases from about 10 pptr at the lowest OH^- concentration to 50-100 pptr at the two highest.

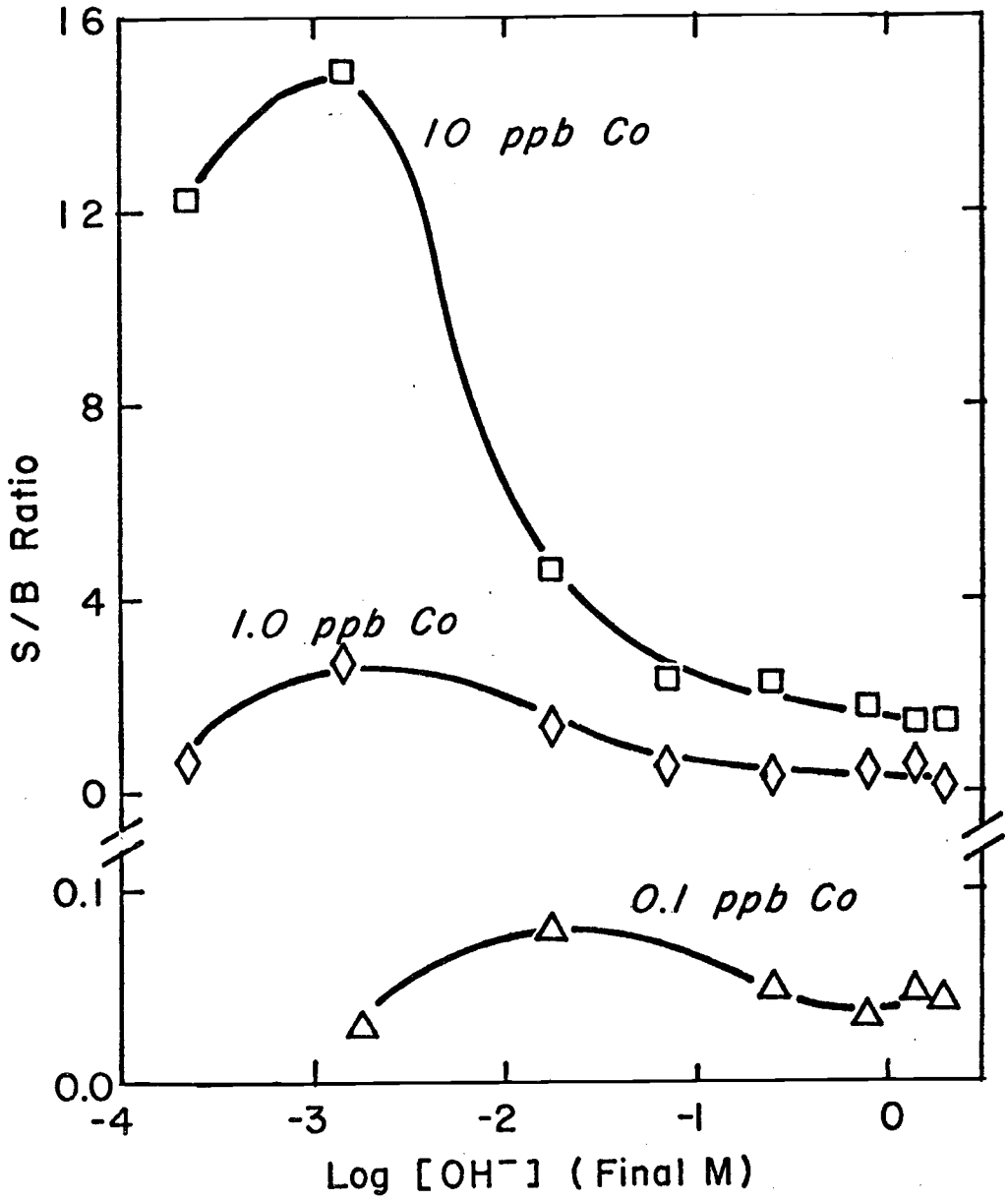

Figure 23. S/B ratio versus final OH^- concentration. Initial conditions: H_2O_2, 0.10 M; Lc, 4.8×10^{-5} M.

The increase at the two highest OH^- concentrations is caused mainly by an increase in the irreproducibility of the blank signal. For the rest of the OH^- concentration range, the detection limit only increases by a factor of three. Peak times do not change markedly as the OH^- concentration changes so analysis time is not a factor in the optimization of pH.

The choice of the optimum final OH^- concentration again involves compromises because the most convenient OH^- concentrations for analysis are not optimum (largest) for the S/B ratio and analytical signal. It was felt, however, that working at a high pH would be best because then the pH of the CL solution would remain constant under the influence of various acidic metal solutions which would eventually be added. The hope was that the reaction could be carried out without the use of a buffer or adjustment of the pH of samples and this is true if the concentration of KOH injected into the cell is 5.0 M or greater. Experiments showed that even if a pH 0.5 metal solution is added in place of water, the final pH of CL solution will still be 14 if the initial OH^- is 5.0 M. Accordingly, a final concentration of 1.0 M was chosen as the optimum OH^- concentration. At this OH^- concentration, the Co calibration curve is linear over a large concentration range and the detection limit is still quite low (25 pptr). The analytical signal of 0.10 ppb Co is a third of its optimum value which occurs at 1.7×10^{-2} M and the S/B ratio of 0.10 ppb Co is about half

of its optimum value. The detection limit is three times larger than that for the lowest OH^- concentrations. The reproducibility of the blank is better here than at larger OH^- concentrations, but the analytical sensitivity is not as large as that at the lower OH^- concentrations.

Comparison of the optimum reagent concentrations just proposed with those of previous workers shows that there are differences. In Table VIII, which shows the optimum reagent concentrations for Co analysis found by Dubovenko (7), the final pH was 13.5, the optimum Lc was 1×10^{-5} M, and the optimum H_2O_2 was 5×10^{-3} M. However, in Dubovenko's study the sample cell volume was twice as large as in this study, so it would be best to compare final Lc and H_2O_2 concentrations for the two systems. Accordingly, his final Lc concentration was 1×10^{-6} M (9.6×10^{-6} M in this study), and the final H_2O_2 concentration was 1.1×10^{-3} M (2.2×10^{-2} M in this study). This difference occurs because the Russian workers employed photographic light detection in their system (exposure time 5 minutes). Their lower Lc and H_2O_2 concentrations imply that analysis time for a single run would be longer than in this system, but the actual analysis time may not be much longer because the blank and standards can be run concurrently. They accomplished this by placing several sample cells on one photographic plate and running them all at once. In all CL metal analysis work done by Dubovenko, the optimization criteria employed

was S/B ratio (defined by them as metal signal/blank signal) so this means they would tend to use lower Lc and H_2O_2 concentrations.

Miscellaneous Optimization Parameters

The temperature of a CL reaction solution was believed to be an important parameter so during the optimization studies the cell temperature was maintained at 25.0°C. Upon completion of the pH study the effect of changing the cell temperature was investigated. At this time the Lc, H_2O_2, and KOH reservoirs were thermostatted in the constant temperature bath. Since the Co (or H_2O) was the first solution placed in the cell, the combination of the temperature controlled cell holder and the remaining three reagents would ensure that the cell temperature would be that of the water bath. The temperature range investigated was 15.5°-35°C with the procedure employed by Hoyt (8). Figure 24, which is a plot of the blank and 1.0 ppb Co signal versus the cell temperature, shows that the signals increase as the temperature increases. However, the analytical signal is nearly constant over this temperature range and the S/B ratio increases only slightly at the lower temperatures. The peak time for the blank decreases from 230 s at 15.5°C to 38 s at 35°C. At 25°C it is 90 s. The data indicate that only two criteria can be optimized by changing the cell temperature, S/B ratio and analysis time. There is no clear advantage in using a low cell temperature to increase the S/B ratio

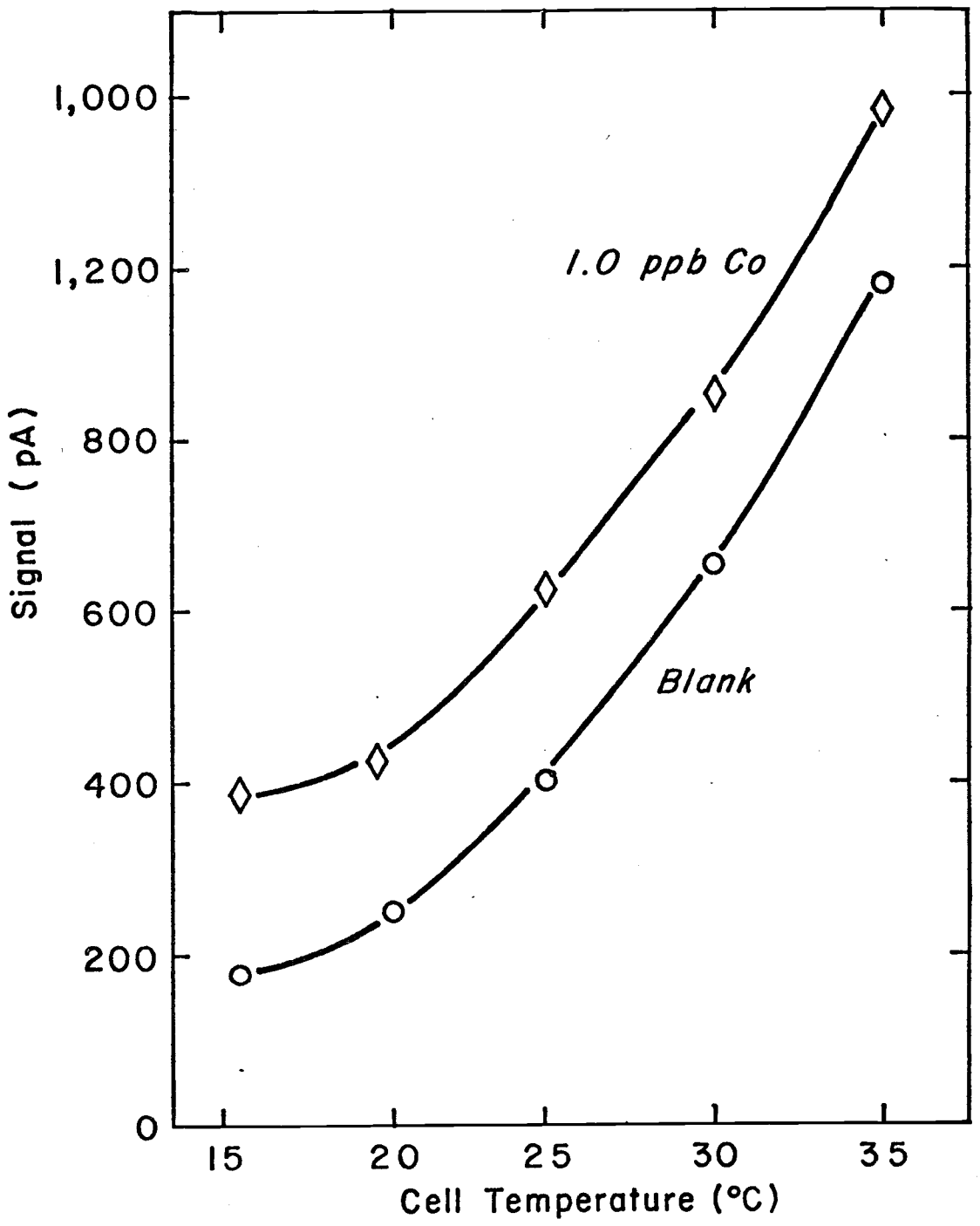

Figure 24. Signal versus sample cell temperature. Conditions in Figure 25.

because the improvement is small and the analysis time increases greatly. Decreasing the analysis time by increasing the cell temperature was not explored because it was known that anslysis time could be controlled by the choice of H_2O_2 and Lc concentrations. Consequently, the cell temperature for the remainder of the study was maintained at 25.0°C.

An Arhenius plot of the temperature data (ln signal versus the reciprocal of the absolute temperature) was linear for the blank and 1.0 ppb Co. Calculation of the activation energies from the slopes gave 15.9 and 12.7 kcal/mole for the blank and 1.0 ppb Co, respectively. These data do not prove that the height of the second CL peak is proportional to the rate of the CL reaction, although this is a reasonable assumption.

Upon completion of the optimization studies and the interference study two refinements were made to improve the analysis procedure for the real samples. The first change was to increase the initial Lc concentration from 4.8×10^{-5} to 6.8×10^{-5} M. This factor of 1.5 increase in Lc concentration decreased the peak time of a blank run from 1.5 to 1 minute. This was a substantial time saver when it is considered that 150-250 runs were being made daily. As noted in the Lc optimization study, such an increase would be expected to result in a decrease in the S/B ratio and an increase in the detection limit. At low Co concentrations the decrease in S/B ratio is small (Figure

17) and it was expected that real samples and Co standards for them would be in the range of 0.1 to 0.5 ppb. The change in the detection limit was not significant (t-test, 95% confidence level) and remained at about 25 pptr. The data from the Lc optimization suggested that small changes in the Lc concentration would not markedly affect the criteria important to this study and this was found to be true.

The second change made was the increase in volume of the Co solution added to the sample cell. This volume was increased from 0.5 to 1.0 mL so that it would not be necessary to add the 0.5 mL of water which accompanied the Co solution in each run. The reagent volumes were now 1.0 mL Co, 0.5 mL Lc, 0.5 mL H_2O_2, and 0.5 mL KOH. This change meant that one less reagent transfer for each Co run was required and this resulted in a simplification of the procedure. The time saved during each Co injection sequence was about 5 s. No change in the reagent volumes for blank runs was needed. This increase in volume of Co solution added to each Co run resulted in a lowering of the detection limit and an increase of the S/B ratio. Based on seven detection limit determinations before this change in Co volume and eight determinations after, it was found that the detection limit decreased from an average 25 pptr to about 13 pptr. In spite of the variabilities of detection limit determinations this difference is significant (t-test, 95%). The Co analytical signals for this comparison were obtained during the course of development of an extraction

procedure for Co and represent nominal detection limits obtainable with no extra effort to improve the detection limit. Data before and after the change were taken over a 17 and 22 day period, respectively. The reason the detection limit decreased by a factor of two is that the slope of the Co calibration curve near the detection limit doubled and the reproducibility of the blank did not change. The S/B ratio increased significantly from 1.17 to 1.32 for 0.50 ppb Co measurements. The numerical changes in detection limit, slope of the calibration curve, and analytical sensitivity were expected because the Co concentration in the cell had doubled with the increase in volume of the Co solutions.

Co Calibration Curve

Figure 25 is the Co calibration curve (analytical signal versus Co concentration) using the optimum conditions obtained during the optimization study. The log-log plot is linear over seven orders of magnitude and has a slope of about 0.5. A linear plot of analytical signal versus Co concentration shows that near the detection limit the slope is 1.2×10^{-10} A/ppb and the plot is linear over an order of magnitude above the detection limit.

During the analysis of real samples the Co concentration usually analyzed was limited to the range of 0.1 to 1.0 ppb. By this time, the two procedural refinements mentioned earlier had been instituted.

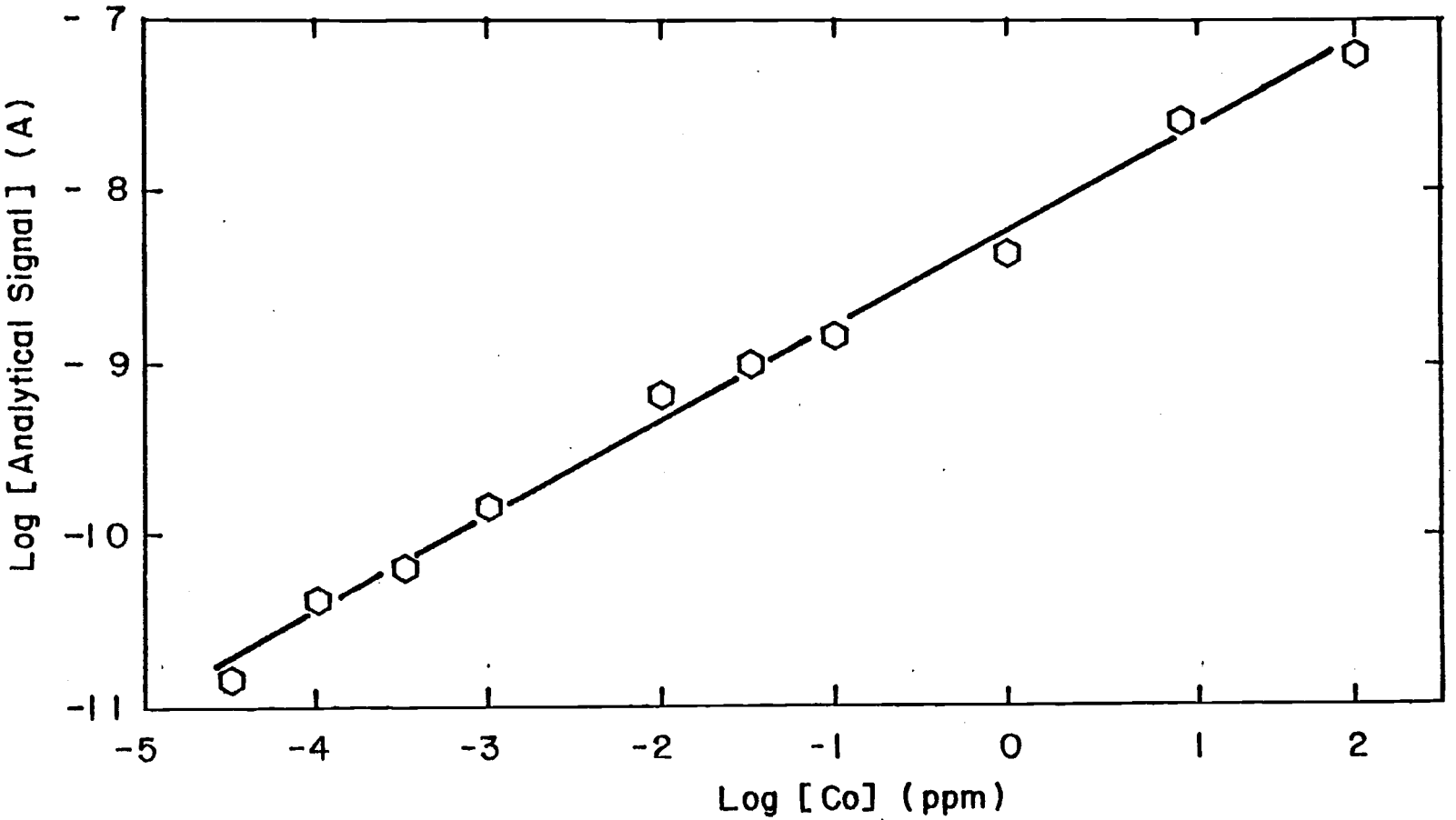

Figure 25. Co calibration curve. Initial conditions and volumes: H_2O_2, 0.10 M (0.5 mL); Lc, 4.8 x 10^{-5} M (0.5 mL); KOH, 5.0 M (0.5 mL); Co (0.5 mL); H_2O (0.5 mL).

A typical Co calibration curve under these conditions is shown in Figure 26. The initial conditions are shown in the figure caption. The slope near the detection limit is 4.2×10^{-10} A/ppb and the detection limit is about 15 pptr. The linear portion of the curve is from 0.1 to 0.5 ppb which is typical of the 20 or so working curves prepared near the end of the study.

The importance of a reproducible blank signal and the minimization of contamination when working at these low Co concentrations cannot be over emphasized. In regard to contamination, it was felt that the use of Eppendorf pipets with their plastic, disposable tips for reagent handling was a definite advantage compared to conventional pipets or syringes. These pipets also have about 1% accuracy and 0.3% precision and are faster to use than glass pipets. The precision liquid dispenser, with its closed system for injecting the base into the sample cell, also helped to minimize contamination. The measured accuracy and precision are about 0.1% and 0.03%, respectively, and with this device the injection of the base is faster than with a syringe. The pipet rack, covered reservoirs for all reagents, and scrupulous glassware cleaning are all important in minimizing contamination.

The precision of blank measurements was carefully investigated and it was found that cell temperature, reagent preparation, and condition of the sample cell are all important. A change in sample cell

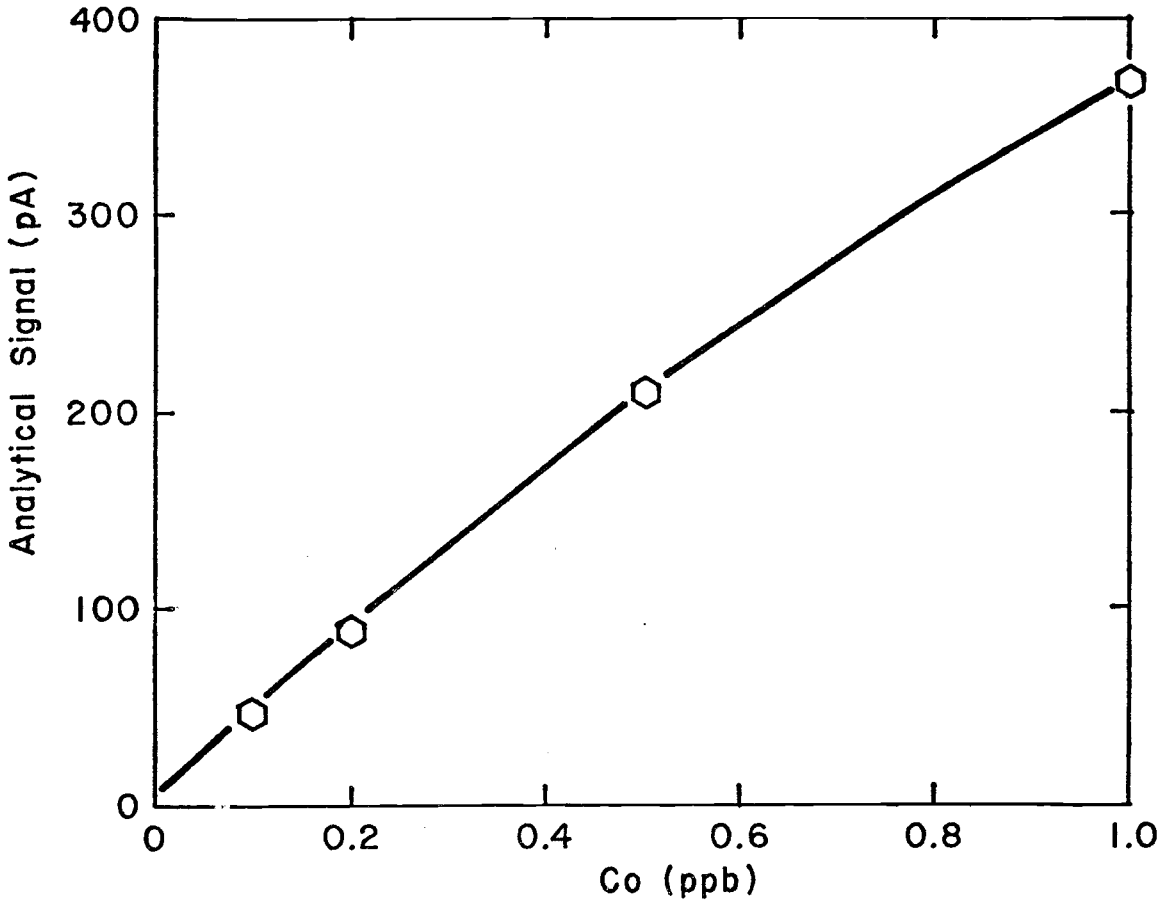

Figure 26. Co calibration curve. Initial conditions and volumes: H_2O_2, 0.10 M (0.5 mL); Lc, 6.8×10^{-5} M (0.5 mL); KOH, 5.0 M (0.5 mL); Co (1.0 mL).

temperature of 0.25°C was noticeable if repetitive blank measurements were being made. Studies showed that if the temperature of the injected KOH was 19°C (versus 25°C) it would cause the resulting blank signal to decrease by 6%. This is why the KOH and other reagent reservoirs were placed in the constant temperature bath.

In the early parts of this study, 0.10 M H_2O_2 solutions were prepared daily by diluting concentrated H_2O_2. The pH of these solutions was not adjusted within the range of 4-4.5. The result was an essentially constant drift in the blank signal during the day. This downward drift, which was as large as 5% on some days, could not be arrested except by preparing H_2O_2 solutions at least 24 hours before they were needed. Because dilute solutions of H_2O_2 are unstable, the pH was adjusted to 4-4.5 and they were refrigerated until needed.

As mentioned in the Procedure chapter, an insoluble reaction product is produced during the Lc reaction which is probably dimethylbiacredene from the studies of Legg and Hercules (61). This proved to be a source of imprecision for blank measurements. After 20-30 blank runs, enough of this substance accumulates on the cell walls and stirring bar to influence subsequent blank reactions. The effect is always to increase the blank signal so when consecutive blank runs showed increasing peak heights, the cell was cleaned. The procedure was to fill the cell for 5 minutes with 50% HNO_3 and then rinse 20 times with water. If the cell has not been rinsed thoroughly, the next

few blanks will have low signals. Apparently, the interior surface of the cell and/or the stirring bar have some effect on the reaction. This conjecture is supported by the finding that the blank and analytical signal are larger when the sample cell is glass rather than plastic.

Once the above problems with contamination and irreproducibility were recognized the precision of blank measurements was improved. Blank signals for an entire day were made with a relative precision of 0.5 to 2% and the absolute magnitude of the blank signal did not vary by more than 10% for the last 8 months of the study. The relative precision of Co signals is independent of Co concentration and it is comparable to that observed for the blank. The light output of the Lc reaction under the conditions of this study is large and no noise is obvious in the CL signal of the blank or Co. The imprecision in making CL measurements seems to be due to changes in the rate of the reaction from run to run. These may be caused by changes in the interior surfaces of the sample cell or variations in the mixing when the last reagent is injected into the cell.

Interference Study

The applicability of CL analytical techniques is sometimes limited by chemical interferences that occur. Accordingly, a comprehensive interference study was undertaken to determine which

elements or complexing agents would present problems in the analysis of Co via Lc CL. The expected interferents were those metals for which Lc CL based analytical techniques had been previously reported. However, most of the available data were not directly applicable to this study because the effects of various elements had been determined under different conditions and with different instrumentation. Since the effect of many elements on the Lc CL reaction had not been reported previously, this interference study also served as a survey to determine if Lc CL analysis for other elements was possible.

The approach to this study was to first obtain a calibration curve for all the metals, anions, and complexing agents. This would extend from the detection limit up to a starting concentration which was 100 ppm for most metals, and 10,000 ppm for anions and complexing agents. The data obtained in this section were then analyzed in light of the expected concentration of elements and anions in various real samples, and an indication of the serious interferences was obtained. It was then necessary to determine what the nature of the interference was for mixtures of the interferent and Co, and if necessary, devise an appropriate masking or separation procedure.

The experimental procedure, for a metal, was to prepare a 100 ppm solution according to the method described in the Procedure chapter. The pH of metal solutions was 0.8 to 2 and an acid blank for each metal was always made. Using the same conditions as for the

Co calibration curve in Figure 25, the analytical signal for the metal was measured. If the analytical signal was greater than twice the standard deviation of the two blank signals (run before and after the metal), the metal solution was diluted and another analytical signal measurement made. Subsequent dilutions were made until the detection limit for the metal had been reached. The signal of the acid blank was always subtracted from the analytical signal of the metal solution so that the effect of the metal alone could be recorded.

Interference studies for anions and complexing agents were carried out in the same manner as metal solutions, with the only exceptions being the higher starting concentration and the absence of an acid blank. There are some exceptions for the starting concentration as metals of particular interest were tested at concentrations greater than 100 ppm and some complexing agents could not be prepared at concentrations as high as 10,000 ppm. The data were treated by calculating the slopes of the calibration curve on a log-log plot for the entire concentration range studied and the slope of the linear plot near the detection limit. In both cases, the analytical signal versus the concentration of the species in ppm was plotted. The detection limit was calculated as previously described for Co.

Table XI is a presentation of the data accumulated for metals in this study, grouped by family for comparison. An indication of a positive slope for the calibration curve means that the element

Table XI. Metals which enhance or inhibit the Lc run.

Metal	Positive Slope (pA/ppm)	Negative Slope (pA/ppm)	Detection Limit (ppm)
Li(I)	-	-	> 100
Na(I)	-	7.7×10^{-4}	6,000
K(I)	-	-	>7,100
Rb(I)	-	-	> 100
Cs(I)	-	-	> 100
Be(II)	1.7×10^{-1}	-	30
Mg(II)	-	1.4×10^{-1}	0.35
Ca(II)	2.9×10^{-2}	-	120
Sr(II)	-	-	> 100
Ba(II)	1.1×10^{-1}	-	20
Sc(III)	3.6×10^{-1}	-	10
Y(III)	-	1.3×10^{-1}	55
La(III)	-	-	> 100
Ce(III)	2.3×10^{-1}	-	20
Pr(III)	3.7×10^{-1}	-	10
Nd(III)	-	2.1	2
Sm(III)	-	1.5	3
Eu(III)	-	8.9	0.9
Gd(III)	-	2.2	4
Tb(III)	-	5.6	1
Dy(III)	-	1.2	5
Ho(III)	-	2.4	0.2
Er(III)	-	4.2	0.3
Tm(III)	-	5.5×10^{-1}	0.06

(Continued on next page)

Table XI. (Continued)

Metal	Positive Slope (pA/ppm)	Negative Slope (pA/ppm)	Detection Limit (ppm)
Yb(III)	-	5.8	0.03
Lu(III)	-	3.9	1.5
Th(IV)	-	6.8	85
U(VI)	2.4×10^{-2}	-	20
Ti(IV)	2.4	-	1
Zr(IV)	1.3	-	1.5
Hf(IV)	-	2.5×10^{-1}	7
V(V)	-	8.3×10^{-1}	4.5
Nb(V)	-	4.4×10^{-1}	10
Ta(V)	3.3×10^{-1}	-	14
Cr(III)	4.6×10^{1}	-	0.20
Cr(VI)	1.1	-	3
Mo(VI)	-	-	> 100
W(VI)	-	-	> 100
Mn(II)	-	4.9	0.6
Re(VII)	-	-	> 113
Fe(II)	1.8×10^{2}	-	0.03
Fe(III)	1.2×10^{2}	-	0.04
Ru(III)	2.8×10^{3}	-	0.001
Os(VIII)	8.6×10^{4}	-	0.00003

(Continued on next page)

Table XI. (Continued)

Metal	Positive Slope (pA/ppm)	Negative Slope (pA /ppm)	Detection Limit (ppm)
Co(II)	1.2×10^{5}	-	0.00002
Rh(III)	9.1×10^{-1}	-	4.0
Ir(IV)	5.1×10^{-1}	-	8.0
Ni(II)	2.2×10^{1}	-	0.3
Pd(II)	1.1×10^{-1}	-	25
Pt(IV)	3.3	-	1
Cu(II)	2.0×10^{1}	-	0.1
Ag(I)	8.0×10^{1}	-	0.03
Au(III)	3.3	-	1
Zn(II)	9.4×10^{-2}	-	75
Cd(II)	-	3.6×10^{-1}	10
Hg(II)	-	2.1×10^{-1}	20
Al(III)	4.2×10^{-1}	-	6
Ga(III)	3.7×10^{-1}	-	18
In(III)	-	-	>103
Tl(I)	-	5.4×10^{-2}	59
Ge(IV)	-	-	>103
Sn(IV)	-	1.9×10^{-1}	9
Pb(II)	4.7×10^{-1}	-	9
Sb(III)	5.1	-	1
Bi(III)	8.7×10^{-1}	-	4

enhances the Lc reaction, just as Co does. A negative slope means that the element inhibits the Lc reaction such that the height of its second peak is less than the corresponding peak height for the blank reaction. In these cases, metal determination is still possible, but detection limits for these elements is not nearly as low as those elements which enhance the Lc reaction.

The most striking feature of these data is the fact that so many metals enhance or inhibit the Lc reaction. The alkali metals are the only family that has little effect on the reaction. It seems possible that the small negative signal observed at a high Na concentration was due to a contaminant present in the Na compound used to prepare the 10,000 ppm Na solution. For the rest of the data, comment will be made only on those features which seem to imply unusual chemistry or possible analytical applications for metal determination. It is difficult to be specific because the mechanism by which the metals influence the reaction is not known.

Group IIA metals enhance the Lc reaction, if they have any effect, except Mg. This metal was found to be a powerful inhibitor and its detection limit of 0.35 ppm appears to indicate that an analytical technique for it would be possible. However, the calibration curve for Mg is linear over a rather small range (0.35 to 3 ppm) and the signal is independent of Mg concentration from 10 to 10,000 ppm.

In Group IIIB, Sc and Y have the opposite effect on the Lc reaction. Not surprisingly, the Lanthanides exhibit similar effects on the Lc reaction with only three exceptions. Ce and Pr are the only two elements which enhance the Lc reaction and La has no effect at concentrations below 100 ppm. The remaining elements (Nd through Lu, Pm not included) all inhibit the reaction, and the slopes of the calibration curves near the detection limit are all quite large compared to other elements which also inhibit. The detection limit for two of the Lanthanides are quite low (30 and 60 ppb for Er and Tm, respectively), but all have a calibration curve with essentially the same shape as the Mg plot. The linear range extends about an order of magnitude above the detection limit then the curve bends off such that the signal is independent of metal concentration from 10 to 100 ppm. Of the two Actinides run, Th inhibits the reaction and U enhances it. Neither element has a very low detection limit.

The behavior of Ti was unusual. At concentrations of 60 ppm or greater Ti inhibits the reaction strongly, but below this concentration it enhances the reaction. From 1 to 10 ppm the calibration curve has a positive slope and beyond 10 ppm the slope is negative. Accordingly, the detection limit and positive slope shown in Table XI are indicative of the enhancement that occurs at low Ti concentrations. The congeners of Ti, which were expected to have a similar effect on

the Lc reaction, did not do so. Zr enhances the Lc reaction, but Hf clearly inhibits the reaction.

In group VIB, Cr is the only element which has en effect at concentrations below 100 ppm. Cr(III) and Cr(VI) enhance the reaction with Cr(VI) having the greater slope near the detection limit and Cr(III) the lower detection limit. In the adjacent family, group VIIB, Mn inhibits and enhances the reaction while Re has no effect at 113 ppm or less. Mn is like Ti in that it exhibits two effects depending on its concentration. From the detection limit to 10 ppm, the calibration curve has a negative slope and beyond this concentration the slope becomes positive. At concentrations of 35 ppm or greater, the analytical signals are positive and remain so up to 100 ppm.

Group VIII, which contains those elements known to be good catalysts for a variety of reactions, is the area of the periodic chart where the metals which best enhance the Lc reaction occur. Fe(II), Fe(III), Ru, and Os all exhibit large slopes near their detection limit and the detection limit decreases in going from Fe to Os. Co, of course, has the lowest detection limit of any element tested, but that of Os is not much higher. The congeners of Co are not as active as Co itself and this lack of ability to greatly enhance the reaction is in sharp contrast to what was seen for the congeners of Fe. Ni, Pd, and Pt also enhance the reaction with the lowest detection limit observed

for the lightest element. None of the elements in this last set have detection limits as low as those observed for Fe, Ru, Os, and Co.

Group IB metals all enhance the reaction, as does Zn the first element in group IIB. Cd and Hg have the opposite effect as Zn which is unusual, because in many respects the chemistry of Zn and Cd is more alike than the chemistry of Cd and Hg.

The remaining metals, which are not transition series elements, are not as reactive as those discussed earlier. Tl and Sn inhibit the reaction while Al, Ga, Pb, Sb, and Bi enhance it. In and Ge have no effect at concentrations less than 103 ppm.

Generalizations about what is common among all elements which inhibit the Lc reaction are difficult to make. In some cases, elements which have similar chemical behavior exhibit opposite effects on the Lc reaction. Examples of this are the differences between Hf and Zr or Zn and Cd. It was not surprising that most of the Lanthanides have the same effect on the reaction (inhibition), but two of them definitely enhance the reaction (Ce and Pr). Other unexpected inhibitors were Mg and Mn, which seem to have dissimilar chemistries. In the area of inhibition, it seems unlikely that a single mechanism would be operative for all the metals which show this effect.

Equally complex is the classification of elements which enhance the Lc reaction. In retrospect, it seemed likely that most known transition metal catalysts would also enhance the Lc reaction.

Specifically, these would include the elements in group VIII as well as Cu, Ag, and Au. The ability of these elements to form complexes and exist in variable valence states may be the key to their effect on the Lc reaction. This must be qualified, however, since there are several main block transition elements which either have no effect or inhibit the reaction. These latter elements possess the same basic chemical characteristics as those elements which enhance the reaction so other factors must be important. The major problem in delineating what is common among metals which enhance or inhibit the Lc reaction is the lack of knowledge as to what form they exist in during the reaction. Before the KOH is injected, each metal is in solution with H_2O_2 and Lc. Complexation with either of these species is possible for many metals and redox reactions involving H_2O_2 are also likely. Upon KOH injection (when the pH of the solution increases from 4 to 14) a wide variety of reactions can occur. The chief reactions would be precipitation for some metals (if they are at a high enough concentration), redox reactions, and olation or oxolation. The effect of many metals (including Co, Os, Ru, and Fe at low concentrations) is on the second peak of the Lc reaction, which under the conditions in the interference study, appears about 90 s after the KOH injection. It seems unlikely that very many metals would be in the same state after 90 s at pH 14 (in the presence of Lc and H_2O_2) as they were in the original pH 0.8 to 2 solution. No attempt was made to determine

what the state of these metals was after the Lc reaction. As noted earlier, the mechanism of the blank reaction is unknown and so it is difficult to propose a likely mechanism for the enhancement or inhibition of the reaction by metals.

In spite of the fact that no optimization was attempted for any other metal except Co, the interference data indicate that analysis for several metals is feasible under the conditions used in this part of the study. The criteria that are important in this selection are a low detection limit, a large dynamic range for a linear calibration curve (log-log plot), and good analytical sensitivity. The elements which meet these requirements are shown in Table XII, and Co is included for comparison. For all elements, the calibration curve is linear (on a log-log plot of analytical signal versus metal concentration) from the detection limit up to 100 ppm.

When compared to Table VII, these data show that with Lc CL lower detection limits were observed for Os, Ag, Cu, and Cr(III). Comparable detection limits were found for Ni and Bi. An element for which this technique has great potential, Ru, apparently has not been studied previously. There are better conditions for analysis of some elements as evidenced by the fact that lower detection limits, via Lc CL, have been reported for Mn, Tl, Pb, and Fe(II). Of course, Co is the most favorable element for analysis because it has

Table XII. Metals for which analysis by Lc CL is possible.

Metal	Slope (log-log)	Slope (linear, near detection limit) (pA/ppm)	Detection Limit (ppm)
Co(II)	0.56	1.2×10^5	0.00002
Os(VIII)	0.86	8.6×10^4	0.00003
Ru(III)	0.88	2.8×10^3	0.001
Fe(III)	0.81	1.2×10^2	0.04
Fe(II)	0.90	1.8×10^2	0.03
Ag(I)	1.31	8.0×10^1	0.03
Cu(II)	1.48	2.0×10^1	0.1
Ni(II)	1.13	2.2×10^1	0.3
Cr(III)	1.44	4.7×10^1	0.2

the lowest detection limit and best analytical sensitivity compared to any previous CL system (Table VIII).

Table XIII shows the data obtained for the non-metals, anions, and complexing agents in the interference study. As expected, these species are relatively unreactive. Concentrations as great as 10,000 ppm were used for the halogens and common anions because this would be the maximum concentration that could be expected after the digestion of a real sample. These data also served as a check on the metals run previously, since it was possible to determine if any effect seen for a metal was due to it alone or caused by the anion present in the metal solution.

Si and the halogens are the only non-metals which had any effect on the reaction. All of the halogens, except I, have no effect except at concentrations above 1,300 ppm. F is the only halogen which enhances the reaction. Of the common anions studied, only peroxodisulfuric ($S_2O_8^{2-}$) and bicarbonate had an appreciable effect on the reaction. The $S_2O_8^{2-}$ ion is a strong oxidant, but whether or not this property is important to its inhibition of the Lc reaction is not known. EDTA also inhibited the reaction, but in contrast to $S_2O_8^{2-}$ its signal is independent of concentration from 1 to 1,000 ppm. This may indicate that at concentrations greater than 1 ppm, EDTA is able to complex whatever metals are present in the blank reaction solution and prevent them from enhancing the reaction. At concentrations

Table XIII. Nonmetals, anions, and complexing agents which enhance or inhibit the Lc run.

Species	Positive Slope (pA/ppm)	Negative Slope pA/ppm)	Detection Limit (ppm)
B	-	-	>100
Si	-	1.5×10^{-1}	20
As	-	-	>100
Se	-	-	>105
Te	-	-	>100
F	2.7×10^{-3}	-	1,300
Cl	-	2.8×10^{-3}	1,500
Br	-	2.9×10^{-3}	1,800
I	-	1.8×10^{-2}	400
NO_3^-	-	1.7×10^{-3}	2,600
SO_4^{2-}	-	-	>10,000
NH_4^+	-	-	>10,000
PO_4^{3-}	-	8.8×10^{-4}	3,400
ClO_4^-	-	-	>5,000
$S_2O_8^{2-}$	-	2.0×10^{-1}	20
CO_3^{2-}	3.3×10^{-3}	-	1,600
HCO_3^-	6.8×10^{-2}	-	74
OCl^-	-	4.4×10^{-1}	20

(Continued on next page)

Table XIII. (Continued)

Species	Positive Slope (pA/ppm)	Negative Slope (pA/ppm)	Detection Limit (ppm)
CH_3COO^-	-	-	>10,000
$C_2O_4^{2-}$	9.7×10^{-3}	-	240
EDTA	-	8.9	0.6
TBP[1]			> 77
Acac[2]			> 90

[1] Tributylphosphate

[2] Acetylacetonate

below 1 ppm, the EDTA is unable to tie up those metal contaminants present and so the signal increases to the value normally seen when making blank runs.

The result of this comprehensive interference study (72 elements, 8 anions, and 3 complexing agents) is unfavorable, if the criterion for Co analysis is specificity. With so many elements that enhance or inhibit the Lc reaction, it would appear that Co analysis would be impossible in a real sample. The available literature pertaining to metal analysis via Lc CL does not contain any cases where the technique was used to analyze anything but laboratory standards containing no interferents. In spite of these obstacles, Co analysis is possible due to the low detection limit of Co and its relative concentration in the samples picked for analysis. An examination of the certified and provisional concentrations of elements in NBS (101) orchard leaves (OL) showed that after digestion of a 250 mg sample and dilution to 100 mL, only three elements would be present at concentrations greater than their detection limit. The elements are Co, Fe, and Mg and their final concentrations would be about 0.5 ppb, 0.75 ppm, and 15 ppm, respectively. Because of the extremely low detection limit for Co, all other potential interferents (except Fe and Mg) can be essentially diluted away. This makes the application of Lc CL for real samples more attractive because nearly all of the potential interferents present no problem during actual analysis of the

sample. The same is true for analysis of other biological samples and for direct analysis of river water. In these samples, it appears that only Fe and Mg would be present at a concentration large enough to interfere with a Co determination. Direct analysis of sea water (typically 0.3 ppb Co) would not be as simple because five elements would normally be present at a concentration large enough to interfere. These are Fe, Mg, Ag, Ca and Cl. Similarly Co analysis of most rocks would be possible if three interferents (Fe, Mg, and Al) could be controlled. Naturally, the concentration of every element in these samples can vary considerably and perhaps an element which was presumed to be a noninterferent would actually interfere. However, this first approximation did point out that the major interferents in the samples most likely to be analyzed in this study would be Fe and Mg. Consequently, the focus of the remainder of the interference study was to determine how to handle these two interferents.

Fe and Co enhance the Lc reaction so it is impossible to determine the contribution of each metal to the total analytical signal. It was anticipated, however, that the Fe concentration in real samples could be determined via atomic absorption spectroscopy so the problem remaining was to discover if the Co concentration in an Fe + Co mixture could be estimated if the Fe concentration were known. The experiment proceeded by measuring the analytical signals of 0.2 ppb Co and five Fe solutions whose concentration ranged from 24 to

500 ppb. Analytical signals were also determined for mixtures of 0.2 ppb Co with each of the five Fe solutions. Subtraction of the analytical signal of Fe alone from the analytical signal of an Fe + Co mixture, and subsequent estimation of the Co concentration from a Co calibration curve results in a Co concentration that is at least 10% low. However, a satisfactory determination of the Co concentration in a Fe + Co mixture can be obtained by using a Co calibration curve to convert the analytical signal of the mixture (and Fe solution alone) to an "apparent" Co concentration. Subtraction of the apparent Co concentration of the Fe solution from the apparent concentration observed for a Fe + Co mixture results in the Co concentration that was present in the mixture. These data should be compatible with the conditions encountered in a real sample because the ratio of Fe to Co in this experiment varied from 120 to 2,500. The expected ratio for NBS OL is 1,500. Figure 27a is an interference plot which shows how the analytical signal of Fe and Co mixtures varies with Fe concentration. The Co concentration is constant at 0.20 ppb. The plot indicates that in the presence of 20 ppb Fe or less a 0.2 ppb Co analytical signal can be determined without any interference. It is not known if all metals which enhance the Lc reaction will behave in the same manner, since no studies were conducted with metals other than Fe.

An attempt was made to find a suitable masking agent for Fe(III). This would greatly simplify the analysis if some species could be

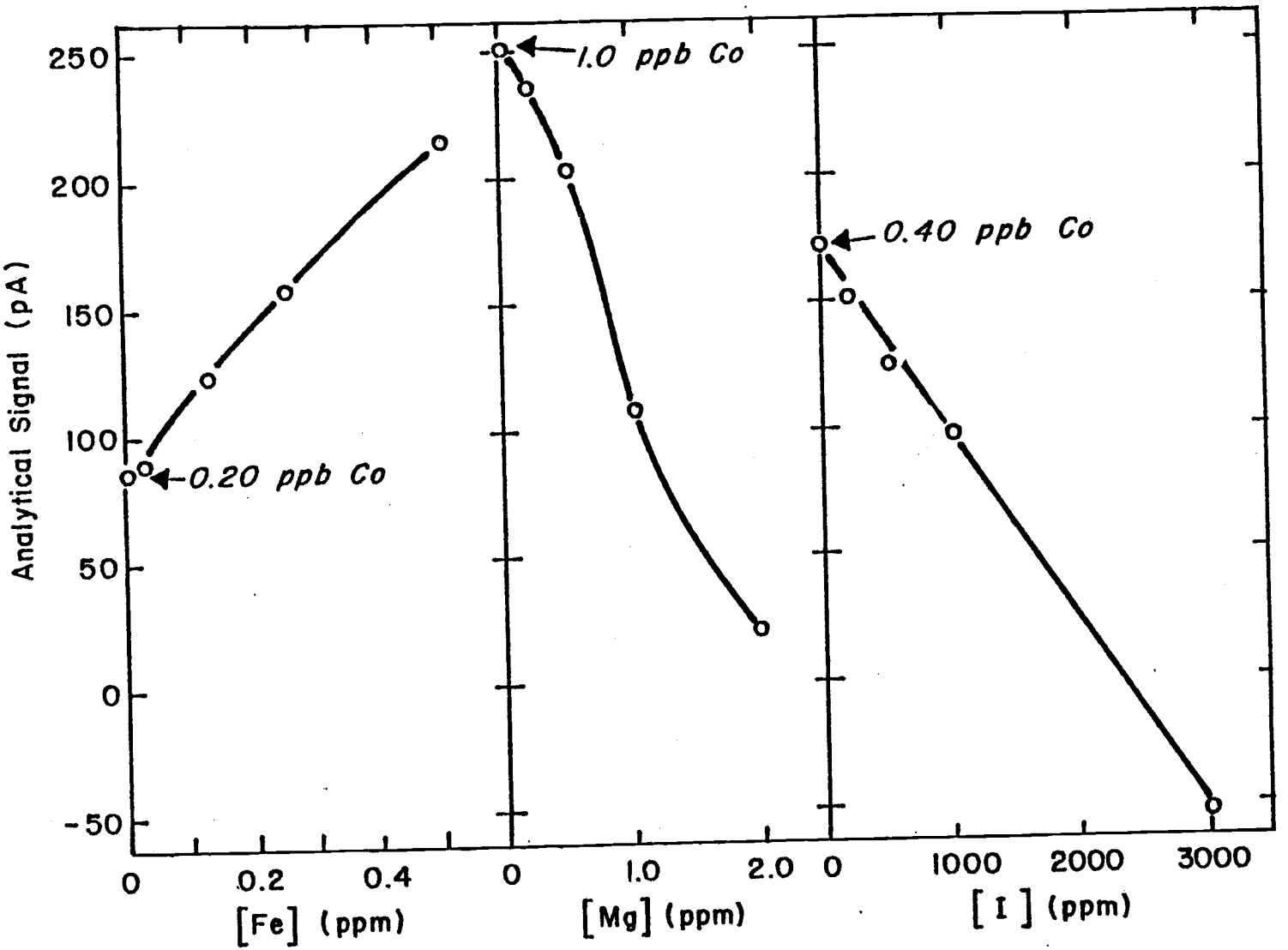

Figure 27. Interference plots for Fe, Mg, and I.

found which would tie up the Fe(III) in a Co + Fe mixture such that the analytical signal observed would be that of Co alone. The procedure for these studies was to mix various anions and complexing agents with Fe(III) and then run this solution as a regular sample. The Fe(III) concentration was 1.0 ppm and the potential masking agent was present in a 100-fold molar excess over the Fe(III). Analytical signals were compared for Fe(III), the masking agent, and a mixture of the two. The Fe(III) analytical signal in the mixture was at least 90% of its value for Fe(III) alone with F^-, Acac (acetylacetonate), and $P_2O_7^{2-}$ as masking agents. EDTA inhibits the Lc reaction and in a mixture with 0.1 ppm Fe(III) the analytical signal remains negative relative to the blank. The analytical signal of the mixture is positive with respect to the analytical signal of EDTA alone, indicating that the Fe(III) is still able to exert some of its enhancing effect on the reaction. Accordingly, these four species were judged not to be effective masking agents because they could not completely mask the enhancing effect of Fe(III).

A similar study was carried out to see if 1.0 ppm Fe(II) could be masked by citrate, Acac, F^-, or EDTA. The analytical signals for mixtures of the first three species with Fe(II) were at least 95% of the value for 1.0 ppm Fe(II), so they do not mask Fe(II) effectively. EDTA lowers the Fe(II) analytical signal, but again, it does not completely mask the enhancing effect of Fe(II).

An attempt was made to find a masking agent for Co because this would permit the evaluation of the Fe analytical signal in mixtures of Fe and Co. The same procedure was used and the species investigated were TBP (tributylphosphate), EDTA, F^-, and CN^-. Mixtures of these species with 1.0 ppb Co did not decrease the Co analytical signal markedly (20% decrease for TBP, less than 5% for the others) so they were judged not to be useful masking agents for Co.

The data indicate that formation of complexes by Fe and Co does not affect the ability of these metals to enhance the Lc reaction. This may result because the complexes are destroyed at the high pH the reaction is run at, permitting the metals to react as they would when no complexing agents are present. It could also be that the mechanism by which the metals enhance the Lc reaction is such that complexation of the metal is immaterial to the process.

The initial approach in handling the Mg interference problem was based on the finding that the Mg signal is independent of Mg concentration from 10 to 1,000 ppm. By adding Mg to the sample to ensure that its concentration would fall in this range (e.g. 100 ppm), it should be possible to establish a new baseline signal which would be constant in spite of changes in Mg concentration from sample to sample. If the Co analytical signal could be referenced to this new baseline, Co determination in the presence of Mg could be accomplished quite simply. This approach did not work, however, because

Mg is such an effective inhibitor of the Lc reaction. The analytical signals of 1 and 10 ppb Co solutions (above the blank which consists of 100 ppm Mg) in 100 ppm Mg were essentially zero. In the absence of Mg, their analytical signals were 150 and 560 pA, respectively. In OL and river water, the Co concentrations expected for determination were 0.5 and 0.2 ppb so it is obvious that attempting to swamp out the Mg interference would not be successful.

The next approach was to prepare interference plots for mixtures of Co and Mg. Figure 27 shows such a plot in which the Co concentration in various Mg and Co mixtures is constant at 1.0 ppb. The data indicate that in order to determine the analytical signal of a dilute Co solution accurately, the concentration of Mg must be about 0.06 ppm or less. This Mg concentration is lower than the detection limit for Mg (0.35 ppm) which may indicate that in the presence of Co, Mg is a more effective inhibitor.

An interference plot for mixtures of I and Co is also shown in Figure 27. The Co concentration in these solutions was 0.4 ppb. Again, the concentration at which the I has no effect on the Co analytical signal (about 50 ppm) is lower than the detection limit for I alone (400 ppm).

The conclusions reached at the end of the interference study, regarding analysis of real samples, are these:

1. A great number of potential interferents exist and they can

enhance or inhibit the Lc reaction (some do both).

2. The expected interferents in some real samples (e.g. OL) are limited to Fe and Mg because after digestion and dilution all other potential interferents would be at a concentration below their detection limit in this system. The interferences expected in direct analysis of river water are the same. In both samples, the Co concentration would still be above its detection limit for this method.

3. The Fe interference can be easily handled as long as the Fe concentration can be determined by another analytical method. In such cases, the analytical signal of a mixture of Fe and Co can be resolved to yield the concentration of Co in the solution.

4. The Mg interference is difficult to handle because in mixtures of Mg and Co the Mg concentration must be quite low before the Co analytical signal can be determined accurately. In light of the samples intended for analysis, this means that some prior separation of Mg and Co must occur before analysis.

5. Masking of Co or Fe is not possible with those masking agents investigated.

Sample Analysis

NBS Orchard Leaves

NBS orchard leaves (OL) were chosen for analysis because the matrix is well defined and the Co concentration is low (0.2 ppm based on dry weight of material). Comparison of the certified values of constituent elements to the known interferences for this method indicated that only Fe and Mg (300 and 6,200 ppm, respectively, by dry weight) would be interferents in a Co determination. Since these two remaining interferences could not be masked or diluted to the point where they would not interfere (while keeping the Co concentration above its detection limit), an appropriate separation scheme was needed. The development of an effective method to separate Co from its matrix would have the added advantage of ensuring that none of the other potential interferents would present any problems in analysis. This would broaden the applicability of Co analysis via Lc CL to include all liquid and solid samples.

The separation technique used in the analysis was solvent extraction, with the chelating agent being 1-nitroso-2-naphthol (1N2N). The procedure was based on the colorimetric determination of Co via its 1N2N complex (λ_{max} 530 nm) taken from Stary (102). Co forms a 1:3 (Co(III):1N2N) complex which is stable in the presence of relatively concentrated acids and bases. 1N2N is capable of oxidizing

Co(II) to Co(III), but usually H_2O_2 is added to speed up the process. The application of this extraction procedure for alloys, ores, and biological samples has been reported (103, 104, 105). Extraction of Co via its acetylacetonato complex proved to be unacceptable due to the low extraction efficiencies.

In previous studies, the main interferent was also Fe, but it can be masked by addition of citrate. Subsequent extraction (usually with chloroform, $CHCl_3$) leaves the Fe in the aqueous solution and transfers Co (and other metal-1N2N complexes) to the organic phase. Back extraction with 2.0 M HCl strips interferring ions back into the aqueous phase without dislodging the Co-$(1N2N)_3$ complex from the organic phase. Another back extraction with 2.0 M KOH can be used to strip the excess 1N2N into the aqueous layer. The combination of these two back extractions permits the selective separation of Co from its matrix. It had been reported (102) that Mg is not extracted by 1N2N, so Fe and Mg were not expected to interfere with Co CL analysis of any sample.

The digestion procedure employed for OL analyses was dry ashing. Acid digestion was not used because of its inherent problem with metal contamination from the acids. The disadvantages of dry ashing are difficulty in removing the ash from the container and a longer digestion time compared to acid digestions. However, dry ashing is simple to perform and reagent blanks are usually not large.

Before digestion the OL were thoroughly dried at 120°C for 1.5 hours. When cool, three 250 mg samples were weighed out and placed into 50 mL Erlenmeyer flasks. The digestion and extraction procedure is outlined below:

1. The three samples were placed in a muffle furnace (initially at 200°C) and the temperature was increased to 450°C, in 125°C increments, during the first hour. Two blanks (empty 50 mL Erlenmeyer flasks) were also placed in the furnace and all flasks were covered with 2 in. watchglasses. The samples were left overnight and removed after an 18 hour ashing period.
2. The flasks were allowed to cool and then a few drops of Millipore water was added to moisten the ash. This was followed by 5.0 mL of 50% HCl (V/V), which dissolved the ashed material. The HCl was evaporated to dryness and the residue taken up with 2.0 mL of 0.10 M HCl. The two reagent blanks were also subjected to the 50% HCl, evaporation, and 0.10 M HCl. At this point, the reagent blank solutions were clear and the samples varied in color from pale yellow to brown.
3. To clarify the sample solutions, they were filtered through 1.2 μ filter paper (Millipore Catalog No. 97403-15). The receiving vessels were 10 mL volumetric flasks and 0.10 M HCl was used to quantitatively transfer from the Erlenmeyer flasks to the funnels. It was also used to rinse the filter

papers and dilute each 10 mL volumetric flask to the mark. Two reagent blanks were filtered in the same manner as the samples. This completed the digestion, with the Co concentration expected to be about 5 ppb in each sample.

4. The extraction began by adding 1.0 mL of 18% citrate solution, 1.2 mL of 0.50 M KOH, and 1.0 mL of 8.8×10^{-3} M 1N2N, and 1.0 mL of 0.10 M H_2O_2 to each of the three samples and two blanks. The pH of the samples and blanks was then checked and, if necessary, it was adjusted to 3.5 with 0.50 M KOH or 0.10 M HCl. All solutions were then allowed to stand at room temperature for one hour. The 18% citrate solution was prepared by dissolving 50 g citric acid (Mallinckrodt #0627) in 15 mL H_2O and then adding 50 mL concentrated NH_4OH (Mallinckrodt #9721). This solution was diluted to 250 mL after adjusting its pH to 3.4 with 6 M HCl. The 1N2N was prepared by dissolving 0.0382 g 1N2N (Baker's #S519) in 25 mL of 0.10 M KOH. The solution must be filtered as the 1N2N is not completely soluble. The 0.50 M KOH was prepared by dilution of the stock 5.0 M KOH used in CL determinations and the 0.10 M H_2O_2 is the stock H_2O_2 used in CL determinations.

5. To check the efficiency of the extraction, under the exact conditions that were used for the samples, three 10.0 mL Co standards were also extracted. Their concentrations were 4.0,

5.0, and 6.0 ppb, and they were prepared by diluting appropriate volumes of 100 ppb Co stock solution with 0.10 M HCl. These extraction standards were treated in the same manner as the samples and reagent blanks.

6. The actual extraction involved quantitative transfer of the sample to a 125 mL separatory funnel which held 25 mL of reagent grade $CHCl_3$. After shaking for 3 minutes, the layers were allowed to separate and the organic layer was transferred to another 125 mL separatory funnel which held 20 mL of 2.0 M HCl. The second separatory funnel was agitated for 30 s and the layers were allowed to separate. The organic layer was transferred to a third separatory funnel which contained 20 mL of 2.0 M KOH. After shaking for 30 s, the organic layer was transferred to a 100 mL beaker and the process repeated two more times with fresh 25 mL portions of $CHCl_3$. When this had been completed for the three samples, two blanks, and three extraction standards, the respective beakers were placed on a hotplate and the $CHCl_3$ evaporated to dryness.

7. Then, 0.5 mL of concentrated H_2SO_4 and $HClO_4$ was added to each 100 mL beaker, the beaker was covered with a watchglass, and then the solution was refluxed at high heat for one hour. The watchglasses were removed and the $HClO_4$ and H_2SO_4 (in that

order) were evaporated away. This rigorous treatment was required to breakup the Co-(1N2N)$_3$ complex.

8. To the residue in each beaker, 10 mL of 0.01 M HNO_3 was added and then heated gently to achieve full dissolution. The contents were quantitatively transferred to a 100 mL volumetric flask and diluted to the mark with 0.01 M HNO_3. The pH of the samples, blanks, and extracted Co standards was now the same as the Co standards used to prepare the calibration curve. The expected concentration of Co in the samples was now about 0.5 ppb and the extracted Co standards were about 0.4, 0.5, and 0.6 ppb.

The analyses of the samples were carried out by preparing a Co calibration curve for Co concentrations from 0.1 to 1.0 ppb, and then determining the analytical signals of the samples, blanks, and extraction standards. The average percent recovery of the extraction standards was used to determine the percent recovery of the samples.

To verify that the extraction procedure was effective in separating Co from its two principal interferents, Fe and Mg, extractions were performed on 5 ppb Co solutions containing 10 ppm Fe(III) and 200 ppm Mg. These concentrations are about what is expected for Fe after digestion of OL (0.75 ppm) and in 13-fold excess for the expected concentration of Mg (16 ppm). After extraction (steps 4 and

6 above), Atomic Absorption analysis (Varian AA-6) showed that the concentration of the two interferents had remained unchanged in the aqueous phase.

The efficiency of the extraction was not constant from day to day, which is why extraction standards were used in the OL analysis. During the last 3 days before OL analysis, the average efficiency for three replicate extractions of 5.0 ppb Co was 105 $\pm$ 5%, 92 $\pm$ 10%, and 101 $\pm$ 6%. Contamination from glassware or reagents was judged to be minimal because the analytical signal of extraction blanks was consistently small. The cause of the variations in extraction efficiency could not be determined, although it was discovered that freshly prepared 1N2N solution gave a higher extraction efficiency than solutions that were 2 or more days old. Digestion of the Co-$(1N2N)_3$ complex with any other acid or combination of acids other than $H_2SO_4 + HClO_4$ resulted in consistently low extraction efficiencies. Those acids which were tried include concentrated HNO_3, H_2SO_4, $HNO_3 + H_2SO_4$, and $HNO_3 + HCl$. Thirty percent H_2O_2 and 5.0 M KOH were equally ineffective.

The actual OL analysis was carried out twice, each time with three replicate samples of about 250 mg each. The result of the first attempt showed that the extraction efficiency of the three extraction standards was 86 $\pm$ 16%. Based on this extraction efficiency and the analytical signals of the three samples, the Co

concentration in the OL (dry weight basis) was 0.11 ppm. The relative precision of the Co concentration in the samples was small, being about 2%. The listed Co concentration in this particular reference material is 0.2 ppm, but this value is not certified. It is considered uncertifiable because the Co analysis was not based on the results of either a reference method or two or more independent methods. This underscores the importance of developing analytical techniques which can be used to determine trace level Co concentrations.

The second analysis of OL indicated that the Co concentration was 0.14 ppm, but in this case the relative precision of the Co determinations was poor. The value for one sample was much lower than the other two and was rejected (Q-test, 95% confidence level). The relative precision of the two remaining determinations was 20%. The extraction efficiencies of the Co standards was also poor compared to previous attempts, $61 \pm 23\%$.

The estimated Co concentration based on five determinations of OL is 0.12 ppm, with the relative standard deviation of the measurements being 18%. The greatest source of imprecision is the uncertainty of the extraction efficiency, which was 18 and 37% (relative precision) for the two analyses. Higher extraction efficiencies, with better precision, were obtained in the last phase of the development of the procedure. It could not be determined what caused the extraction

efficiencies to deteriorate when sample analyses were being carried out. Sample digestion was not complete, as evidenced by the need to filter the samples before extraction. The sample loss at this point could be a contributing factor in the low values obtained. It must be remembered, however, that the Co concentration of 0.2 ppm in OL is uncertified.

Tap Water

The other sample picked for analysis was tap water. The expected Co concentration in such a sample was about 0.2 ppb, which means that direct analysis (no extraction) of the sample should be possible with this technique. Atomic Absorption analysis of the sample indicated that the Fe and Mg concentrations were 0.11 and 3.17 ppm, respectively. Dilution by a factor of five will be sufficient to eliminate the Fe interference, but a 50-fold dilution is required for the Mg interference. A factor of 50 dilution would certainly reduce the Co concentration to a value below its detection limit for this technique so direct analysis of tap water is not possible. When direct analysis was tried on the tap water sample (diluted 1:8 to eliminate Fe interference) the standard additions plot clearly indicated the presence of a negative interferent. No estimation of the Co concentration in this diluted tap water sample was possible because the analytical signal for this solution was negative. To demonstrate that

analysis without prior separation of Co is possible, the tap water was spiked with a small volume of a concentrated Co solution (0.10 mL 1.0 ppm Co added to 20.0 mL tap water). The Co concentration in the tap water was 5 ppb and the other species in the matrix were within 1% of their original value. The Co determination was carried out by first diluting the spiked tap water sample by 50, and then performing the CL analysis. By the standard additions method and the Co calibration curve, the Co concentration in the diluted sample was 0.095 and 0.098 ppb, respectively. The expected Co concentration was 0.10 ppb so the analysis was accurate to about 3.5%. The accuracy of the Co determination using the Co calibration curve indicates that interferences were no problem in the diluted sample.

The conclusion reached after the analysis of OL and tap water is that trace level determinations of Co are feasible with this technique. Direct analysis of water samples is possible if the concentration of Co is large enough to permit the elimination of the Fe and Mg interferences by dilution. Analysis of rock, soil, and biological samples is possible if an appropriate separation scheme can be worked out. The 1N2N solvent extraction procedure appears to be effective but work still needs to be done to improve the reproducibility of the extraction.

Additional Kinetic Data

Background Reaction

As mentioned in the discussion of the mechanism of the Lc reaction, the presence of H_2O_2 is not required for the production of CL if the base concentration is large. Under the conditions used for this study (a final pH of 14), this background CL is readily detected. The maximum CL intensity of the blank is a factor of 25 times smaller than the blank observed when H_2O_2 is present. The peak shape is different for this reaction in that there is no sharp, initial peak when the KOH is injected into the sample cell (compare with Figure 13). The peak time for a background blank reaction is 5 minutes or five times longer than the blank when H_2O_2 is present (the Lc concentration was 6.8×10^{-5} M). It was not determined if the peak time for the background reaction increases as the Lc concentration decreases.

Unlike Lc CL in the presence of H_2O_2, Co(II) inhibits the background reaction. A Co concentration of 200 ppm completely quenches the background reaction, but at 0.20 ppm or less it has no effect on the reaction. Also in contrast to CL runs with H_2O_2, is that the peak time of Co runs is the same as it is for the background blank (compare with Figure 13).

The effect of Fe(III) on the background reaction is more complicated than that of Co(II). At low Fe concentrations (1.0 to 10 ppm),

its effect is to inhibit the background reaction, with the inhibition increasing as the Fe concentration increases. At 30 ppm the background reaction (peak at 5 minutes) is completely quenched. From 10 to 100 ppm, a new quick CL peak (0.5 s duration) appears upon KOH injection and this peak increases in size with increasing Fe(III) concentration.

Hypochlorite ion (OCl^-) inhibits the background reaction as for the normal CL reaction. At 10,000 ppm, OCl^- completely inhibits the background reaction, but its effect on the reaction ceases when its concentration is 10 ppm.

In summary, the data clearly indicate that the nature of background reaction is different than the normal Lc CL reaction. Tamamushi and Akiyama reported in 1939 (53) that reducing agents (hydrazine, hydroquinone, sodium hydrosulfite) enhanced the CL at 50-70°C in the absence of H_2O_2. They did not report the effect of metals or oxidizing agents on the background reaction.

Lucigenin CL Reaction

The CL of the Lc reaction is known to last for about an hour (52, 40) with its duration considerably decreased in the presence of metals which enhance the intensity of the CL. To determine if the decrease in CL intensity with time is exponential, several measurements of the CL intensity as a function of time for the blanks and Co runs were

made. As shown in Figure 28, which is plot of the ln signal versus time, the blank decay is exponential for 50 minutes after initiation of the reaction. The slope of the blank curve is -0.085 min^{-1}. The three Co solutions (0.5, 3.5, and 100 ppb Co) do not decay exponentially for the entire duration of the runs, although the 0.5 ppb Co CL decay is close to the form followed by the blank. As shown in Figure 28, the 100 ppb Co curve crosses over the blank curve at the 19 minute mark. For 3.5 ppb Co, the cross over point is at the 28 minute mark.

It has been implied during the discussion of the Lc CL reaction that any base can be used in the reaction. While it is true that the same peak shape and Co effect is found when NaOH and KOH are used (because the cations do not affect the reaction), the nature of the reaction changes when NH_4OH is used. With the same reagent volumes and concentrations as those in Figure 25 (except 5.0 M NH_4OH replaces 5.0 M KOH), the blank signal is one sharp peak after the NH_4OH is injected. The height of this peak is comparable to the height of the second peak of the blank when KOH is the base, and the CL decays linearly (by about 5-10%) for the first minute of the reaction. Addition of Co(II) in concentrations of 2 to 200 ppm inhibits the CL such that the height of the peak in a Co run is less than the blank. The decay of Co peaks is much faster than for blank peaks. A Co calibration curve is linear over the Co concentration range studied (log-log plot) with a slope of 0.85. The detection limit for Co is about

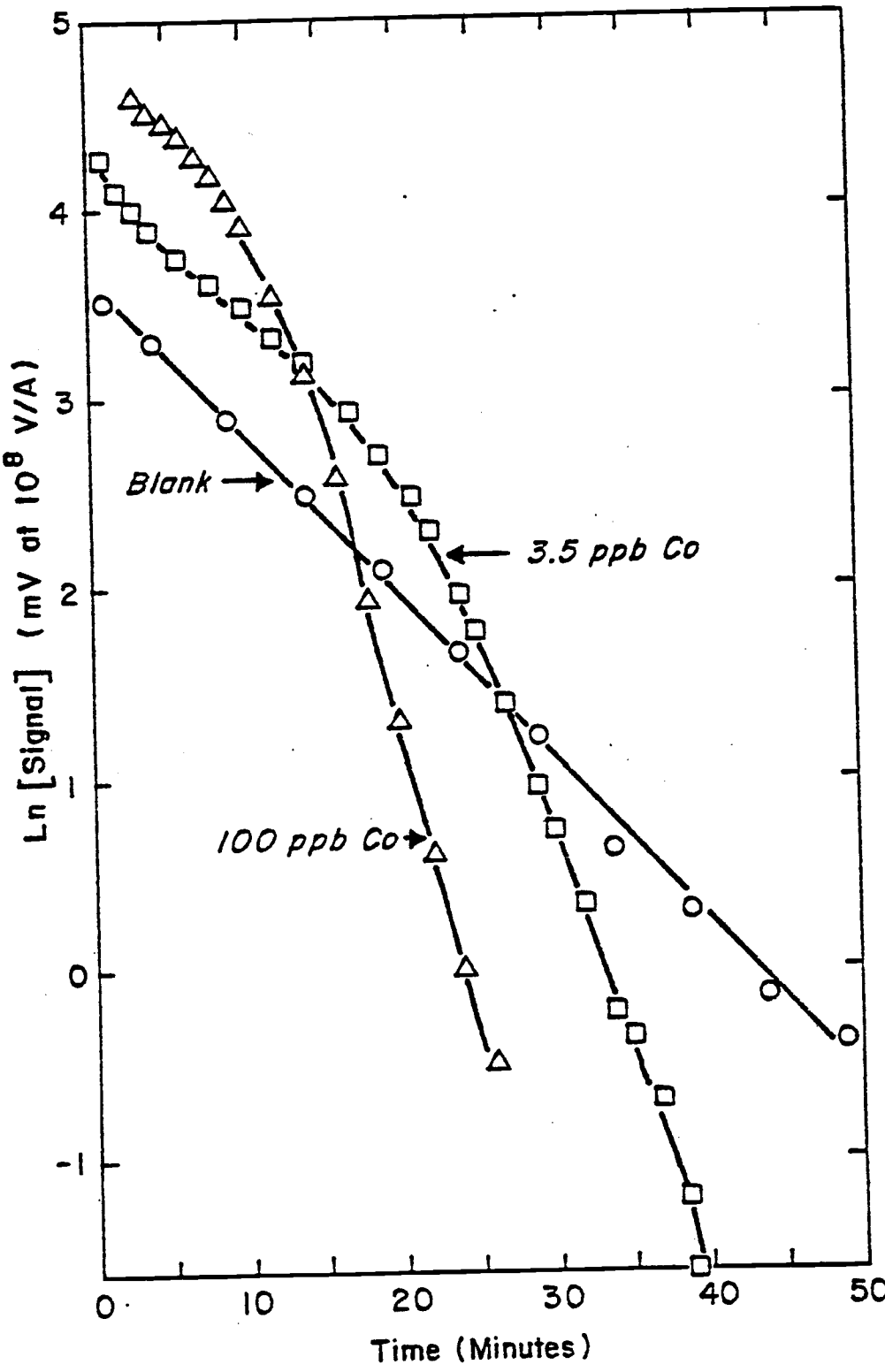

Figure 28. Decay of CL for blank and Co reactions.

1 ppm. The interference study showed that NH_4^+ had no effect on the reaction at 10,000 ppm, but when present at about 9 times this concentration the Lc reaction has different characteristics. The advantage of using NH_4OH as the base for Lc CL is that the peak time for blank and Co runs is very small (about 1 s), but the detection limit for Co is not very low. It was found that Ag behaves essentially the same as Co when NH_4OH is the base.

The necessity of dissolved molecular O_2 for the production of Lc CL (in the absence of H_2O_2) has been demonstrated by several authors (52, 53, 59), but to date there are not reports on the effect of deoxygenating CL solutions when H_2O_2 is present. Therefore, a study was undertaken to determine the effect of bubbling N_2, O_2, H_2, and Ar gases through the sample cell during CL reactions. At this time the reagent volumes and concentrations were those used for the analysis of the samples (Figure 26). The various gases were introduced into the sample cell with a glass capillary connected to the appropriate gas cylinder through one of the extra bulkhead swagelock fittings (g) of the sample module. The glass capillary went all the way to the bottom of the sample cell, and because it was in the corner of the cell, it did not interfere with the operation of the stirring bar. A tee in the gas line was installed so the reservoir of the precision liquid dispenser could also be bubbled with the gas used for the sample cell. A 5 minute period of vigorous bubbling was used to displace the

dissolved gases in the solutions. The sample cell solution (Co or $H_2O + H_2O_2$ + Lc) and KOH were degassed prior to KOH injection, and the gas flow continued in the sample cell throughout the CL run. The results of these experiments for the blank and Co enhanced reactions are as follows:

1. Degassing the solutions with O_2 resulted in a 75% increase in the blank and 1 ppb Co peak times. The peak shapes for both kinds of runs remained the same, but the signal (second peak) of the blank was 20% below its normal value and the 1 ppb Co signal was also 35% low. The overall effect is to decrease the analytical signal.
2. Degassing with pre-purified N_2 decreases the peak time by about half for the blank and 1.0 ppb Co. The blank signal is about 20% larger than normal, but the 1.0 ppb Co signal is 10% smaller. The analytical signal for 1.0 ppb Co is smaller.
3. Degassing with H_2 has some of the same effect as N_2. The blank peak time is shorter than normal as is the 1.0 ppb Co peak time. The peak shapes are different in that the maximum of the second peak is much broader (blank and 1.0 ppb Co) than when the cell is degassed with N_2 or not bubbled at all. The blank signal is about 30% larger than normal, but in contrast to the N_2 data, the 1.0 ppb Co signal is about 20% larger than normal.

4. The effects of degassing with Ar are similar to the results when N_2 is used. The blank and 1.0 ppb Co peak times are about half their normal values of one minute. The blank signal is 15% greater than normal and the 1.0 ppb Co signal is 25% below its normal value.

The result of this study is the conclusion that dissolved molecular O_2 in the CL solutions tends to inhibit the Lc blank reaction. When it is displaced by N_2, H_2, or Ar the blank signal increases and the peak time decreases. It was concluded that these effects are not due to some reaction involving the gases used to displace the O_2 because the effects of using N_2, H_2, and Ar were so similar. The enrichment of the CL solution in O_2 by bubbling with O_2 produced the opposite effects, which supports the basic conclusion that O_2 inhibits the blank reaction.

The study of CL systems usually involves examination of pertinent spectra and this was included in this study. This involved the examination of the CL spectrum as well as the fluorescence emission spectrum of Lc and N-methylacridone. UV-visible absorption spectra of the reactants and CL runs were also obtained. The relationships of the Lc absorption spectrum, the CL spectrum, and the fluorescence emission spectrum of Lc and N-methylacridone are shown in Figure 29. The fluorescence and CL spectra were obtained with a fluorometer constructed and described by Wilson (106). A Cary model 118

Figure 29. Absorption, chemiluminescence, and fluorescence spectra.

Letter	
a	Absorption; Lc, 6.8×10^{-6} M; pH, 5.5; auto slit; period, 5 s; scan rate, 1 nm/s; gain, 4.
b	CL; blank reaction under the conditions in Figure 26; gain, 10^6 V/A; scan rate, 50 nm/min.
c	Fluorescence; Lc, 1.4×10^{-4} M; pH, 5.5; λ_{ex}, 366 nm; gain, 10^6 V/A; scan rate, 50 nm/min.
d	Fluorescence; blank reaction under conditions in Figure 26; λ_{ex}, 366 nm; gain 10^6 V/A; scan rate, 50 nm/min; scan started two minutes after KOH injection.

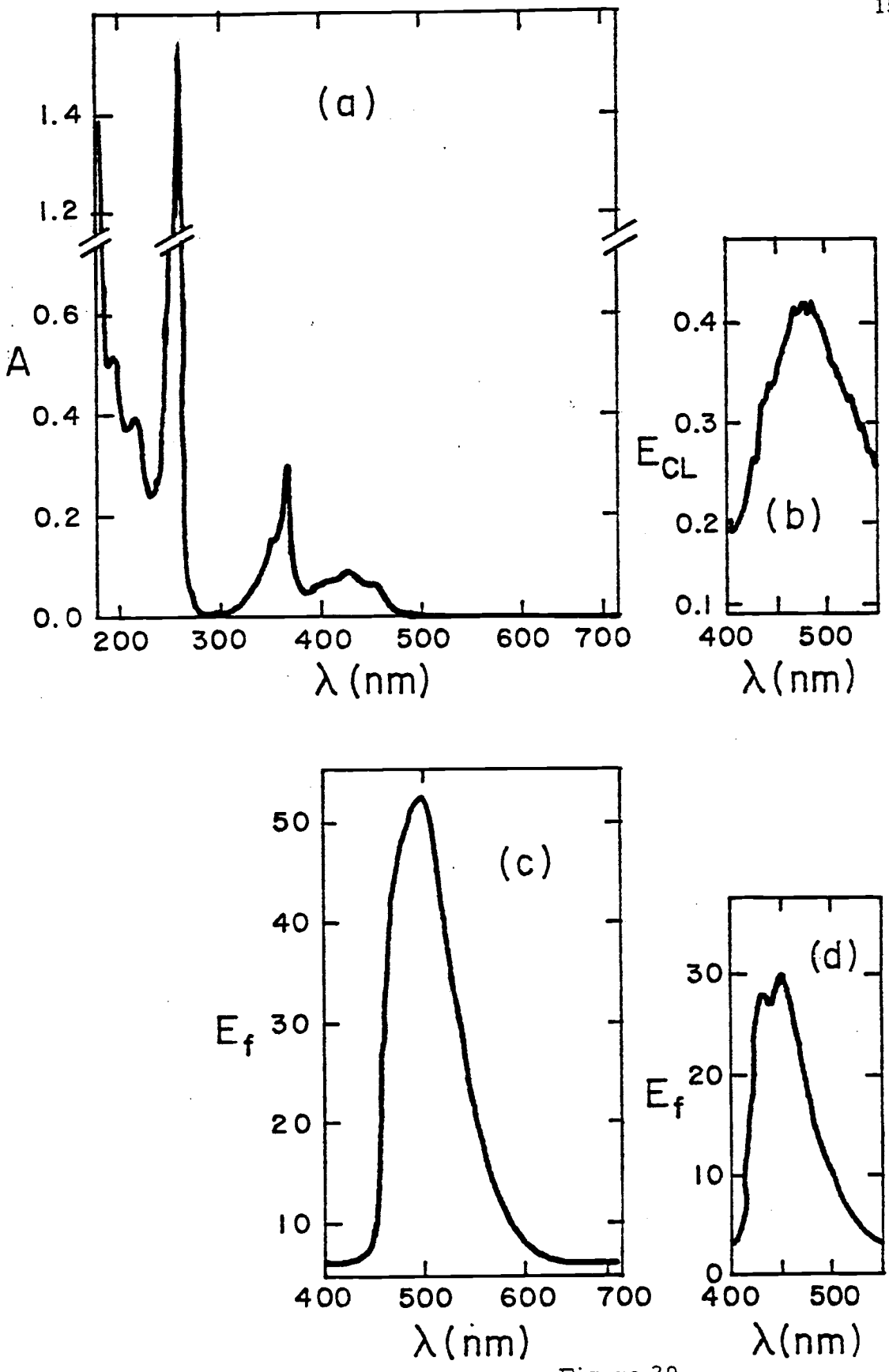
(a)
1.4
1.2
0.6
A
0.4
0.2
0.0
200
300
400
500
600
700
λ (nm)
(b)
0.4
0.3
E_{CL}
0.2
0.1
400
500
λ (nm)
(c)
50
40
E_f
30
20
10
400
500
600
700
λ (nm)
(d)
30
E_f
20
10
0
400
500
λ (nm)

Figure 29

spectrophotometer was used for the UV-visible spectra. The solutions and instrumental conditions are in the figure caption. The absorption peaks and logarithms of their molar absortivities for the UV-visible spectrum (Figure 29a) are: 193 nm (4.88), 218 nm (4.76), 260 nm (5.36), 367 nm (4.65), and 428 nm (4.08). The CL spectrum (Figure 29b) was taken for a blank reaction and it shows that the maximum emission is at 475 nm. A scan of the CL of a single run over a large wavelength region could not be made because the intensity of the CL decreases rather rapidly once the peak reaches its maximum value one minute after KOH injection. To obtain the spectrum shown in the figure, a 1.5 minute scan over 150 nm was made, starting as soon as the KOH was injected. This procedure allows the observation of a true spectral maximum which does not reflect decreasing CL intensity. It was not possible to obtain spectra of Co enhanced reactions because the scan speed of the fluorometer was rather slow (50 nm/min). CL spectra of metal enhanced Lc reactions have not been published due to the necessity of having an instrument which can take CL spectra quickly. The fluorescence emission spectrum of Lc (λ_{ex} = 366 nm) shows a maximum at 503 nm (Figure 29c). The absorption peaks locations, molar absortivities, maximum CL wavelength, and maximum fluorescence emission for the species in Figures 29a, 29b, and 29c all agree with published literature values (55, 56). A spectrum which has not been published is that shown in Figure 29d. This is the

fluorescence emission spectrum (λ_{ex} = 366 nm) of a blank CL run taken within the first 8 minutes after initiation of the reaction. The two peaks at 430 and 450 nm are characteristic of N-methylacridone (Table III), one of the end products of the Lc reaction. The CL of the reaction is not apparent in the spectrum because its intensity is about 1/100th of the intensity of the N-methylacridone fluorescence. The fluorescence emission peak of Lc is not apparent in the spectrum because its fluorescence quantum efficiency is about half that of N-methylacridone (61) and apparently a large fraction of the Lc had reacted. A scan over the same wavelength region one hour after this spectrum was completed indicated that the fluorescence intensity of the N-methylacridone peaks had increased by a factor of four with no new peaks apparent. This points out a convenient way to monitor the rate of the Lc reaction--using fluorescence to follow the increase in concentration of the end product of the reaction. This has not been done before and it could prove to be a helpful tool in characterizing the mechanism of the reaction.

The UV-visible spectra of the reactants and CL runs were taken in order to determine if the formation of a Co-H_2O_2 or Cl-Lc complex was occurring, and what changes in the spectra took place during CL. The attempt to demonstrate that a Co-H_2O_2 or Co-Lc complex exists under the conditions of the reaction was based on the belief that complexation of either of these species could be a factor in the

enhancement of the Lc reaction. A great number of catalytic reactions involve complexation of a reactant by a transition metal and there are indications that complexation of Co with Lc (or a reduction product of Lc) does occur. As mentioned in the History chapter, Metal-"Lc" complexes have been extracted from CL solutions, where the metals are Bi, Cu, Pb, and Co (7, 32, 51, 62). In each case, the metal is believed to be complexed with a reduction product of Lc, but the reduction product has not been identified and the necessity for such complexation to the production of CL has not been proved. Comparison of the UV-visible spectra (190-700 nm) of Co, Lc, H_2O_2, and mixtures of Co + Lc and Co + H_2O_2 did not indicate that complexation was occurring.

A study of the UV-visible spectrum during a blank CL reaction showed that the rate of Lc disappearance could be followed quite easily. The large Lc absorption peak at 260 nm is obscured when KOH is introduced into a mixture of Lc and H_2O_2, but the 367 nm Lc peak remains resolvable. Repeated spectral scans of the same blank CL reaction for 40 minutes showed that this peak steadily decreases in concentration and no new peaks appear. By stopping the scan and observing the absorbance of the 367 nm peak alone, it was possible to see that in a Co run the Lc concentration decreases much faster than when a blank reaction is run. During the first 5 minutes of each reaction the Lc concentration (based on the absorbance of its 367 nm

peak) decreases by 50% in a Co enhanced reaction. The decrease in Lc concentration during the same time span is about 10% for a blank reaction.

The spectral data presented actually shed very little light on the kinetics of the Lc reaction, but they do provide some direction for future studies. The most important findings were that the course of the Lc reaction can be followed by two means other than the total CL output. Correlation of the rate of disappearance of Lc (by absorption spectroscopy) and the rate of production of N-methylacridone (by its fluorescence) with the observed CL could be a powerful tool in the elucidation of the Lc reaction mechanism.

The Co Enhanced Reaction

A useful feature for study of the Co enhanced Lc reaction is the differences that exist in the chemistry of Co(II) and Co(III). Co(III) complexes are kinetically inert, in contrast to Co(II) complexes which are not. Dubovenko (7) reported that substitution of Co(III) complexes for Co(II) resulted in a "quenching" of the Lc reaction, but did not perform a systematic study of very many Co(III) complexes or elaborate further on the nature of the quenching effect. As part of this study, a number of Co(III) complexes were obtained[1] and their effect

[1]Supplied by Dr. J. T. Yoke, Oregon State University, Corvallis.

on the Lc reaction studied. A 100 ppm Co solution (or less, depending on the solubility of the complex) was prepared for each complex. Calibration curves were then prepared for each Co(III) complex and compared to the Co(II) calibration curve. As shown in Figure 30, none of the Co(III) complexes exhibit as large an analytical signal as Co(II) if equal concentrations are compared. A ranking of the Co(III) complexes studied according to their ability to enhance the Lc reaction as effectively as Co(II) would show: cyanocobalamin < $Co(en)_3^{3+}$ < $Co(NH_3)_6^{3+}$ < $Co(NH_3)_2(NO_2)_4^- \approx Co(NO_2)_6^{3-} \approx Co(acac)_3 \approx$ Co(II). To a first approximation, this series of Co(III) complexes corresponds to the expected order of stability based on the number and nature of ligands attached to the Co(III) atom. As stated in the History chapter, Co forms its strongest bonds to N donating ligands such as en, NH_3, and NO_2^-. Coordination to NO_2^- ligands is not expected to be as strong as coordination to NH_3 because in NO_2^- the N donor atom is not as basic. In general, Co forms weaker bonds with O donors compared to N donors, so the relative stability of the acac complex is expected to be less than the other complexes. The corrin ring system of the cyanocobalimin (Vitamin B_{12}) complex is expected to impart stability to the molecule beyond the fact that 5 coordinate bonds in the complex are to N atoms (see Figure 10). Thus, the data imply that the effects of these Co(III) complexes on the Lc reaction can be related to their relative stabilities, but without knowing the mechanism of the

Figure 30. Reactivity of Co(III) complexes.

Co(III) complexes

cyanocobalamin (vitamin B_{12})

$[Co(en)]I_3$

$[Co(NH_3)_6]Br_3$

$Na_3[Co(NO_2)_6]$

$Co(acac)_3$

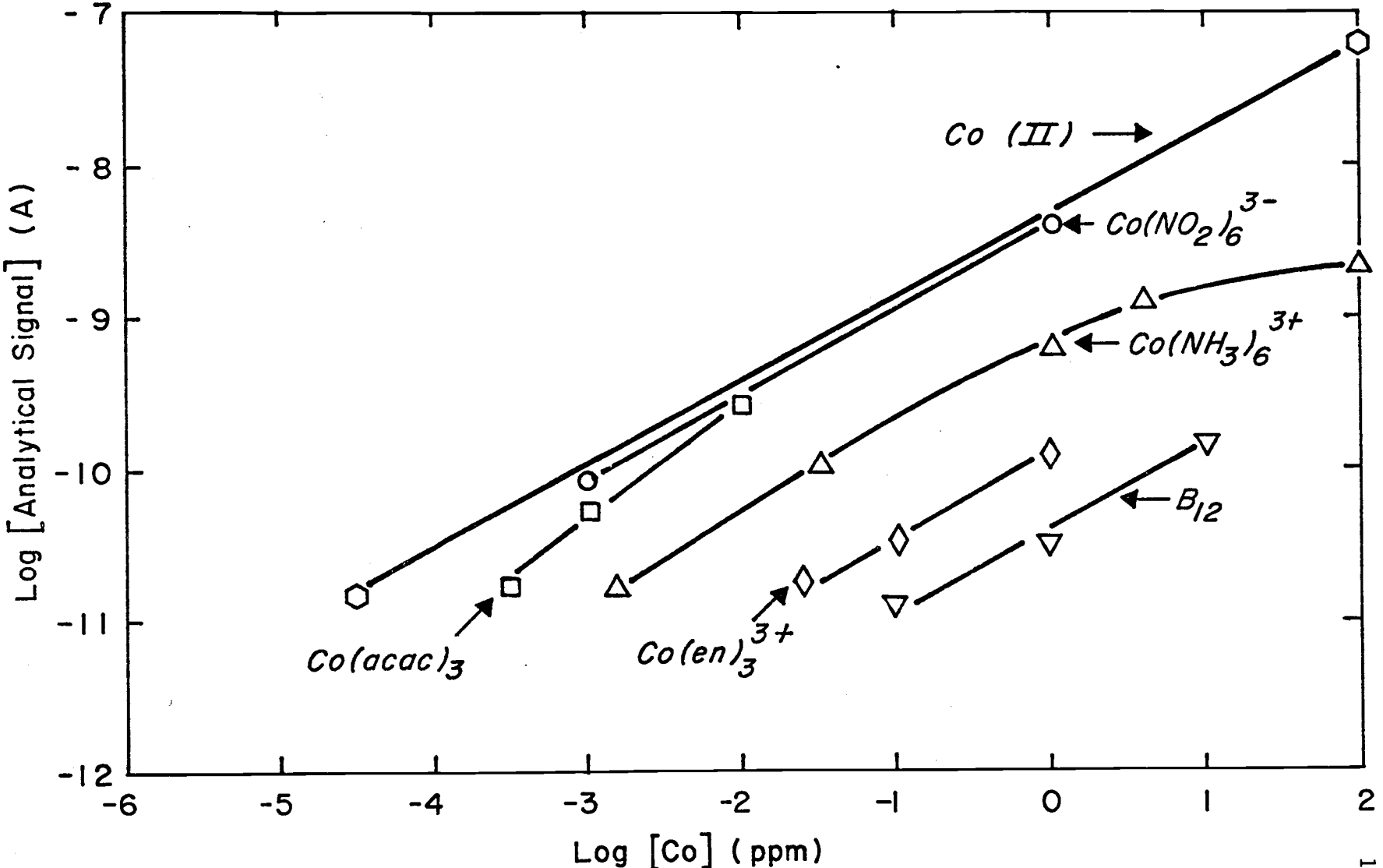
Log [Analytical Signal] (A)
-7
-8
-9
-10
-11
-12
-6
-5
-4
-3
-2
-1
0
1
2
Log [Co] (ppm)
Co (II)
Co(NO2)6 3-
Co(NH3)6 3+
B12
Co(acac)3
Co(en)3 3+

Figure 30

Lc reaction it is impossible to discern how this stability affects the reaction or even if it is important.

Another experiment conducted in this study was the determination of the ability of Co to enhance the Lc reaction after it had participated in the Lc reaction one time. A 100 ppb Co run was initiated and the CL was allowed to continue for 80 minutes. A 0.10 mL portion of this solution was then diluted to 10.0 mL with 0.01 M HNO_3. One mL of this solution (which should have been 1.0 ppb Co) was then used in another CL reaction. The analytical signal was less than 4% of the value normally observed for a 1.0 ppb Co reaction, so it must be concluded that after participating in the Lc reaction the Co is no longer in the same state it started out. This is not too surprising considering the pH of the CL reaction, but it does emphasize that Co cannot be properly regarded as a catalyst in the Lc reaction.

CONCLUSIONS

Analysis

The application of Lc CL to the determination of trace level concentrations of Co(II) has been described. The technique has a very low detection limit (15 pptr) and the linear range extends up to 100 ppm. The method provides a lower detection limit for Co(II) than that reported with any previous CL system or other instrumental technique.

The optimization of the mixing order, reagent concentrations, and other parameters involved several compromises due to conflicts in the criteria monitored. The H_2O_2 concentration (0.10 M), the Lc concentration (6.8×10^{-5} M), and the KOH concentration (1.0 M final) chosen were not necessarily optimal considering S/B ratio, detection limit and analysis time. These concentrations do, however, represent a reasonable compromise between S/B ratio, detection limit, and analysis time. The detection limit can be improved by a factor of two or three by adjusting concentrations, but only at the expense of a much longer analysis time. The high KOH concentration is also advantageous because it does offer the convenience of not having to use a buffer or carefully control the pH of the reagents, standards, and samples.

A comprehensive interference study indicated that many species are capable of enhancing or inhibiting the Lc reaction. Most of these interferences would not actually be a problem in the analysis of a real sample because they would be present at a concentration below their respective detection limits by Lc CL. The interferents that could not be diluted away in the samples analyzed in this study were Fe and Mg. While it is possible to determine the Co contribution to the analytical signal of a mixture of Co and Fe (knowing the Fe concentration) the Mg interference necessitated the development of an extraction scheme based on 1-nitroso-2-naphthol to isolate Co from its matrix. The technique is thus applicable to a wide range of samples because the extraction procedure is specific for Co. The interference study also indicated that under the conditions used for Co determination, the technique can be applied to the determination of trace concentrations of Os, Ru, Fe, Ag, Cu, Ni, and Cr(III).

To test the effectiveness of the digestion, extraction, and analysis procedures NBS OL were analyzed. Five determinations indicated that the Co concentration was 0.12 ppm (dry weight basis), with the relative precision of the measurements being 18%. The relative precision of the extraction efficiency is the greatest source of imprecision in the analysis. A direct analysis of a tap water sample was not possible because of the Mg interference. Analysis of a spiked tap water sample showed that if the Co concentration were 5 ppb or

greater the Mg interference (and all others) could be diluted away. Determination of Co in the dilution of the spiked tap water sample was accurate to about 3.5%.

Several instrumental and procedural improvements were made in order to obtain good blank reproducibility, minimize contamination, and decrease the analysis time. The major improvement in instrumentation was the installation of the precision liquid dispenser to inject the KOH.

Kinetics

The analytical applications of the Lc reaction are well characterized, but the mechanisms of the background, blank, and metal enhanced reactions remain unknown. Because of this the kinetic data obtained are difficult to interpret, but they provide some insights.

A brief examination of the background reaction (Lc + KOH, no H_2O_2 present) showed that there are several differences between it and the blank reaction. In the optimization of the H_2O_2 concentration study, it was noted that the height of the initial, quick peak decreases as the H_2O_2 concentration decreases. Since the peak is entirely absent in the background reaction this CL must result from a reaction dependent on the presence and concentration of H_2O_2. Co(II) inhibits the background reaction in contrast to its enhancing effect on the blank reaction.

The result of the gas bubbling experiments showed that O_2 tends to inhibit the blank reaction. Previous literature reports indicate that O_2 is required for the background reaction which again points out the dissimilarities between the background and blank reaction.

The results of spectra obtained as part of this study verified previous literature reports as to the location and intensity of the Lc absorption peaks, the location of the maximum in the CL spectrum (second peak of the blank), and the location of the maximum of the fluorescence emission spectrum of Lc. A result that has not been reported previously is that N-methylacridone can be readily detected during a blank CL reaction by its fluorescence at 430 and 450 nm. The intensity of the N-methylacridone peak increases as the reaction progresses and this could be a valuable aid in studying the kinetics of the reaction. Another findings, perhaps important for future studies, is that the decrease in Lc concentration can be followed by observing the Lc absorption peak at 367 nm and it was found that Lc is consumed much faster during a Co enhanced reaction than a blank reaction.

Studies of the ability of Co(III) complexes to enhance the Lc reaction showed that their ability to do so was dependent on the nature of the ligands in the complex. Ligands with N donor atoms are bound more strongly to Co than those with O donor atoms, and complexes with ligands like en or NH_3 were the least effective in enhancing the

reaction. Conversely, $Co(acac)_3$ was the Co(III) complex which most closely matched the behavior of Co(II).

Other work in this laboratory has shown that the rate of H_2O_2 decomposition is greatly enhanced by the presence of CL activators such as Co(II) and Ag(I), but not by CL inhibitors such as Mg(II). Quite possibly, the activation of CL by metal ions is related to the effect of the metal ion on the decomposition of H_2O_2.

Future work in the area should be concerned with correlation of the rates of Lc and H_2O_2 consumption and rate of N-methylacridone formation with the observed CL intensity of the blank and Co enhanced reactions. Also, the precise effect of metals on the Lc reaction must be determined to understand the different activation efficiencies of different metals and the difference between metals which inhibit and enhance the Lc CL.

BIBLIOGRAPHY

1. W.R. Seitz and M.P. Neary, Anal. Chem., 46, 188A (1974).

2. U. Isaacsson and G. Wettermark, Anal. Chim. Acta, 68, 339 (1974).

3. W.R. Weitz and D.M. Hercules, in "Chemiluminescence and Bioluminescence," M.J. Cormier, D.M. Hercules, and J. Lee, Ed., Plenum Press, New York, N.Y., 1973, pp. 427-449.

4. W.R. Weitz and M.P. Neary, in "Methods of Biochemical Analysis," D. Glick, Ed., Vol. 23, Wiley and Sons, New York, N.Y., 1976, pp. 161-188.

5. A.K. Babko and N.M. Lukovskaya, Zavod. Lab., 29, 404 (1963). From Chemical Abstracts No. 59:3301d.

6. S. Stieg and T.A. Nieman, Anal. Chem., 49, 1322 (1977).

7. L.I. Dubovenko and N.V. Beloshitskii, J. Anal. Chem. USSR, 29, 85 (1974).

8. S.D. Hoyt, Thesis, Oregon State University, Corvallis, 1976.

9. S.D. Hoyt and J.D. Ingle, Jr., Anal. Chim. Acta, 87, 163 (1976).

10. S.D. Hoyt and J.D. Ingle, Jr., Anal. Chem., 48, 232 (1976).

11. O. Shimomura, F.H. Johnson, and Y. Saiga, Science, 140, 1339 (1963).

12. W.L. Crider, Anal. Chem., 37, 1770 (1965).

13. R.K. Stevens and J.A. Hodgeson, Anal. Chem., 77, 572 (1965).

14. G.W. Nederbragt, A. van der Horst, and J. Van Duijn, Nature, 206, 87 (1965).

15. A.K. Babko, L.I. Dubovenko, and L.S. Mikhailova, Sov. Prog. Chem. 32, 471 (1966).

16. W.R. Seitz, W.W. Suydam, and D.M. Hercules, Anal. Chem., 44, 957 (1972).

17. I.E. Kalinichenko, Ukr. Khim. Zh., 35, 755 (1969).

18. I.E. Kalinichenko and O.M. Grischenko, Ukr. Khim. Zh., 36, 610 (1970).

19. W.R. Seitz and D.M. Hercules, Anal. Chem. 44, 2143 (1972).

20. A.K. Babko and N.M. Lukoskaya, Zh. Anal. Khim., 17, 50 (1962).

21. L.I. Dubovenko and T.A. Bogoslovskaya, Ukr. Khim. Zh., 37, 1057 (1971).

22. A.K. Babko, L.I. Dubovenko, and L.S. Mikhailova, Metody. Anal. Khim. Reakt., Prep. No. 13, 139 (1969).

23. L.I. Dubovenko and Chan Ti Huu, Ukr. Khim. Zh., 35, 637 (1969).

24. L.I. Dubovenko and Chan Ti Huu, Ukr. Khim. Zh., 35, 957 (1969).

25. L.I. Dubovenko and A.P. Tovmasyan, J. Anal. Chem. USSR, 25, 812 (1970).

26. L.I. Dubovenko and A.P. Tovmasyan, Sov. Prog. Chem., 37, 83 (1971).

27. A.K. Babko, A.V. Terletskaya, and L.I. Dubovenko, J. Anal. Chem. USSR, 23, 809 (1968).

28. A.K. Babko, L.I. Dubovenko, and A.V. Terletskaya, Sov. Prog. Chem., 35, 64 (1969).

29. A. Ya. Brin, S.E. Kashlinskaya, N.P. Strel'nikova, and V.I. Petrovichera, Anal. Teknol. Blagorod. Met., 1971, 86-90. From Ref. Zh. Khim., 1972, Abstract No. 6G100. Chemical Abstract No. 78:66575h.

30. L.I. Dubovenko and A.P. Tovmasyan, Ukr. Khim. Zh., 37, 845 (1971). From Chemical Abstracts No. 75:126070q.

31. L.I. Dubovenko and L.D. Guz, Sov. Prog. Chem., 36, 61 (1970).

32. L.I. Dubovenko and A.P. Tovmasyan, Sov. Prog. Chem., 39, 85 (1973).

33. L.I. Dubovenko and A.P. Tovmasyan, Sov. Prog. Chem., 39, 68 (1973).

34. L.I. Dubovenko and E. Ya. Khotinets, J. Anal. Chem. USSR, 26, 683 (1971).

35. A.K. Babko, L.I. Dubovenko, and A.V. Terletskaya, Sov. Prog. Chem., 32, 1326 (1966).

36. L.I. Dubovenko and V.G. Drokov, Izv. Vyssh. Ucheb. Zavod., Khim. Khim. Teknol. 16, 1010 (1973). Chemical Abstracts No. 79:142551k.

37. L.I. Dubovenko, M.M. Tananaiko, and V.G. Drokov, Ukr. Khim. Zh., 40, 758 (1974). From Chemical Abstracts No. 81:98896s.

38. L.I. Dubovenko and A.M. Guta, Izv. Vyssh. Ucheb. Zavod., Khim. Khim. Teknol., 18, 1211 (1975). Chemical Abstracts No. 84:38257m.

39. L.I. Dubovenko and A. Yu. Nazarenko, Ukr. Khim. Zh., 41, 1205 (1975). From Chemical Abstracts No. 85:13306j.

40. R.M. Acheson, "Acridines," Interscience Publishers, New York, N.Y., 1956.

41. Decker and Dunant, Ber., 42, 1176 (1909).

42. Decker and W. Petsch, J. Prakt. Chem., 143, 211 (1935).

43. L. Erdey and I. Buzas, Anal. Chim. Acta, 22, 524 (1959).

44. Ju. Lurie, "Handbook of Analytical Chemistry," Mir Publishers, Moscow, 1975.

45. L. Erdey, J. Takacs, and I. Buzas, Acta. Chim. Acad. Sci. Hung., 39, 295 (1964). From Chemical Abstracts No. 60:9878h.

46. I. Sarudi, Fresenius' Z. Anal. Chem., 260, 114 (1972). From Chemical Abstracts No. 77: 134779j.

47. G. Soli, U.S. Patent No. 3,564,388 (1971). From Chemical Abstracts No. 75:P148444s.

48. J.R. Totter, V.J. Medina, and J.L. Scoseria, J. Biol. Chem., 235, 238 (1960).

49. L. Greenlee, I. Fridovich, and P. Handler, Biochem., 1, 779 (1962).

50. W.S. Oleniacz, M.A. Pisano, and R.V. Insolera, Photochem. Photobiol. 6, 613 (1967).

51. L.I. Dubovenko, M.M. Tananaiko, and V.G. Drokov, Izv. Vyssh. Uchen. Zavod., Khim. Khim. Teknol. 18, 1068 (1975). From Chemical Abstracts No. 83:174969b.

52. K. Gleu and W. Petsch, Angew. Chem., 48, 57 (1935).

53. B. Tamamushi and H. Akiyama, Trans. Faraday Soc., 35, 491 (1939).

54. A.V. Kariakin, Optics and Spec., 7, 75 (1959).

55. J.R. Totter, Photochem. Photobiol. 3, 231 (1964).

56. K. Maeda and T. Hayashi, Bull. Chem. Soc. Japan, 40, 169 (1967).

57. F. McCapra and D.G. Richardson, Tet. Letters, 43, 3167 (1964).

58. E.G. Janzen, J.B. Picket, J.W. Happ, and W. DeAngelis, J. Org. Chem., 35, 88 (1970).

59. K. Maeda, T. Kashiwabara, and M. Tokuyama, Bull. Chem. Soc. Japan, 50, 473 (1977).

60. F. McCapra and R.A. Hann, Chem. Comm., 442 (1969).

61. K.D. Legg and D.M. Hercules, J. Am. Chem. Soc., 91, 1902 (1969).

62. L.I. Dubovenko, L.M. Korotun, and A.P. Kostyshina, Ukr. Khim. Zh., 42, 1194 (1976). From Chemical Abstracts No. 86:61208w.

63. F.A. Cotton and G. Wilkinson, "Advanced Inorganic Chemistry," Interscience, New York, N.Y., 1972, pp. 875-890.

64. D. Dubos, "Electrochemical Data," Elsevier Scientific Publishing, New York, N.Y., 1975.

65. "The Vitamins," Volume 2, W.H. Sebrell, Jr., and R.S. Harris, Ed., Academic Press, New York, N.Y., pp. 119-259.

66. J.M. Pratt, "Inorganic Chemistry of Vitamin B_{12}," Academic Press, New York, N.Y., 1972.

67. E.J. Underwood, "Trace Elements in Human and Animal Nutrition," 4th Edition, Academic Press, New York, N.Y., 1977.

68. H.R.V. Arnstein and A.M. White, Annals New York Acad. Sci. 112, 807 (1964).

69. H.J. Evans and Mark Kliewer, Annals New York Acad. Sci. 112, 735 (1964).

70. "Cobalt Monograph," Edited by Centre D'Information Du Cobalt, M. Weissenbrach, Brussels, Belgium, 1960.

71. R.S. Young, "The Analytical Chemistry of Cobalt," Volume 27 of the International Series of Monographs in Analytical Chemistry, Pergamon Press, New York, N.Y., 1966.

72. I.V. Pyatnitskii, "Analytical Chemistry of Cobalt," Ann Arbor-Humphrey Science Publishers, Ann Arbor, Mich., 1969.

73. "Trace Analysis," J.D. Winefordner, Ed., John Wiley and Sons, New York, N.Y., 1976.

74. V.A. Fassel and R.N. Kniseley, Anal. Chem., 46, 1110A (1974).

75. Varian Techtron Publication #85-100044-00, 1975.

76. K.W. Olsen, W.J. Haas, and V.A. Fassel, Anal. Chem. 49, 632 (1977).

77. E.B. Sandell, "Colorimetric Determination of Traces of Metals," 3rd Edition, Interscience Publishers, New York, N.Y., 1959.

78. H. Aiginger, P. Wobrauschek, and C. Brauner, Meas., Detect. Control Environ. Pollut. Proc. Int. Symp., 197 (1976). From Chemical Abstracts No. 87:110810t.

79. D.C. Burrel, "Atomic Spectrometric Analysis of Heavy-Metal Pollutants in Water," Ann Arbor Science, Ann Arbor, Mich., 1975.

80. H.J. Evans, M. Kliewer, R. Lowe, and P.A. Mayeux, Plant and Soil, 21, 153 (1964).

81. B.K. Hovsepian and I. Shain, J. Electroanal. Chem., 12, 397 (1966).

82. W.C. Schumb, C.N. Satterfield, and R.L. Wentworth, "Hydrogen Peroxide," Reinhold Publishing, New York, N.Y., 1955.

83. K.J. Laidler, "Chemical Kinetics," McGraw-Hill, New York, N.Y., 1965, p. 485.

84. F.R. Duke and T.W. Haas, J. Phys. Chem., 65, 304 (1961).

85. J.F. Goodman and P. Robson, J. Chem. Soc., 2871 (1963).

86. E. Koubek, M.L. Haggett, C.J. Battaglia, K.M. Ibne-Rasa, H.Y. Pyun, and J.O. Edwards, J. Am. Chem. Soc., 85, 2263 (1963).

87. D.B. Broughton, R.L. Wentworth, and M.E. Farnsworth, J. Am. Chem. Soc., 71, 2346 (1949).

88. J.H. Baxendale and C.F. Wells, Trans. Farad. Soc., 53, 800 (1957).

89. I. Budek and G. Davies, Inorg. Chem., 14, 2580 (1975).

90. C.F. Wells and M. Husain, Trans. Farad. Soc. 67, 760 (1971).

91. M. Bobtelsky and A.E. Simchen, J. Am. Chem. Soc., 64, 2492 (1942).

92. I.M. Reibel, Russian J. Phys. Chem., 36, 1036 (1962).

93. J. Bognar and L. Sipos, Mikrochim. Ichnoanal. Acta., 3, 442 (1963).

94. A. Hartkopf and R. Delumyea, Anal. Lett., 7, 79 (1974).

95. T.L. Sheehan and D.M. Hercules, Anal. Chem., 49, 446 (1977).

96. W.R. Seitz, W.W. Suydam, and D.M. Hercules, Anal. Chem., 44, 957 (1972).

97. W.R. Seitz and D.M. Hercules, Anal. Chem. 44, 2143 (1972).

98. M.P. Neary, W.R. Seitz, and D.M. Hercules, Anal. Lett., 7, 583 (1974).

99. S.A. Wise and W.E. May, Res. Delv., 10, 54 (1977).

100. M.L. Parsons, B.W. Smith, and G.E. Bentley, "Handbook of Flame Spectroscopy," Plenum Press, New York, N.Y., 1975.

101. National Bureau of Standards, Standard Reference Material No. 1571, Orchard Leaves, 1971 (Revised 1976).

102. J. Stary, "Solvent Extraction of Metal Chelates," Macmillan Company, New York, N.Y., 1964.

103. R. Lundquist G.E. Markle, and D.F. Boltz, Anal. Chem., 27, 1731 (1955).

104. B.E. Saltzman, Anal. Chem., 27, 284 (1955).

105. E. Cogan, Anal. Chem., 32, 973 (1960).

106. R.L. Wilson, Thesis, Oregon State University, Corvallis, 1977.